




12-2022

## **INTRA-SKELETAL VARIATION IN STABLE ISOTOPES THROUGH NON-DESTRUCTIVE APPROACHES: APPLICATIONS OF THE PATTERNS OF SKELETAL REMODELING TO BIOLOGICAL ANTHROPOLOGY**

Armando Anzellini

*University of Tennessee, Knoxville, aanzelli@vols.utk.edu*

Follow this and additional works at: [https://trace.tennessee.edu/utk\\_graddiss](https://trace.tennessee.edu/utk_graddiss)

 Part of the [Analytical Chemistry Commons](#), [Bioethics and Medical Ethics Commons](#), [Biological and Physical Anthropology Commons](#), and the [Musculoskeletal System Commons](#)

---

### **Recommended Citation**

Anzellini, Armando, "INTRA-SKELETAL VARIATION IN STABLE ISOTOPES THROUGH NON-DESTRUCTIVE APPROACHES: APPLICATIONS OF THE PATTERNS OF SKELETAL REMODELING TO BIOLOGICAL ANTHROPOLOGY." PhD diss., University of Tennessee, 2022.  
[https://trace.tennessee.edu/utk\\_graddiss/7699](https://trace.tennessee.edu/utk_graddiss/7699)

This Dissertation is brought to you for free and open access by the Graduate School at TRACE: Tennessee Research and Creative Exchange. It has been accepted for inclusion in Doctoral Dissertations by an authorized administrator of TRACE: Tennessee Research and Creative Exchange. For more information, please contact [trace@utk.edu](mailto:trace@utk.edu).

To the Graduate Council:

I am submitting herewith a dissertation written by Armando Anzellini entitled "INTRA-SKELETAL VARIATION IN STABLE ISOTOPES THROUGH NON-DESTRUCTIVE APPROACHES: APPLICATIONS OF THE PATTERNS OF SKELETAL REMODELING TO BIOLOGICAL ANTHROPOLOGY." I have examined the final electronic copy of this dissertation for form and content and recommend that it be accepted in partial fulfillment of the requirements for the degree of Doctor of Philosophy, with a major in Anthropology.

Dawnie W. Steadman, Major Professor

We have read this dissertation and recommend its acceptance:

Benjamin M. Auerbach, Alex Bentley, Jonathan Bethard

Accepted for the Council:

Dixie L. Thompson

Vice Provost and Dean of the Graduate School

(Original signatures are on file with official student records.)

INTRA-SKELETAL VARIATION IN STABLE ISOTOPES  
THROUGH NON-DESTRUCTIVE APPROACHES:  
APPLICATIONS OF THE PATTERNS OF SKELETAL  
REMODELING TO BIOLOGICAL ANTHROPOLOGY

A Dissertation Presented for the  
Doctor of Philosophy  
Degree  
The University of Tennessee, Knoxville

Armando Anzellini  
December 2022

Copyright © 2022 by Armando Anzellini  
All Rights Reserved

## ABSTRACT

Stable isotope analysis is a well-established method in biological anthropology used to deliver data on residence, diet, and life history. Samples for these analyses are often collected from the diaphyses of long bones with an assumption of an expected rate of turnover between five and ten years, depending on the skeletal element. However, the biological foundations of this assumption are still uncertain, especially concerning the intra-skeletal and intra-element variation of isotopic signatures that may relate to patterns of remodeling. Exploring these gaps in intra-element isotopic variation requires fine-grained work using multiple bones from multiple individuals, but such work is limited by the destructive nature of current mass spectrometry technology. Traditional stable isotope analysis techniques typically destroy the skeletal sample, which can be damaging for the prospect of justice, if the entire representative sample must be used, and is detrimental for the stewardship of curated skeletal collections. Destructive analyses of skeletal material can also be perceived as disrespectful and intrusive by descendants and descendant communities, and ultimately lead to the exploitation and marginalization by scientists of already marginalized communities. This project, therefore, tested a non-destructive approach using Raman Spectrometry, called Isotope Ratio Infrared Spectrometry (IRIS), to explore its application to isotopic ratio analyses in human skeletal remains for the assessment of  $\delta^{13}\text{C}$  and  $\delta^{18}\text{O}$  from bioapatite. Using this method as well as the traditional method of isotope ratio mass spectrometry, intra-element variation in  $\delta^{13}\text{C}$  and  $\delta^{18}\text{O}$  was explored in two populations, an archaeological population from Transylvania, Romania and a contemporary collection of donors to the University of Tennessee Skeletal Collection. Results suggest that, while IRIS appears promising for  $\delta^{13}\text{C}$ , it is not reliable for  $\delta^{18}\text{O}$  values. Results from both methods also demonstrate that intra-element variation is well within the expected ranges of intraskeletal variation, likely

because bulk sampling is too coarse a method to tease apart potential differences based on the processes of remodeling. Future work must continue to search for reliable non-destructive methodologies while simultaneously ensuring all research follows ethical principles to reduce marginalization of descendant communities.

## DEDICATION

I dedicate this dissertation to my rock, my partner, and my best friend. This is all thanks to you,

Jess. I love you more than I can ever show.

## ACKNOWLEDGMENTS

First and foremost, I would like to begin by thanking the community of Patakfalva-Papdomb and the donors to the University of Tennessee Skeletal Collection, without whom neither this project nor so many others would have ever occurred. Their selflessness extends throughout their lives and I'm deeply grateful to have been allowed to contribute to some of the work for which they have been so indispensable. I would also like to thank Dr. Jon Bethard, Dr. Katie Zedjlik, Ms. Katie Kulhavy, Ms. Renee Reinman, Dr. Zsolt Nyárádi, and everyone else involved in the Papdomb project, for allowing me to be a part of their work and welcoming me with open arms.

For their financial support through the Lucas Grant, I would like to thank the Forensic Sciences Foundation of the American Academy of Forensic Sciences. Without that support, most of the analyses conducted for this project would not have been possible. They risked their funding on this dream project and I never could have completed it without them.

I would like to thank Dr. Tiffany Saul for her support and mentorship throughout this process. Without her emotional and academic assistance, I could not have done much of what I managed to do in my limited time at the University of Tennessee and at Middle Tennessee State University. I'm lucky to count her as a mentor and a friend and only hope I can be as much of a help for her in the future as she has been for me. While at Middle Tennessee State University, I also could not have conducted my research without the amazing support and openness of Dr. Ngee Sing Chong. He not only opened his lab for me but was willing to do anything necessary to help me complete my research. This dissertation, in part, I owe to him.

I have spent a number of years working in the Forensic Anthropology Center and want to thank everyone with whom I've ever worked. You have all been amazing, supportive colleagues



and I could not have asked for a better group of people with whom to work. In addition, I would like to thank Middle Tennessee State University for their support through the Diversity Dissertation Fellowship program. This program supported me through a salary, an office, laboratory space, and wonderful colleagues. I hope it continues for many years to come and I will forever be grateful for the support of the university and my colleagues.

I would like to thank my committee members, Dr. Ben Auerbach, Dr. Alex Bentley, and Dr. Jon Bethard for their mentorship and flexibility. I know I pushed and rushed through this process, and it would not have been possible without their openness, their care, and their willingness to pivot as needed and take time off their busy schedules to make sure I finished on time and with a great project. Their guidance has been invaluable, and I certainly could not have done this without them.

I would like to thank my advisor, Dr. Dawnie W. Steadman, for being the best advisor I could ever have imagined. Without her, this experience would never have been as great as it was. For her unerring support, her willingness to listen to my crazy ideas, her amazing concern for my personal well-being and that of my spouse. I am so lucky to have been chosen to be a part of this program under her mentorship. Thank you, Dawnie, I will forever be grateful.

And last, but certainly not least, I would like to thank my spouse Jessica Purvis, without whom this dream of earning a Ph.D. would not have been possible. I will forever be in her debt for her care through the best of times and the worst of times, her unwavering belief in my abilities and competence, and her willingness to do whatever it took to get me to the finish line in this process. I could never have done this without her.

## TABLE OF CONTENTS

|   |    |
|---|----|
| CHAPTER ONE INTRODUCTION .....  | 1  |
| Research Questions .....  | 3  |
| Biogeochemistry and the Human Skeleton.....   | 4  |
| A Critical Theory of Destructive Analyses in Biological Anthropology .....                | 6  |
| Vibrational Spectrometry and its Applications in Bioarchaeology and Forensic Anthropology | 7  |
| The Potential for a Non-Destructive Stable Isotope Analysis .....                         | 9  |
| Summary of Individuals Analyzed .....   | 10 |
| The Patakfalva-Papdomb Site.....  | 10 |
| The University of Tennessee Skeletal Collection.....                                      | 11 |
| Research Hypotheses .....   | 12 |
| Significance of Research .....  | 13 |
| Chapter Organization.....   | 14 |
| CHAPTER TWO SKELETAL STRUCTURE, SKELETAL REMODELING, AND STABLE<br>ISOTOPE ANALYSES.....  | 16 |
| Skeletal Structure and Remodeling.....  | 17 |
| Bones: From Micro to Macro .....  | 17 |
| Processes of Bone Modeling and Remodeling .....   | 20 |
| Biomechanics and Bone Remodeling .....  | 23 |
| Biogeochemistry and Bone Turnover .....   | 26 |

|  |    |
|--|----|
| Biogeochemistry in Bioarchaeology and Forensic Anthropology..... | 29 |
| Inter- and Intrasketal Variation in Isotopic Analyses .....      | 32 |
| Diagenesis .....   | 35 |
| Vibrational Spectrometry in Biological Anthropology .....        | 37 |
| Raman Spectrometry.....  | 38 |
| Isotope Ratio Infrared Spectrometry (IRIS) .....                 | 42 |
| Summary.....   | 44 |
| <br>   |    |
| CHAPTER THREE A CRITICAL THEORY OF DESTRUCTIVE ANALYSES IN       |    |
| BIOLOGICAL ANTHROPOLOGY .....                                    | 46 |
| Introduction.....  | 46 |
| Biopower and Capital in Biological Sciences.....                 | 49 |
| Necropolitics and the Meaning of the Dead .....                  | 53 |
| The Agency of Biological Material .....                          | 56 |
| Defining Necrodominance .....                                    | 58 |
| To Whom Belong the Data .....                                    | 59 |
| Solutions .....  | 61 |
| Solutions as Applied to this Project .....                       | 66 |
| Summary.....   | 67 |
| <br>   |    |
| CHAPTER FOUR INDIVIDUALS ANALYZED AND METHODS .....              | 70 |
| Individuals Analyzed .....                                       | 71 |

|   |            |
|---|------------|
| The Székelyfold and the Site of Patakfalva-Papdomb.....   | 71         |
| The University of Tennessee Skeletal Collection.....  | 78         |
| Raman Spectrometry.....   | 82         |
| Isotope Ratio Mass Spectrometry (IRMS) and Correlation to Isotope Ratio Infrared Spectrometry (IRIS)..... | 85         |
| Calculating Diagenesis for Archaeologically Recovered Individuals .....                                   | 87         |
| Intra-element Variation in Biogeochemical Data .....  | 91         |
| Reassociation of Individuals using Biogeochemical Data.....   | 92         |
| Summary.....  | 94         |
| <b>CHAPTER FIVE RESULTS .....</b>   | <b>96</b>  |
| Raman Analysis and IRIS Protocol for Human Skeletal Remains.....  | 97         |
| Diagenesis, IRMS, and IRIS.....   | 100        |
| Intra-element Variation in Biogeochemical Data .....  | 106        |
| Reassociation of Skeletal Remains using Biogeochemistry .....   | 109        |
| Summary.....  | 114        |
| <b>CHAPTER SIX DISCUSSION .....</b>   | <b>116</b> |
| IRMS, IRIS, and the Future of Isotopic Analysis of Human Skeletal Remains.....                            | 117        |
| Diagenesis, Isotopes, and IRIS .....  | 122        |
| Intra-Element Isotopic Variation .....  | 125        |
| Commingling and Isotopic Reassociation .....  | 129        |

|                                     |     |
|-------------------------------------|-----|
| The Context of Necrodominance ..... | 132 |
| Summary .....                       | 133 |
| CHAPTER SEVEN CONCLUSION.....       | 135 |
| Research and Limitations.....       | 136 |
| Future Considerations .....         | 138 |
| REFERENCES .....                    | 141 |
| APPENDIX.....                       | 173 |
| VITA.....                           | 185 |

## LIST OF FIGURES

- Figure 1. Example of hydroxyapatite crystal demonstrating replacements of carbonate for the phosphate (B-type) and for the hydroxyl group (A-type). Drawn using VESTA (Momma & Izumi, 2008) from the Crystallographic Information File obtained from Sudarsanan and Young (1969) ..... 18
- Figure 2. Energy diagram demonstrating the differences between Rayleigh, Stokes, and anti-Stokes scattering as the molecule goes to a higher virtual energy state and then returns to a real energy state.  $\Delta E$  is the energy difference between the states which translates to a difference in wavelength for the scattered photons.  $V$  values represent the “real energy states” to which the electrons return after excitation ..... 39
- Figure 3. Sample Raman spectrum of unprocessed bone with complete baseline fluorescence removal. Vibrational modes and bands frequently encountered in bone samples are indicated..... 43
- Figure 4. Map of the counties in Romania. Highlighted are the modern counties that encompass the area known as the Székelyfold. Inset shows the county of Harghita, the town of Székelyudvarhely (Odorheiu Secuiesc), and the site of Patakfalva-Papdomb is marked with a cross. .... 72
- Figure 5. Scatter and marginal box plots of  $\delta^{18}\text{O}$  and  $\delta^{13}\text{C}$  isotopic data from bone apatite derived from individuals recovered from intact or almost intact graves at the site of Patakfalva-Papdomb. Data from Bethard, Zejdlik, Nyárádi, and Gonciar (2022)..... 76

Figure 6. Map of tap water values for  $\delta^{18}\text{O}$  of the contiguous United States with pins denoting the residence location for selected donors from the University of Tennessee Skeletal Collection. All  $\delta^{18}\text{O}$  values are in reference to SMOW. Adapted from data by Bowen, Ehleringer, Chesson, Stange, and Cerling (2007)..... 81

Figure 7. Example of sampling locations for a left femur. Orange circles represent sampling locations. Only sampling locations visible in this anterior view are represented, but sampling occurred on anterior and posterior aspects of each element with the exception of rib 2 which was only sampled on the ventral surface. .... 83

Figure 8. Scatter plot of the  $\delta^{13}\text{C}_{\text{apatite}}$  and  $\delta^{18}\text{O}_{\text{vpdb}}$  results from IRMS analysis of bone apatite. Results are grouped by mortuary context (burial or unassociated) and age category (adult or subadult). Burial apatite data from Bethard et al. (2022). Marginal scatter plots summarize the grouped data. .... 98

Figure 9. Correlation plots of IRIS derived and IRMS derived isotopic ratio values for  $\delta^{13}\text{C}_{\text{apatite}}$  (left) and  $\delta^{18}\text{O}_{\text{vpdb}}$  (right). Bands demonstrating the MMD (Pestle et al., 2014) are visible on the correlation plot for  $\delta^{13}\text{C}$  but the spread of original values for  $\delta^{18}\text{O}$  is too close for the MMD bands to be visible..... 101

Figure 10. Error for the  $\delta^{13}\text{C}_{\text{apatite}}$  (left) and  $\delta^{18}\text{O}_{\text{vpdb}}$  (right) models for each sample spectrum in the testing dataset. Box plots on the right margin of each scatter plot show the distribution of the error and dashed lines in the error scatter plots show the MMD value (Pestle et al., 2014). .... 102

Figure 11. Boxplots showing the correlations between the calculated indices of diagenesis and

|  |     |
|--|-----|
| the assessed quality control categories. ....  | 104 |
| Figure 12. Visual representation of the mean deviation of $\delta^{13}\text{C}_{\text{IRIS}}$ for the right second rib. View is superior. Colors represent magnitude and sign of deviation. Adapted from Šavlovskis and Raits (2021).....  | 111 |
| Figure 13. Visual representation of mean deviation of $\delta^{13}\text{C}_{\text{IRIS}}$ for the right upper limbs: (A) humerus, (B) radius, and (C) ulna on both the anterior (left) and posterior (right) views. Colors represent the magnitude and sign of the deviation. Adapted from (Bauer, 2016).<br>..... | 112 |
| Figure 14. Visual representation of mean deviation of $\delta^{13}\text{C}_{\text{IRIS}}$ for the right lower limbs: (A) fibula, (B) tibia, and (C) femur on both the anterior (left) and posterior (right) views. Colors represent the magnitude and sign of the deviation. Adapted from (Bauer, 2016).<br>.....  | 112 |



## LIST OF TABLES

|  |     |
|--|-----|
| Table 1. Raman band positions and assignments most often encountered in analyses of skeletal remains.....  | 43  |
| Table 2. Summary table of skeletal elements of individuals from the Patakfalva-Papdomb site analyzed in this study. The N of elements represents the individual isolated skeletal elements while the N of samples represents the total number of samples representing each skeletal element.....   | 77  |
| Table 3. Summary table of data from selected University of Tennessee Skeletal Collection donors. $\delta^{18}\text{O}_{\text{water}}$ values have been estimated from an isoscape of tap water isotopic ratios across the United States and the $\delta^{18}\text{O}_{\text{carbonate}}$ values have been estimated using the formula by Daux et al. (2008). $\delta^{18}\text{O}$ values shown are in the VSMOW scale. .... | 81  |
| Table 4. Formulae for the calculation of the indices of diagenesis from Raman Spectrometry used in this study and their associated ranges for determining the extent of diagenetic alteration in bone.....   | 90  |
| Table 5. Raman bands and their molecular assignment selected for the IRIS linear regression model. Their relationship and the strength of that relationship in the model are presented. ....   | 101 |
| Table 6. Summary statistics for indices of diagenesis calculated from all Raman spectra. ....  | 102 |
| Table 7. Mean deviation table for skeletal element and location demonstrating that no sampling location deviates by more than the 95% C.I. of the distribution of $\delta^{13}\text{C}_{\text{IRIS}}$ values.....  | 110 |

## CHAPTER ONE

### INTRODUCTION

Since the 1970s, anthropologists have analyzed stable isotopes in skeletal remains, also known as biogeochemistry, to deliver rich data on diet, migration, and life history in bioarchaeological contexts (Bethard, 2013; Brätter, Gawlik, Lausch, & Rösick, 1977; Katzenberg, 2008; van der Merwe, 1982; Vogel & Van Der Merwe, 1977). Bioarchaeological studies have interpreted these isotopic data to explore social inequality in access to food (Bethard, Zejdlik, Nyárádi, & Gonciar, 2022; Le Huray & Schutkowski, 2005; Somerville, Fauvelle, & Froehle, 2013; Toyne et al., 2014), permanent and seasonal migration patterns (Balasse, Ambrose, Smith, & Price, 2002; Bower, Getty, Smith, Simpson, & Hoffman, 2005; Groves et al., 2013; Hufthammer et al., 2010; Knudson & Price, 2007), weaning of children and their health outcomes (Burt, 2013; Dupras & Tocheri, 2007; Nehlich et al., 2011; Reynard & Tuross, 2015; Richards, Mays, & Fuller, 2002; Wright & Schwarcz, 1998), and even metabolic differences between individuals and the expression of pathological conditions in the past (Jaouen & Pons, 2016; Katzenberg & Lovell, 1999; Olsen et al., 2014). Forensic anthropologists have more recently begun to use stable isotopes derived from bone to aid with the identification of missing individuals by providing cultural and residential markers that may help narrow down the identity of the deceased from a pool of missing persons through interpretations of their diet and residential history (e.g., Bartelink & Chesson, 2019) and potentially reassociate commingled remains (Berg, Chesson, Yuryang, Youngsoon, & Bartelink, 2022). And while variation between skeletal elements in a single individual, known as intraskeletal variation, has been explored (Berg et al., 2022; Olsen et al., 2014; Sealy, Armstrong, & Schrire, 1995), the implications of

intra-element variation of isotopic signatures, potentially affected by differential patterns of remodeling, has not yet been thoroughly examined (Bell, Cox, & Sealy, 2001; Birkhold et al., 2016; Fahy, Deter, Pitfield, Miskiewicz, & Mahoney, 2017; Hsieh, Robling, Ambrosius, Burr, & Turner, 2001; Maggiano, White, Stern, Peralta, & Longstaffe, 2019). Biogeochemical studies comparing isotopic values from different sections of a skeletal element (e.g., endosteal versus intracortical, newer osteons versus older osteons) have found significant differences related to differential patterns of remodeling such that newer bone has a significantly different value than older bone (Bell et al., 2001; Fahy et al., 2017; Maggiano et al., 2019). Although differences in remodeling rates have also been found between anterior and posterior, and proximal and distal aspects of long bones (Hsieh et al., 2001; Lanyon, Goodship, Pye, & MacFie, 1982; Schulte et al., 2013), no study has yet explored the potential resulting isotopic differences from these different sampling locations.

Exploring this gap in our understanding of isotopic deposition requires fine-grained work sampling multiple bones from multiple individuals and selecting a number of samples from each bone, but such work is made impractical by the destructive nature of current mass spectrometry technology that would ultimately destroy the skeletal remains being studied. Standard stable isotope analysis techniques necessitate the mechanical breakdown of the skeletal remains and include chemical processing that typically destroy the skeletal sample. Destructive processes may be damaging for the prospect of justice in forensic contexts if the entire representative fragment is destroyed and can be problematic for the stewardship of curated skeletal collections. This project, therefore, aims to test a non-destructive spectrometric technique called Raman spectrometry and explore its application as a proxy to traditional isotopic ratio analyses using a mass spectrometer (Kerstel, 2004; Vitkin et al., 2020; Wiesheu et al., 2018). The Raman

instrument can then be used to explore the effect of differential patterns of bone remodeling within skeletal elements on isotopic fractionation. Vibrational spectrometric tools, such as Raman spectrometers, have a multitude of advantages over traditional isotope ratio mass spectrometers (IRMS) since they can be operated in a field lab without the need for engineering safety measures, time-consuming sample preparation, or expensive consumable products, thereby significantly expediting the results in investigations and protecting the integrity of the skeletal remains and simultaneously calculate indices of diagenesis to examine the reliability of the isotopic results (Weiner, 2010b).

### **Research Questions**

This project sought to answer the following research questions:

1. Can Raman spectrometry be applied to human skeletal remains to estimate light-weight isotopic ratio values?
2. Does diagenesis significantly impact the application of Raman analysis as a non-destructive proxy for biogeochemical analysis?
3. Does the location of isotopic sampling, both between and within skeletal elements, significantly affect stable isotope ratio values?
4. Can a method based on spectral and biogeochemical data be created that out-performs osteometric methods of reassociation of commingled remains?

These questions were explored in an archaeological context through the analysis of individuals represented by the skeletal remains from the archaeological site of Patakfalva-Papdomb, Romania, and in more recent, and less likely to be diagenetically altered, contexts through the analysis of contemporary donors to the University of Tennessee Skeletal Collection.

## Biogeochemistry and the Human Skeleton

Isotopes are variations of a chemical element such that the number of protons remains the same while the number of neutrons changes. The change in the number of neutrons alters the reactions of these atoms in the natural world. The products of these natural reactions in plants, animals, and the water cycle affect the isotopic composition of food and water ingested by humans, and the isotopic composition of these “isotopic pools” is then incorporated into human bone, with a slight divergence due to physiological processes. These differences in the abundance of isotopes allows for biogeochemistry to be used to interpret the diet and water source of an individual from their skeletal remains. The focus of biogeochemistry in biological anthropology are the stable forms of isotopes as they become incorporated into the skeleton. These stable isotopes can either be radiogenic, heavier elements that are usually the result of radioactive decay, or light isotopes that are naturally occurring but less abundant forms of a common element. Radiogenic isotopes like strontium and lead are often used to explore residential location (Bartelink & Chesson, 2019; Bentley, 2006). Lighter isotopes such as nitrogen and carbon are used for interpretations of diet (Bethard, 2013; Katzenberg, 2008) while oxygen is used in the study of residential location (Bethard, 2013; Daux et al., 2008; Katzenberg, 2008). The ratios of the less abundant isotopes to the more abundant isotopes are compared with an internationally defined standard and are presented as  $\delta$  values representing the difference in the ratio between the sample and the reference in parts per thousand (‰). Light isotopes can be recovered from either bioapatite, as in this study, or collagen, and each provide a different interpretive value. Isotopic analyses of carbon ( $\delta^{13}\text{C}$ ) from collagen and carbonate can provide information on dietary choices related to the plants and proteins being consumed. Isotopic

analyses of oxygen ( $\delta^{18}\text{O}$ ) can provide information on the water source being consumed as those values relates to precipitation and evaporation in the water cycle related to geography. This geographic basis for isotopic data has been used to narrow the location of residence for unknown individuals through the use of isoscapes, or maps that show the isotopic distribution across a region (Bartelink & Chesson, 2019; Chesson, Tipple, Ehleringer, Park, & Bartelink, 2017).

To assess the isotopic ratio values from human skeletal remains requires a destructive process. Samples of skeletal remains undergo both mechanical and chemical preparations that break down the sample into constituent parts prior to vaporization and mass spectrometry analyses. Minor variations in the preparation of the sample or the reference material each laboratory utilizes for the purposes of calibration can affect the precision of the isotopic analysis, with research demonstrating that  $\delta^{13}\text{C}$  from bone apatite can vary as much as 1.2‰ and  $\delta^{18}\text{O}$  can vary as much as 3.1‰ between laboratories analyzing the same sample (Pestle, Crowley, & Weirauch, 2014). These variations have been termed the minimum meaningful differences (MMD) such that only differences between individuals above these values should be interpreted as biologically meaningful and have also become the standard variability expected between laboratories (Pestle, Crowley, et al., 2014).

The process of grinding and homogenizing the sample, often referred to as bulk sampling, averages intra-element differences that have previously been found with a more focused isotopic analysis of individual osteons and of the endosteal surface (Bell et al., 2001; Fahy et al., 2017; Maggiano et al., 2019). However, remodeling rates may also affect the length of the diaphysis differently as bone reacts to mechanical stimuli (Birkhold et al., 2016; Lanyon et al., 1982), differences that may lead to varied incorporation of isotopes into the bone along the diaphysis. These differences, related to patterns of remodeling, can only be explored with more

locally focused analyses of the bone, but the highly destructive nature of the methodology makes the exploration of this question impractical using currently established methods. The process of isotopic analysis is always highly destructive for any skeletal material and has been considered problematic for some marginalized communities, as have other destructive analyses (Fox & Hawks, 2019; Kaufmann & Rühli, 2010; Sadongei & Cash Cash, 2007; Squires, Booth, & Roberts, 2019; Tsosie, 2007).

### **A Critical Theory of Destructive Analyses in Biological Anthropology**

Destructive analyses of human remains, such as those required for the collection of isotopic data, can be problematic from many perspectives. Western scientific thought has historically placed human remains in the category of objects of study (Gold, 1996; Highet, 2005; Kaufmann & Rühli, 2010; Rabinow & Rose, 2006). This perspective is founded on Cartesian dualism, the idea that body and mind are separate entities, such that the body is seen as merely a vessel for a soul/mind (Campbell, 2003; Gold, 1996). Such a vessel, therefore, can easily be separated and damaged postmortem without harm to the individual. However, not all cultures see the body in this detached way (Deloria Jr., 1992; Riding In, 1992; Sadongei & Cash Cash, 2007; Tsosie, 2007). Even in western thought, the body represents a symbol on which all stakeholders, those with an interest in the body, can place their own ideologies and meaning (Andrews & Nelkin, 1998; Harper, 2010; Verdery, 1999). This imposition onto the body as separate from its own agency is a form of dominance perpetrated by those with authority, such as scientists, through direct action, and such dominance is perpetuated by the legal structures of society. In the vein of Mbembé's (2003) necropolitics, I call this form of dominance of human remains necrodominance. In recent years, anthropologists have grappled with the discipline's history of

necrodominance by acknowledging the agency of the skeletal remains as individuals, by understanding the cultural harm perpetrated by acts of necrodominance, and by increasingly seeking the most ethical treatment of human skeletal remains (Arnold, 2014; Geller & Suri, 2014; Kreissl Lonfat, Kaufmann, & Rühli, 2015; Walker, 2008; Zuckerman, Kamnikar, & Mathena, 2014). From these efforts, a few suggestions have arisen for a more ethical treatment of human remains, especially concerning invasive/destructive analyses (Kreissl Lonfat et al., 2015; T. R. Turner, 2012; T. R. Turner, Wagner, & Cabana, 2018). Suggestions for a more ethical biological anthropology include: complete collaboration with descendant communities beginning at the stage of hypothesis development, data privacy and a stewardship model of both data and samples collected from individuals, giving back to the descendant communities using the results of all research, and methodological advancements should place an emphasis on discovering non-invasive and non-destructive methods for all analyses in biological anthropology (Arbour & Cook, 2006; Kreissl Lonfat et al., 2015; Sadongei & Cash Cash, 2007; Squires et al., 2019; T. R. Turner et al., 2018). The current project seeks to provide one alternative, non-destructive approach that, when applied in conjunction with all other suggestions, will further the efforts of the field for a more ethical understanding of the skeletal remains of individuals.

### **Vibrational Spectrometry and its Applications in Bioarchaeology and Forensic Anthropology**

Some attempts to reduce the potential for needless destruction of skeletal material have included the prescreening of skeletal remains for isotopic analysis using vibrational spectrometry prior to removal and destruction (Halcrow et al., 2014; Madden, Chan, Dundon, & France, 2018; Mays, Elders, Humphrey, White, & Marshall, 2013; Pestle et al., 2015; Sponheimer et al., 2019).



Vibrational spectrometry is a form of non-destructive chemical analysis that uses the physical properties of molecules, in particular their inherent vibrational frequency, to identify their concentration in the composition of some material. Vibrational spectrometry has been frequently applied in bioarchaeology in the study of diagenesis, the process by which the molecular composition of bone is altered in the burial environment (Beasley, Bartelink, Taylor, & Miller, 2014; Berna, Matthews, & Weiner, 2004; Hedges, 2002; López-Costas, Lantes-Suárez, & Martínez Cortizas, 2016; Stathopoulou, Psycharis, Chryssikos, Gionis, & Theodorou, 2008). Diagenetic alteration of bone may significantly affect the results of isotopic analyses, making any interpretations from those isotopic values unreliable. Therefore, the effect of diagenesis on skeletal remains has been the focus of several studies on the application of vibrational spectrometry (Beasley et al., 2014; France, Thomas, Doney, & Madden, 2014; Madden et al., 2018; Muhamadali, Chisanga, Subaihi, & Goodacre, 2015; Pestle et al., 2015).

This study focuses on the application of Raman spectrometry, a form of vibrational spectrometry that applies a low-powered laser at a particular frequency to excite the molecules in a material and then collects the photons released by those molecules at their inherent frequencies. Raman spectrometry has been used in the study of human skeletal remains for decades, especially in the study of diagenesis, but more recently in other applications such as the estimation of time since death in forensic contexts (France et al., 2014; Halcrow et al., 2014; Khan et al., 2013; Madden et al., 2018; McLaughlin & Lednev, 2011; Penel, Leroy, Rey, & Bres, 1998; Pestle et al., 2015). Outside of anthropology, Raman spectrometry has also been successfully used in the application of a non-destructive approach to isotope ratio analyses often called Isotope Ratio Infrared Spectrometry (IRIS) (Dalou, Furi, Caumon, & Laumonier, 2018; Kerstel, 2004; McKay, Dettman, Downs, & Overpeck, 2013; Muhamadali et al., 2015; Vitkin et

al., 2020; Wiesheu et al., 2018). This study, therefore, applies Raman spectrometry-based IRIS to the isotopic study of human skeletal remains.

### **The Potential for a Non-Destructive Stable Isotope Analysis**

While reducing needless destruction through pre-screening of samples is important, non-destructive analyses would be the ideal solution by providing an alternative method. To this end, the current study attempts to develop a protocol for the use of Isotope Ratio Infrared Spectrometry (IRIS) using Raman spectrometry. While IRMS is a destructive method, it directly measures the ratios of isotopes present in the material based on their atomic mass. IRIS, on the other hand, is a non-destructive protocol that uses the physics of vibrational spectroscopy to estimate the ratio of molecules with a heavier isotope to those with a lighter isotope. The vibrational frequency of a molecule in Raman spectrometry is based on the relationship between the atomic weight of the chemical elements in the molecule and their bonding energy (Keresztury, 2006). Since IRIS is an indirect method of estimating isotopic ratios, for any new material being studied using IRIS, the protocol must be correlated and calibrated to IRMS-derived values to create a standard model. While anthropology has yet to apply IRIS to the question of isotopic ratio analysis of human skeletal remains, other disciplines have previously found promising results in applying Raman spectrometry-based IRIS to the study of isotopic ratios for several materials, both biological and non-biological (Dalou et al., 2018; McKay et al., 2013; Muhamadali et al., 2015; Vitkin et al., 2020; Wiesheu et al., 2018).

A great potential benefit of IRIS is its ability to sample multiple elements without any destruction. A reliable IRIS approach allows for the study of intra-element and intraskeletal variation without comprising the skeletal remains of the individuals being studied. With a better

understanding of this variation in isotopic values, both intra-skeletal and intra-element, IRIS may also provide the potential for reassociation of remains using biogeochemistry. Previous research has found some success in biogeochemical reassociation of skeletal remains in commingled contexts, mostly through exclusionary methods (Berg et al., 2022). The most frequent approach to reassociation in commingled contexts is the use of osteometric techniques (Lynch, 2018), but techniques using molecular composition may provide more replicable results. The destructive nature of isotopic analyses has limited the application of reassociation using biogeochemistry, but a non-destructive method may be more readily applied. In order to develop such a method, however, intra-element and intra-skeletal variation in isotopic ratios must be better understood.

### **Summary of Individuals Analyzed**

To explore the research questions presented, individuals from two populations were selected for this study. The individuals in this study derive from both the archaeological site of Patakfalva-Papdomb located in modern day Romania and the University of Tennessee Skeletal Collection.

#### ***The Patakfalva-Papdomb Site***

The site of Patakfalva-Papdomb, located in the town of Văleni (Hungarian: Patakfalva), has been investigated since 2014 in collaboration between the Haáz Rezső Museum, ArchaeoTek Canda, LLC, and the Văleni descendant community. Contemporary interments within this currently in-use cemetery had been encountering historical graves surrounding what had previously been recorded as the site of a Medieval church (Zejdlik, Gonciar, Bethard, & Nyárádi, 2020). The descendant community of Văleni requested the excavation and recovery of the skeletal remains from the director of the Haáz Rezső Museum, Zsolt Nyárádi, who in turn

requested assistance in the excavation and analysis of the skeletal remains to learn more about the history of their community (Zejdlik et al., 2020). Over 700 burials have been excavated since the project began, and three main interment strategies have been observed at the site, one primary and two secondary interments: 1) traditional primary Christian interments, extended and facing East-West with little to no disturbance; 2) a secondary interment of skeletal remains mixed into the overburden of intact medieval burials, likely excavated to create space for more recent burials; and 3) a collective ossuary located on the northern side of the historical church. This project focused on a small subsample of the remains found in the secondary interments covering the more recent intact graves, comparing their isotopic values with results from the previously conducted isotopic analysis of complete burials, to explore one of the questions posed by the community of the potential reasons for the differing mortuary treatments. Individuals from this site aided in the development of the IRIS protocol, intra-element variation in isotopic data, and to better understand the effects of diagenesis on IRIS and IRMS methods.

### ***The University of Tennessee Skeletal Collection***

The University of Tennessee skeletal collection is composed of over 1800 individuals who donated their bodies to the Forensic Anthropology Center for research. Donors to the Forensic Anthropology Center are placed at the Anthropology Research Facility for decomposition research. Once the remains have fully decomposed, they have given permission for their skeletal remains to be cleaned, inventoried, and curated. These donors or their families provide background information, life history, and consent for their remains to be used in research. To maintain respect and safeguard the integrity of the collection, non-invasive analysis is often preferred to any destructive analysis. This project, therefore, applied non-destructive

analyses using Raman spectrometry to explore questions related to isotopic deposition and patterns of remodeling in a small subsample of these individuals. The collection of 30 individuals for this study were selected for their broad geographic residential range between individuals and their diversity in age. These donors aided in the exploration of intraskeletal and intra-element variation in isotopic data and in the testing of methods for the reassociation of skeletal remains using spectrometry.

### **Research Hypotheses**

Through the analysis of these individuals, the following hypotheses, based on the research questions, were tested:

1. Application of IRIS from Raman spectra to human skeletal remains provides a reliable non-destructive proxy for IRMS  $\delta^{13}\text{C}$  and  $\delta^{18}\text{O}$  isotopic values from bioapatite.
  - a. This hypothesis will be supported for  $\delta^{13}\text{C}$  values if those values derived using IRIS are within the 1.2‰ expected variability between isotope preparation laboratories (Pestle, Crowley, et al., 2014).
  - b. This hypothesis will be supported for  $\delta^{18}\text{O}$  values if those values derived using IRIS are within the 3.1‰ expected variability between isotope preparation laboratories (Pestle, Crowley, et al., 2014).
2. Diagenetic alteration of the skeletal remains will not significantly impact stable isotope analysis using IRIS.
  - a. This hypothesis will be supported if IRIS derived isotopic values show a similar relationship to Raman derived indices of diagenesis as traditional IRMS derived isotopic values.

3. With known intra-element and intra-skeletal variation in light-weight isotope fractionation, isotopic ratios may be used to re-associate skeletal remains in commingled contexts with greater accuracy than osteometric methods.
  - a. This hypothesis will be supported if regression models on light-weight stable isotopes or Bayesian Gaussian Mixture Models of Raman spectra can be used to re-associate skeletal elements with an accuracy equal to or above the approximately 95% specificity rates of osteometric methods (Lynch, 2018).

### **Significance of Research**

The increasing popularity and advancement of isotopic analyses have brought some gaps to the fore. Recent research has explored the precision of isotopic data between labs (Chesson, Kenyhercz, Regan, & Berg, 2019) and intraskeletal variation (Berg et al., 2022; Fahy et al., 2017; Jørkov, Heinemeier, & Lynnerup, 2009) that have vastly improved our understanding of isotopic data. The next step, undertaken by this research, is to understand how bone remodeling affects isotopic deposition across individual skeletal elements. This is particularly important because, while differential remodeling between different skeletal elements is known (Jørkov et al., 2009; Sealy et al., 1995), no skeletal element is homogenous in its rate or pattern of remodeling (Allori, Sallon, Pan, & Warren, 2008; Birkhold et al., 2016; Hsieh et al., 2001; Sugiyama et al., 2012). The highly destructive nature of isotopic analyses, however, makes such an exploration difficult both ethically and practically when attempting to protect or curate skeletal remains. The non-destructive approach presented in this study allows us to explore this variation while reducing the impact to skeletal remains.

In addition, Raman Spectrometric technology is accessible, portable, and less expensive

in the long term than traditional isotopic analyses. Any investigator can begin to use this system with a brief training session and without the need for expensive lab consumables or any mechanical or chemical preparation. These analyses can be conducted in remote lab spaces without the need to remove sections of osseous material or export samples (Weiner, 2010b). These tools are relatively inexpensive, compared with traditional isotope ratio mass spectrometers, and can often be found in publicly funded labs, even internationally.

Lastly, vibrational spectrometric methods have been used to assess bone quality and diagenesis, and have been applied to other questions of the biological profile such as discrimination between human and non-human (McLaughlin & Lednev, 2012), estimation of age-at-death (Pedrosa, Curate, Batista de Carvalho, Marques, & Ferreira, 2020), and even estimation of post-mortem interval (Ortiz-Herrero et al., 2021). This project adds two more potential applications of this methodology: 1) the estimation of isotopic values giving diet and residential information and, 2) the potential for reassociation of remains in commingled contexts. This latter potential has already been demonstrated with light weight stable isotopes (Berg et al., 2022) and the correlation between these values and Raman spectrometry allows for the application of a non-destructive approach to this important question of reassociation.

## **Chapter Organization**

This project explores the effects of the patterns of bone remodeling on stable isotope values in human skeletal remains using non-destructive methods. Chapter Two presents the biological patterns of remodeling and explains how these may affect isotopic deposition along a single skeletal element. That chapter also presents background on biogeochemistry and previous research on intraskeletal variation in isotope values and demonstrates that an even more refined

look at isotopic variation is necessary to further our understanding of biogeochemistry in the human skeleton. Chapter Three provides a broad overview of the ethical considerations of destructive research, specifically presented as a form of dominance imposed on descendant communities. That chapter concludes with some suggested solutions that, in addition to less invasive and non-destructive approaches as presented in this project, should be considered in future bioarchaeological investigations. Chapter Four presents the skeletal collections and descendant communities that make this project possible and explains the research design, protocol, and analytical methods. Chapter Five reports the results of this study beginning with the correlation between isotopic data and Raman spectrometry and then following each of the three hypotheses proposed in this project: 1) the application of IRIS to the biogeochemical analysis of human skeletal remains, 2) the effects of diagenesis on IRIS and IRMS methods, and 3) the understanding of intra-element variation and the application of this understanding to reassociation of skeletal remains in comingled contexts. Chapter Six presents a discussion of these results, their significance to the future of non-destructive isotopic analyses, and the implications of the results on intra-element isotopic variation for future biogeochemical studies. Lastly, Chapter Seven concludes with a summation of the work, some final remarks, and potential future directions for research.



CHAPTER TWO  
SKELETAL STRUCTURE, SKELETAL REMODELING, AND STABLE ISOTOPE  
ANALYSES

In this chapter, I present an overview of the physical, biological, and chemical structure of bone, and how each of these inform our current understanding of isotopic analyses and the potential for future non-destructive approaches to biogeochemistry. First, I describe the structural and chemical composition of bone. This discussion forms the foundation for understanding the processes of bone remodeling, the interactions between biomechanical stimuli and patterns of remodeling across the skeleton, and how these patterns of remodeling interact with stable isotope data. Next, I briefly describe the current understanding of biogeochemistry in biological anthropology and our current understanding of intraskeletal variation. The technology of isotope ratio mass spectrometry has been available to biological anthropologists for at least four decades, and more recent explorations of intraskeletal variation have changed our understanding and interpretations of isotopic ratio values derived from skeletal remains. These studies on intraskeletal variation have highlighted the potential for certain isotopic differences between individuals to be of lower magnitude and significance than variation within individuals. Therefore, in this chapter I explore some of the recent work demonstrating natural variation in isotope incorporation. Lastly, I explore the applications of vibrational spectrometry in biological anthropology, especially as they relate to isotopic ratio data, and how some advances in the use of vibrational spectrometry in other fields may provide a non-destructive alternative to collect the same biogeochemical data as with a mass spectrometer, even if this approach has not been applied previously in biological anthropology.

## Skeletal Structure and Remodeling

### *Bones: From Micro to Macro*

In order to understand how vibrational spectrometry, a molecular analytical technique, can be used as a proxy for isotopic data and to explore patterns of bone remodeling, we must first understand the chemical and crystalline structure of bone. Bone is approximately composed of 65% mineral component, 25% organic component, and 10% water (Burr, 2019). The organic component is largely Type I collagen fibrils organized as a series of triple helices of amino acids of the form Glycine-X-Y, where X and Y are most often proline and hydroxyproline but are sometimes replaced by other amino acids. These amino acids are the molecules from which isotopic values of  $\delta^{13}\text{C}$  and  $\delta^{15}\text{N}$  can be derived from bone collagen. Additional non-collagenous proteins are present within bone as they are trapped by the collagen (Burr, 2019). The collagenous fibrils organize into a brick-like lattice where the spaces between the fibrils are packed with mineral crystals and spaces between layers of collagenous fibrils are divided by so-called “plates” of mineral.

The mineral component is characterized by an apatite-like crystal often referred to as hydroxyapatite but more appropriately called bioapatite. Mineralogically, hydroxyapatite has the chemical formula  $\text{Ca}_5(\text{PO}_4)_3\text{OH}$  and is a well-organized and durable crystalline mineral. However, in bioapatite the crystal structure is interspersed with carbonate ions either replacing the  $\text{PO}_4$  component (called B-type carbonated apatite) or replacing the OH ion (called A-type carbonated apatite). These replacements occur in approximately 10% of all biogenic apatite (Figure 1). Additional replacements in the crystal structure can also be observed with elements like strontium and fluorine, which sometimes preferentially bond within the mineral structure

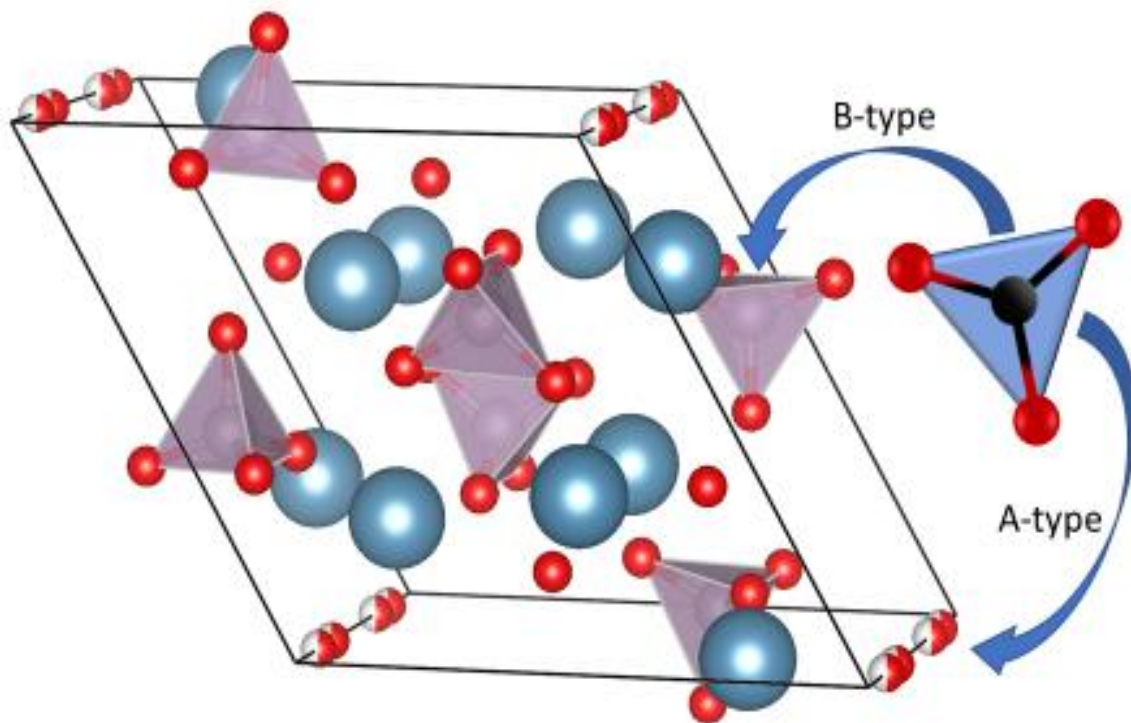


Figure 1. Example of hydroxyapatite crystal demonstrating replacements of carbonate for the phosphate (B-type) and for the hydroxyl group (A-type). Drawn using VESTA (Momma & Izumi, 2008) from the Crystallographic Information File obtained from Sudarsanan and Young (1969)

replacing calcium and hydroxyl groups respectively. The replacements are important since they are either used in isotopic analyses of migration (i.e., strontium) or can inform researchers that bone has undergone some form of post-mortem alteration (i.e., fluorine) (Beasley et al., 2014; Keenan & Engel, 2017; Sponheimer et al., 2019; Wright & Schwarcz, 1996). The molecular replacements in the crystalline matrix form the foundation of isotopic values derived from carbonate bioapatite, such as isotopic ratios for  $\delta^{13}\text{C}$  and  $\delta^{18}\text{O}$ .

Macroscopically, bone can be categorized as either trabecular or cortical, with trabecular bone being more reactive to biomechanical stress. The microscopic structure of cortical bone can generally be subdivided into lamellar bone and osteons. This distinction is important for the discussion of bone remodeling as these two macroscopic structures will remodel differently and react differently to mechanical stress. Lamellar bone is composed of parallel sheets of the collagen-apatite compound material, is dense, and has few vascular apertures (Burr, 2019). Osteons are cylindrical structures built up of circumferential sheets of the same collagen-apatite material with a central haversian canal and a perpendicular Volkmann's canals. Lamellar bone is most often observed on the periosteal and endosteal surfaces and more readily reacts to biomechanical stress than osteonal bone but is still less reactive than trabecular bone (Birkhold et al., 2016; Burr, 2019). Osteons, although less reactive, constitute the majority of the cortical bone volume. Differences in isotopic values have been observed between osteonal and lamellar bone and these have been attributed to differences in modeling and remodeling patterns of these structures (Bell et al., 2001; Birkhold et al., 2016; Brady, White, Longstaffe, & Southam, 2008; Fahy et al., 2017; Maggiano et al., 2019).

## *Processes of Bone Modeling and Remodeling*

The first description of bone functional adaptation, or the reaction of bone to biomechanical stress through modeling or remodeling, was published by Julius Wolff (1886 [1892]). In his seminal book, Wolff described, in engineering terms, the reaction of trabecular bone to mechanical stress and the trabecular buttressing of articular surfaces; however, he did not hypothesize the mechanisms for the signaling or control processes that may have led to his observations. Originally published in the 1960s, Frost's mechanostat theory has come to be the foundation for our understanding of the mechanisms behind bone functional adaptation (Frost, 1987). The name 'mechanostat' is a portmanteau of mechanical and thermostat and defines the foundational hypothesis behind this theory. The mechanostat is founded on the idea that bone has an optimal window of strain within which it neither forms new bone nor reduces bone volume through resorption during remodeling (Frost, 2000). This 'threshold window' of strain acts like a thermostat by increasing bone volume when strain increases and resorbing bone to reduce volume when strain decreases in order to return bone to the ideal strain window. Simply, if strain increases beyond a given point, bone forms, if it decreases under a certain set point, bone resorbs, so that strain on bone remains within an acceptable window.

Frost posits that the mechanostat process is locally controlled, with the osteocyte acting as the primary mechanosensory organ. Some critiques of the model have argued that the mechanostat theory suffers from a 'disuse fallacy,' suggesting that, taken to its natural conclusion, the theory would suggest that a lack of use of a bone would ultimately lead to a complete loss of bone density (C. H. Turner, 1999). Others have argued against a so-called 'lazy zone', a region of the mechanostat model where bone appears to do nothing, an idea that

originates from the strain threshold window hypothesis (Christen et al., 2014). And, of particular importance for studies comparing various skeletal elements, some researchers have critiqued the mechanostat theory for its lack of accounting for osteocyte fatigue and differences in the strain threshold between different skeletal elements (Parfitt, 1994). Each of these critiques has led to adjustments of the model rather than outright rejection (Allori et al., 2008; Christen et al., 2014; Robling, Castillo, & Turner, 2006; Sugiyama, Price, & Lanyon, 2010).

As an attempt to address these critiques and improve the model, the processes for sensation of stress and signaling for remodeling have been extensively studied (Robling et al., 2006; Walsh, 2018). As more detailed study of the mechanisms for osteocyte sensation of mechanical strain have become prominent through *in vitro* studies (Allori et al., 2008), the theory has evolved to include the fluid within the lacunocanalicular network as being heavily involved in the mechanosensation, or sensation of the biomechanical strain, by the osteocytes (Allori et al., 2008). Within the network of canaliculi and the lacunae that interconnect and house osteocytes there is a fluid that encounters shear forces when the bone is under any form of compressive strain and potentially signals for the remodeling process to commence (Allori et al., 2008; Robling et al., 2006). When an osteocyte senses this increase in shear forces resulting from strain on the bone, it begins the process of releasing biochemical factors that signal the basic multicellular unit (BMU) of bone to begin the process of remodeling (Walsh, 2018). This signaling process is called mechanotransduction (Allori et al., 2008; Robling et al., 2006). Mechanotransduction from the osteocytes occurs at the biochemical level with a variety of hormones and transcription factors that regulate the process (Walsh, 2018). However, these factors do not appear to affect the rate of remodeling, but instead affect rates in a broad sense by signaling for remodeling in areas of higher strain (van Oers, Ruimerman, van Rietbergen,

Hilbers, & Huiskes, 2008; Walsh, 2018).

Non-biotic factors that regulate the rate of remodeling rather than the remodeling process itself are the limits of the rates of chemical reactions and the surface area on which resorption and deposition of bone material is occurring. Chemical reactions, such as apatite dissolution through acidification and osteoid removal through protease reactions, take time to develop so osteoclasts are limited in the rate at which they can resorb bone (M. R. Allen & Burr, 2019). Similarly, the rate for osteoid deposition is limited and osteoblasts can only deposit organized osteoid under a particular rate across a limited surface area, any faster and the osteoid is disorganized and mineralizes as woven bone (M. R. Allen & Burr, 2019). As for surface area, bone can only be resorbed and deposited on the surfaces of already existing bone, thus lower surface areas reduce the rate at which bone can be remodeled (M. R. Allen & Burr, 2019; van Oers, Ruimerman, Tanck, Hilbers, & Huiskes, 2008). All of this is to say that the rates at which bone remodels are highly dependent on the chemical and physical limitations of the reactions. The process of resorption is relatively fast, taking approximately a fifth of the time to resorb old bone than to form new bone (M. R. Allen & Burr, 2019). The deposition of osteoid in the form of collagen is also rapid, as osteoblasts create and deposit the osteoid matrix and the BMU moves along the bone surface. However, the beginnings of mineralization are much slower with primary mineralization accounting for approximately 70% of the final mineral composition, occurring over 2-3 weeks and final mineral maturation taking up to a year after osteoid deposition (M. R. Allen & Burr, 2019). However, all of these timing estimates assume homogeneity across the skeleton, but studies on the biomechanical effects on bone remodeling have revealed problems with this assumption.

## ***Biomechanics and Bone Remodeling***

While material properties and bone physiology are relatively homogenous across the body, empirical investigations have demonstrated that osteocytes do not respond equally to new loads (Christen et al., 2014; Hsieh et al., 2001). In fact, some studies have demonstrated marked differences in the responses of bone to loads even within the same skeletal element (Birkhold et al., 2016; Hsieh et al., 2001; Lanyon et al., 1982). Solutions to these problems do not completely overturn our understanding of bone mechanics, or even the application of the mechanostat theory, but instead provide adjustments that help improve the predictions of the model and help explain the heterogeneity of remodeling rates across the skeleton. This heterogeneity of remodeling rates may also in turn affect isotopic deposition and therefore isotopic ratio values, thus a better understanding of differential remodeling resulting from biomechanical stress is imperative.

One solution to understanding differential remodeling rates is the recent arguments against the threshold window as presented by Frost, what some have termed the ‘lazy zone’ of bone remodeling (Christen et al., 2014; Schulte et al., 2013; Sugiyama et al., 2012). Without a ‘lazy zone’, bone is expected to react to all forces that are either above or below a single given strain threshold. If bone is continually reacting when outside of a particular strain or stress threshold, then fluid shear forces are always acting on the osteocyte to either increase or decrease the signaling process for the BMU. Several recent studies have demonstrated that bone resorption and formation, when decoupled, have a linear relationship to the stress imparted on a skeletal element and reach an optimal point of zero net change in bone mass at a level of strain that researchers have termed the minimum effective strain (MES) (Christen et al., 2014; Schulte



et al., 2013; Sugiyama et al., 2012). This model fits with the physics of fluid shear forces that would only exist under changes in load outside of an effective strain that overcomes the viscosity of the fluid. A second assumption made by these models without the threshold window is that bone tends toward resorption and is only counteracted through bone formation if under load (Hsieh et al., 2001; Sugiyama et al., 2010; Yang, Xu, Bullock, & Main, 2019). This assumption again would fit with the idea that the shear forces need to overcome the fluid viscosity to signal for bone formation.

Overcoming this fluid viscosity is related to the strain on the bone, such that higher strains can shear the fluid more effectively than lower strains. Strain, however, is only partially related to stress, with bone density and robusticity playing a significant role. This relationship explains the difference in MES between more gracile bones like the cranium and more robust bones like the femur. The less gracile bones require less stress to signal the remodeling cascade than do more robust bones. However, those more gracile bones may also regularly experience less stress overall, thereby remodeling at rates mediated by physiological processes rather than biomechanical stimulus.

Another factor that may inform this observed difference in remodeling rates across the skeleton is known as osteocyte fatigue. The theory of cellular accommodation, also called osteocyte fatigue, suggests that osteocytes, as the name suggests, accommodate to customary loads (C. H. Turner, 1999). As the osteocyte accommodates to customary loading it fatigues and stops responding to that load over the short term. Over the long term, cellular accommodation suggests that bone responses to load are based on loading history, not just on current peak strain (C. H. Turner, 1999). Cellular accommodation accounts for the lazy zone by suggesting that the cells have become accustomed to customary loads and are thus non-responsive at those peak

strains, but they may begin to react if the peak strain is increased. Although C. H. Turner (1999) provides no mechanism for this accommodation, the model of cellular accommodation does provide one prediction: that disuse and remobilization therapies should conclude with less total bone mass than the individual had prior to disuse, and this bears out in the empirical data (Schlecht, Pinto, Agnew, & Stout, 2012; Sugiyama et al., 2012; Yang et al., 2019).

Differences in skeletal remodeling resulting from increased bone density, osteocyte fatigue, and their relation to mechanostat theory can also be observed within individual skeletal elements, further complicating the heterogeneity of bone remodeling. Studies on sheep and mice have demonstrated that, within a single skeletal element, remodeling rates and volume of bone formation differs across the surfaces of the bone as well as proximo-distally along the diaphysis (Birkhold et al., 2016; Hsieh et al., 2001; Lanyon et al., 1982). In mice, Hsieh et al. (2001) used microCT at the midshaft as well as at 70% and 30% of the length of the element proximally and distally from the midshaft and demonstrated significant differences in bony reaction to mechanical stress even in areas that were relatively close to the original area of interest. In sheep, Lanyon et al. (1982) demonstrated that the medial surface of the radius had greater total remodeling than the lateral, caudal, or cranial surfaces while under the same compressive loads. Comparisons of remodeling as a result of strain between midshaft cortical bone and metaphyseal trabecular bone using microCT have also demonstrated that remodeling and bone formation rates differ significantly for these tissues even within the same element (Yang et al., 2019). Studies on animals have also shown that the bony reactions to strain appear to result in differences in strain distributions rather than differences in total peak strains, but these have all been observed in the short term (Lanyon et al., 1982). These results of differences in remodeling across the skeleton have been replicated in humans through isotopic and histomorphometric analyses of various

elements, demonstrating significant differences in the remodeling rates between the cranium, long bones, and ribs, under even customary loads (Brady et al., 2008; Fahy et al., 2017; Hedges, Clement, Thomas, & O'Connell, 2007).

### ***Biogeochemistry and Bone Turnover***

The elements that comprise the collagenous fibrils and bioapatite that are laid down and nucleated during bone remodeling originate from concurrently available nitrogen from processes of transamination and deamination (France & Owsley, 2015; Schoeller, 1999) and, more importantly for this study as it focuses on bioapatite, body water and dissolved inorganic carbon (DIC)(France & Owsley, 2015). As a result, there is a correlation between formation of new tissues and stable isotope values, which depends on the rate of remodeling and isotopic intake. This fact has been used to biogeochemically study bone tissue turnover. Controlled-diet studies on animals (Balasse, Bocherens, & Mariotti, 1999; DeNiro & Schoeniger, 1983), *in vivo* studies on humans (Babraj et al., 2002), and the study of multiple sampling locations in past populations (Jørkov et al., 2009; Maggiano et al., 2019; Olsen et al., 2014) have provided new insights on rates of remodeling within skeletal elements, the timing of mineralization, and isotopic incorporation. In turn, these more nuanced understandings have suggested better approaches to the exploration of human life in the past from isotopic data. Studies of bone turnover have demonstrated that soft tissues and collagen can begin to approximate a new isotopic pool as quickly as two hours after ingestion but the mineral component of bone will take approximately two weeks to begin to see these differences (Hedges et al., 2007; Matsubayashi & Tayasu, 2019; Warinner & Tuross, 2010)

Other scholars have been successful in demonstrating differences in isotopic values

related to changes in diet and residence from different skeletal elements that correspond to different periods of the individual's life (Jørkov et al., 2009; Sandberg, Sponheimer, Lee-Thorp, & Van Gerven, 2014; Sealy et al., 1995; Waters-Rist & Katzenberg, 2010). While the difficulty in separating remodeling rates from other physiological effects has been shown (Balasse et al., 1999; Beaumont et al., 2018; Katzenberg & Lovell, 1999; Webb, White, & Longstaffe, 2014), isotopic data may still be useful in identifying rates of remodeling, even if they are affected by pathological conditions or nutritional stress (Cerling et al., 2007; Warinner & Tuross, 2010). For example, the Reaction Progress Variable model, as described by Cerling et al. (2007), predicts that a change in the isotopic values of the water source and diet will result in an immediate, noticeable shift toward these new isotopic values in soft tissues. With continued intake of these same sources, the isotopic values in different tissues will gradually continue to shift until they reach equilibrium with the source, and this gradual rate is dependent on the rate of remodeling. Since a single osteon turnover takes approximately 120 days, it is conceivable that with more spatially constricted techniques for isotopic sampling, seasonal or short-term changes in isotopic composition of diet could be observed in humans. Indeed, this bears out in the empirical data (Brady et al., 2008; Maggiano et al., 2019).

Differences in the isotopic composition and relative remodeling rate between adults and subadults have led to conflicting reports on the ability of isotopic analyses to explore isotopic variation resulting from differences in remodeling rates. Subadult data suggests that, within skeletal elements, remodeling rates are consistent enough that there are no significant differences in isotopic incorporation between metaphyses and diaphyses (Waters-Rist & Katzenberg, 2010). However, in adults, histomorphometric and isotopic analyses combined have demonstrated that bulk sampling of the femur and cranial bones may be incorporating values that still include

isotopic incorporation spanning several years, potentially even from adolescence (Bell et al., 2001; Brady et al., 2008; Fahy et al., 2017). This seeming paradox between a lack of resolution in juvenile remains and potentially significant differences in adults may be resolved by the understanding that remodeling rates in youth and adolescence are much faster and that a greater proportion of bone is being remodeled during these periods in life than as an adult. In adulthood, differences between metaphyses, diaphyses, and weight-bearing versus relatively unloaded bones may indeed be demonstrating differences in diet or residential mobility as presented in other isotopic studies based on massive shifts in diet and residential location (Jørkov et al., 2009; Maggiano et al., 2019; Sandberg et al., 2014).

But remodeling rates are not just heterogenous between skeletal elements, they can also vary across a single skeletal element. Studies have explored differences within a single skeletal element by sectioning the cortical bone into the ‘envelopes’ proposed in the biomechanics literature: periosteal, intracortical, and endosteal (Maggiano et al., 2019; Matsubayashi & Tayasu, 2019). Matsubayashi and Tayasu (2019) demonstrated in animals that differences in the endosteal and periosteal surfaces appear to be representative of more recent changes to the isotopic pool rather than consistent isotopic intake while the intracortical bone appears to represent a much longer period of time. Maggiano et al. (2019) have reached a similar conclusion by demonstrating that endosteal bone isotopic data can correlate to seasonal changes in water-source through oxygen isotopes while intracortical bone may not show the same correlation. These results are supported by explorations of remodeling from a biomechanical perspective (Birkhold et al., 2016) as well as studies on remodeling based on radiocarbon (Hedges et al., 2007). Hedges et al. (2007) have also demonstrated that collagen in the intracortical space represents a period closer to adolescence while the periosteal and endosteal

surfaces are likely more recent. These results could be expected by understanding the processes of appositional growth in the skeleton and isotopic analyses have corroborated those expectations. Biogeochemical analyses, however, are most often used for more than just understanding patterns of remodeling.

### **Biogeochemistry in Bioarchaeology and Forensic Anthropology**

Biogeochemistry has been a prominent tool in bioarchaeological research for the past several decades and has been at the forefront of forensic anthropology in more recent years (Bethard, 2013; Chesson et al., 2017). Since its inception in the 1970s, stable isotope analyses have been implemented in bioarchaeological research to explore diet and mobility in ancient humans (Bethard, 2013; Heaton, Vogel, von la Chevallerie, & Collett, 1986; Lee-Thorp, Sealy, & van der Merwe, 1989; Pate, 1994; Reitsema, 2013; Schoeninger, 1988; Sealy et al., 1995). Light isotopes, such as carbon, oxygen, and nitrogen, have been most prominently featured in exploring access to plants, animal protein, and patterns of migration, with heavier elements, such as strontium and lead, being occasionally used for their additional information on residential history. In forensic anthropology, the use of isotopic ratio analyses have provided new lines of evidence for victim identification by tracking residential history and dietary choices and correlating these analyses to specific regions, usually in multi-isotope applications, to reduce the pool of potential victims, the same intent as the biological profile (Bartelink & Chesson, 2019; Chesson et al., 2017). Most often, isotopic data in forensic anthropology relate to geographic region of residence, interpreted using maps of expected isotopic ratio values called isoscapes (isotope landscape), improving the process for the identification of missing persons (Bartelink & Chesson, 2019; Chesson et al., 2017).

Stable isotope analyses of human skeletal remains analyze the proportion of stable isotopes of particular chemical elements in plants and animals to interpret the diet and residential history of an individual. Stable isotopes can either be radiogenic, usually heavier elements that derive from the radioactive decay of unstable chemical elements, or light isotopes, naturally occurring less abundant isotopes of light weight chemical elements. In the stable isotope analysis of the human skeleton, the most often used radiogenic isotopes include strontium and lead, two elements that are most helpful in identifying residential history, while the most commonly used light isotopes include oxygen, for residential location, and carbon and nitrogen, for dietary information (Bethard, 2013; Katzenberg, 2008). The ratio between the more abundant ( $^{12}\text{C}$ ,  $^{16}\text{O}$ ,  $^{14}\text{N}$ ) and less abundant ( $^{13}\text{C}$ ,  $^{18}\text{O}$ ,  $^{15}\text{N}$ ) isotope is the focus of these investigation. Knowing this ratio can provide information related to abundance in the diet of an individual of various plants, animals, and water sources that themselves have different isotopic ratios. Due the low abundance of these isotopes in the natural world, the ratios are usually reported as  $\delta$  values, representing the relative difference between the isotopic ratio in the material being analyzed and the ratio of an internationally recognized standard, in parts per thousand (‰), calculated as:

$$\frac{R_{\text{sample}}}{R_{\text{standard}}} - 1$$

Where R is the ratio between the less abundant and the more abundant isotope for each chemical element. For bioapatite derived  $\delta^{13}\text{C}$  and  $\delta^{18}\text{O}$  values, the standard is usually Vienna PeeDee Belemnite (VPDB), although  $\delta^{18}\text{O}$  may sometimes be referenced to Vienna Standard Mean Ocean Water (VSMOW). While not explored in this study, collagen derived  $\delta^{13}\text{C}$  and  $\delta^{15}\text{N}$  are also often examined in the exploration of past diets, with  $\delta^{13}\text{C}$  also referenced to the VPDB scale and  $\delta^{15}\text{N}$  referenced to the isotopic ratio present in air  $\text{N}_2$  (Air).

Bioapatite-derived  $\delta^{13}\text{C}$  values provide a broad overview of the diet of an individual, specifically interpreted as the ratio of plants being consumed that follow either a  $\text{C}_3$  or a  $\text{C}_4$  photosynthetic pathway. Through photosynthesis,  $\text{C}_3$  plants fixate less  $^{13}\text{C}$  than their  $\text{C}_4$  counterparts, so that individuals consuming  $\text{C}_3$  plants have a much lower  $^{13}\text{C}/^{12}\text{C}$  ratio than individuals consuming  $\text{C}_4$  plants (Still, Berry, Collatz, & DeFries, 2003). The  $\text{C}_3$  photosynthetic pathway is the most common on earth and plants that use this pathway include cereal grains and fruit bearing trees. Tropical grasses, like millet, sorghum, and maize, on the other hand, follow a  $\text{C}_4$  photosynthetic pathway (Still et al., 2003). The  $\delta^{13}\text{C}_{\text{apatite}}$  values for individuals with exclusively  $\text{C}_4$  diets range between approximately  $-4.5\text{‰}$  and  $0.5\text{‰}$  while individuals with exclusively  $\text{C}_3$  diets demonstrate a  $\delta^{13}\text{C}_{\text{apatite}}$  range between  $-25.5\text{‰}$  and  $-10.5\text{‰}$ , based on fractionation from diet to apatite (Hedges, 2003; Katzenberg, 2008; Tykot, 2010). Values of  $\delta^{13}\text{C}_{\text{apatite}}$  between  $-10.5\text{‰}$  and  $-4.5\text{‰}$  are often interpreted to suggest a mixed diet including both  $\text{C}_3$  and  $\text{C}_4$  plants.

For oxygen, the pathway to higher or lower  $^{18}\text{O}/^{16}\text{O}$  ratios is related to precipitation and evaporation in water reservoirs. The most abundant oxygen isotope,  $^{16}\text{O}$ , evaporates more easily than the slightly heavier  $^{18}\text{O}$  while the opposite is true in precipitation. Therefore, a geographic map of oxygen isotopes can be used to predict the isotopic ratios of water sources. This map is called an isoscape and is commonly used in bioarchaeology and forensic anthropology to estimate region of residence for individuals based on their  $\delta^{18}\text{O}$  values with a margin of error of approximately  $\pm 0.5\text{‰}$  (Bartelink & Chesson, 2019; Chesson et al., 2017). Oxygen values can be assessed from bone bioapatite by analyzing either the carbonate ( $\text{CO}_3$ ) present in the crystal matrix or the phosphate ( $\text{PO}_4$ ) that forms one of the primary molecules of the apatite. Carbonate derived oxygen is much easier to access, and the process is less involved leading to fewer



processing errors, thus, it is the most commonly analyzed compound to assess  $\delta^{18}\text{O}$  from human skeletal remains (Bartelink & Chesson, 2019; Chesson et al., 2017). However, multiple studies have found that carbonate-derived  $\delta^{18}\text{O}$  values are less reliable than phosphate-derived isotopic values (Berg et al., 2022; Daux et al., 2008; Pestle, Crowley, et al., 2014), thus the reliability of  $\delta^{18}\text{O}$  values in the study of human skeletal remains is in question.

Previous research has also demonstrated that seasonal changes in diet or water source may affect isotopic results (Maggiano et al., 2019) and that remodeling patterns and changes in diet may also affect isotopic values between osteons in a skeletal element (Bell et al., 2001; Fahy et al., 2017). Understanding the patterns of remodeling across skeletal elements and the effects of these patterns on isotopic ratios therefore becomes an important factor in the application of these methods, both archaeologically and forensically. The destructive nature of the methodology at this time often precludes extensive analyses of intra-element variation, but scholars have explored intra-skeletal variation in isotopic analyses, forming the foundation for this research.

### ***Inter- and Intraskkeletal Variation in Isotopic Analyses***

Physiologically, skeletal elements are not perfectly homogenous due to differential remodeling patterns across the skeleton, or even within skeletal elements, as discussed above (Christen et al., 2014; Matsubayashi & Tayasu, 2019). However, the study of intraskkeletal variation has rarely been undertaken, and only a handful of researchers have explored this topic. Emphasis on the question of intraskkeletal variation is relatively recent (Berg et al., 2022; Olsen et al., 2014), and intra-element isotopic variation has only been examined in adults comparing endosteal, periosteal, and intracortical differences, not longitudinally along a skeletal element or antero-posterior on diaphyses (Bell et al., 2001; Fahy et al., 2017; Maggiano et al., 2019). This

is most likely due to the destructive nature of isotopic analysis, and some studies have tried to find alternatives to explore the question of intraskeletal variation. One example is exploring communities that share isotopic pools. Between individuals raised on monotonous diets, physiological differences can account for an average of 0.6‰ for  $\delta^{13}\text{C}$  and an average of 0.7‰ for  $\delta^{15}\text{N}$  from bone collagen (DeNiro & Schoeniger, 1983), negligible differences when considering that the average intra-laboratory standard deviation is approximately 0.15‰ for both  $\delta^{13}\text{C}$  and  $\delta^{15}\text{N}$  (Pestle, Crowley, et al., 2014). During bone remodeling, some researchers have suggested that the isotopes being incorporated potentially derive from segregated isotopic pools in the body, leading to isotopic ratio differences within individuals (Beaumont et al., 2018). Remodeling rates and seasonal changes to diet and water sources can also affect the incorporation of isotopes and lead to variation in isotopic data within an individual (Jørkov et al., 2009; Maggiano et al., 2019; Olsen et al., 2014).

Intra-element variation in isotopic values is poorly understood (Bell et al., 2001; Berg et al., 2022; Cooper, Lupo, Zena, Schmitt, & Richards, 2018; Fahy et al., 2017; Maggiano et al., 2019), but research has demonstrated differences in the isotopic ratio results correlating to the pattern of remodeling (Jørkov et al., 2009; Maggiano et al., 2019; Matsubayashi & Tayasu, 2019; Olsen et al., 2014), therefore the specific location of sampling even within a single skeletal element may affect the results of the analysis. These slight intraskeletal differences based on rates of remodeling have allowed for the reconstruction of life histories in isotopic analyses by taking samples from femora and ribs and comparing these to enamel and dentine to see changes in diet and residential history recorded in the isotopic data (Sealy et al., 1995). However, while skeletal elements selected for sampling are often presented in the literature, the specific location of this sampling along the skeletal element is rarely addressed.

Recent studies on intraskeletal variation on isotopic ratios in humans have demonstrated intraskeletal variation of 0.8‰ in  $\delta^{13}\text{C}_{\text{collagen}}$  (Berg et al., 2022; Olsen et al., 2014), approximately 1.5‰ in  $\delta^{15}\text{N}$  (Berg et al., 2022; Olsen et al., 2014), approximately 1.6‰  $\delta^{13}\text{C}_{\text{apatite}}$  (Berg et al., 2022), and fluctuations of between 0.9‰ and up to 4.8‰ for  $\delta^{18}\text{O}$  (Berg et al., 2022; Maggiano et al., 2019) within individuals. Intra-element range of variation observed within a single rib were -0.1‰ and 0.1‰ in  $\delta^{13}\text{C}$  and 0.0‰ to 0.5‰ in  $\delta^{15}\text{N}$ , although the authors do not specify the location of sampling (Olsen et al., 2014), and up to 2.5‰ in  $\delta^{18}\text{O}$  when comparing endosteal to intracortical isotopic values on the same humerus (Maggiano et al., 2019). These differences in isotopic composition have been ascribed to the rate of remodeling of each skeletal element and the greater turnover observed on the endosteal and periosteal surfaces (Birkhold et al., 2016; Maggiano et al., 2019). Often cited in the literature is an estimated 7-10 years for complete remodeling of large long bones and 5-7 years for ribs, but these are broad intervals that encapsulate differential remodeling, and that have already been empirically adjusted for some bone sampling locations (Jørkov et al., 2009; Olsen et al., 2014). For example, research by Jørkov et al. (2009) suggests that the petrous portion of the temporal bone may represent such slowed rates of bone apatite turnover that it provides isotopic results that correlate to the formation of the first molar, representing approximately late childhood, while the ribs approximate a five year turnover rate and the femur approximates a 10 to 20 year turnover rate. These findings are consistent with previous studies (Hedges et al., 2007; Manolagas, 2000) and have been corroborated by more recent examinations of bone turnover rates (Matsubayashi & Tayasu, 2019) but continue to be based on bulk sampling of the remains.

Differences between laboratories can also be a concern when interpreting isotopic data, with some interlaboratory differences appearing as large as 3‰ depending on the isotope and

component of origin (Pestle, Crowley, et al., 2014). As a result of intraskeletal differences and potential differences between mass spectrometers and laboratory preparation protocols, researchers have defined a real interpretative difference (RID), also called a minimum meaningful difference (MMD) for use in isotopic studies of bioapatite (Chesson et al., 2019). The MMD can be thought of as a threshold for interpretations, so that any isotopic differences between individuals or between studies should only be interpreted as significant if they surpass that threshold, and not significant if they remain below the threshold. The suggested MMD for enamel-derived apatite are 0.6‰ for  $\delta^{13}\text{C}$  and 1.6‰ for  $\delta^{18}\text{O}$  (Chesson et al., 2019) and closely approximate the values of intraskeletal variation for collagen derived  $\delta^{13}\text{C}$  (0.6‰) and  $\delta^{15}\text{N}$  (0.7‰) for individuals on monotonous diets (DeNiro & Schoeniger, 1983). Differences in the structure of bone lead to slightly increased MMD for bone derived apatite, with those values being established at 1.2‰ for  $\delta^{13}\text{C}$  and 3.1‰ for  $\delta^{18}\text{O}$  from carbonate (Pestle, Crowley, et al., 2014), the latter of which is concerning since interpreted differences in oxygen isotopes often fall below this threshold. This type of biogeochemical variation within skeletal elements has also been observed using vibrational spectrometry. Using a Fourier-Transform Infrared Spectrometer, Gonçalves et al. (2018) demonstrated a significant level of intraskeletal heterogeneity that potentially obscured inter-individual differences. As both isotopic and vibrational spectrometric data have demonstrated similar results, I compare the use of the non-destructive method of analysis to traditional destructive IRMS in this study.

### *Diagenesis*

Skeletal remains in certain burial contexts will undergo a process called diagenesis, which alters the chemical composition of bone and results in unreliable isotopic values. This

complex process involves both chemical and physical alterations that break down organic matter and exchange ions with the surrounding environment, thereby losing the isotopic values of the individual incorporated in life. Diagenesis affects the organic and mineral components of bone differently, and many factors affect diagenetic alteration including humidity, water flow, soil acidity, and the soil microbiome (Berna et al., 2004; Hedges, 2002; Keenan & Engel, 2017; Weiner, 2010a; Wright & Schwarcz, 1996). Microbial processes and acidic soils break down collagen in bone by destroying the bonds between the amino acids (Hedges, 2002; Keenan & Engel, 2017). This breakdown removes the nitrogen and carbon within collagen from the skeletal material, leaving behind altered collagen that does not reflect the tissue while the individual was living. Bioapatite, on the other hand, undergoes a process of dissolution and recrystallization in diagenetic alteration (Berna et al., 2004; Weiner, 2010a). The presence of carbonate in the apatite lattice makes bioapatite a more soluble mineral than non-biological hydroxyapatite. When water is present, either in the soil as humidity or flowing through the soil, it causes the apatite crystals to dissolve into constituent molecules (Berna et al., 2004; Keenan & Engel, 2017). These molecules readily re-crystallize, but into a non-biological hydroxyapatite with little to no carbonate inclusion and replace those removed carbonate molecules with phosphate and hydroxyl ions derived from the surrounding soil (Berna et al., 2004; Keenan & Engel, 2017). This new mineral precipitate is hardened and has a more organized crystalline structure than bioapatite. Importantly, while burial duration has sometimes been correlated with diagenesis, the extent of diagenesis is not directly correlated with time and instead relates to the environmental conditions (Hedges, 2002; Keenan & Engel, 2017). Due to these complications and the potential of misinterpretation of diagenetic altered skeletal remains, bioarchaeologists have used vibrational spectroscopic techniques to assess the extent of diagenetic alterations in skeletal

material they wish to analyze isotopically.

### **Vibrational Spectrometry in Biological Anthropology**

Vibrational spectrometry has been a mainstay of bioarchaeological investigations involving biogeochemical analyses but has mostly been relegated to the analysis and quantification of diagenesis. More recent studies have demonstrated the wide range of applications that vibrational spectrometry can have in biological anthropology. In forensic applications, researchers have demonstrated the ability for vibrational spectrometry to correlate to post-mortem interval (PMI) (Ortiz-Herrero et al., 2021; Woess et al., 2017). Using spectra collected from human skeletal remains of known PMI, researchers have tested vibrational spectrometry to approximate PMI in unknown individuals through either used Principal Component Analysis (PCA) or orthogonal Partial Least Squares regression (OPLS) with great success (Ortiz-Herrero et al., 2021; Woess et al., 2017). Separate of PMI, burial duration has also been studied using vibrational spectrometry, demonstrating a correlation between burial duration and a marked loss of collagenous content (McLaughlin & Lednev, 2011). Another recent application has been the estimation of age-at-death in skeletonized individuals, finding direct correlations between skeletal age and certain indices previously used solely in the study of diagenesis (Pedrosa et al., 2020). And of particular interest for this study, recent applications of vibrational spectrometry have demonstrated significant structural differences in apatite and collagen within single skeletal elements, forming the foundation for the current study (Gonçalves et al., 2018). This project focuses on one form of vibrational spectrometry called Raman spectrometry.

## *Raman Spectrometry*

Raman spectrometry is a molecular vibrational spectrometric technique that relies on the scattering of light by bonded atoms in an analytical sample (Keresztury, 2006; Pestle et al., 2015). Raman spectrometry uses energy in the visible and near-infrared spectral range, emitted from a low-powered laser, to excite the bonds of a molecule into higher virtual energy states, both vibrational and rotational, without affecting the structure of the material. As the bonds return to a lower energy state, they release this accumulated energy in the form of a photon. If the resulting energy state is equivalent to the original state, the released photon will be of the same energy as the incident light and thus the same wavelength/frequency (Figure 2). This is called Rayleigh scattering and accounts for most of the scattered light. However, Raman scattering occurs when the resulting energy state is different from the original state, either lower or higher. The frequency of the released photon is either lower than incoming light (Stokes scattering), the most common and more often analyzed scattered light, or is higher than incoming light (Anti-Stokes scattering) (Figure 2). The magnitude of the shifts (i.e., the difference in energy between the original state and the resulting state) are independent of the wavelength of incident light and are instead characteristic of the vibrational energy of the molecular bond, providing a molecular fingerprint (Keresztury, 2006). The incoming energy can cause vibrations of the molecule in different directions, either bending, stretching, or twisting, and each of these vibrations is called a mode, denoted by a  $\nu$  followed by a number. Each molecule has different potential vibrations and so may have a number of different modes, each appearing as a different frequency in the Raman spectrum. Reporting for Raman spectrometry usually presents the magnitude of the shift in wavenumbers ( $\text{cm}^{-1}$ ) rather than absolute wavelength.

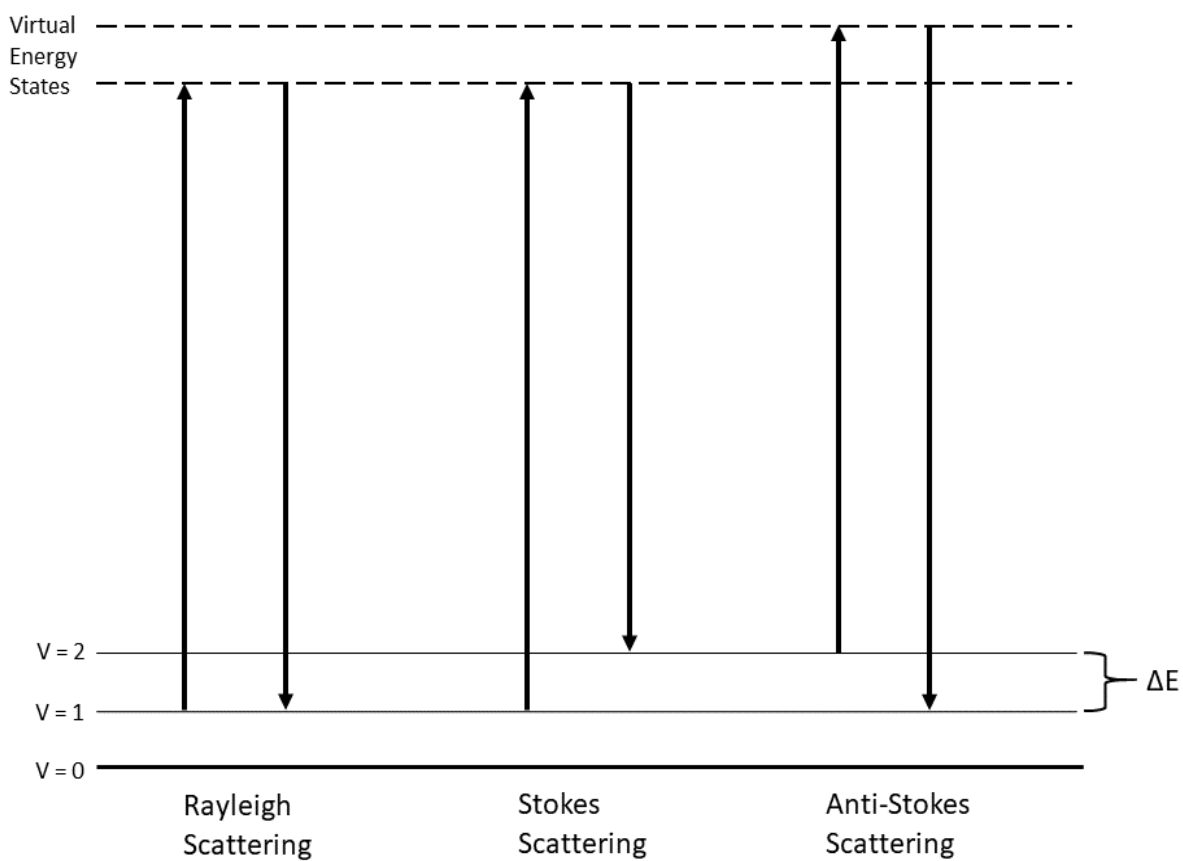


Figure 2. Energy diagram demonstrating the differences between Rayleigh, Stokes, and anti-Stokes scattering as the molecule goes to a higher virtual energy state and then returns to a real energy state.  $\Delta E$  is the energy difference between the states which translates to a difference in wavelength for the scattered photons.  $V$  values represent the “real energy states” to which the electrons return after excitation



The study of human bone using Raman spectrometry has existed for well over the past two and a half decades (Halcrow et al., 2014; Kimura-Suda et al., 2013; Morris & Mandair, 2011; Ortiz-Herrero et al., 2021; Smith & Rehman, 1994). However, in all studies, fluorescence has been a major complication with Raman scattering of untreated bone when compared to deproteinated bioapatite (Bertoluzza et al., 1997; Madden et al., 2018; Smith & Rehman, 1994). Fluorescence is the release of photons unrelated to the molecular structure of the material that can obscure the spectrometric signal, often completely obliterating any signal in the spectrum. Fluorescence in the Raman spectrometry of bone is not well understood, but many researchers believe it originates in organic molecules within the bone matrix that are unrelated to collagen, such as heme or soil derived organics (Barton, Ward, & Hennesly, 2018; Golcuk et al., 2006; Ortiz-Herrero et al., 2021; Shea & Morris, 2002). To deal with this problem, three approaches have been taken by researchers: the selection of excitation wavelength, the photobleaching of bone, and the chemical pre-treatment of bone using either H<sub>2</sub>O<sub>2</sub> or sodium hypochlorite. The last approach, that of chemically pre-treating the sample, appears to provide the most accurate results but negates one of the major advantages of Raman spectrometry, namely the non-destructive nature of the technique by removing organic matter like collagen from the bone (McLaughlin & Lednev, 2011; Ortiz-Herrero et al., 2021; Penel, Leroy, & Bres, 1998; Shea & Morris, 2002). Carefully choosing an excitation wavelength and algorithmically correcting for the minor fluorescence that occurs maintains the non-destructive advantage but may suffer from reduced signal intensity and resolution (France et al., 2014).

Three main excitation wavelengths have been used in the study of bone: 532nm, 785nm, and 1064nm (Madden et al., 2018; McLaughlin & Lednev, 2011; Ortiz-Herrero et al., 2021; Shea & Morris, 2002). Using the 532nm excitation wavelength results in excessive fluorescence from

the untreated bone and is discouraged in the analysis of skeletal material. However, there is a fine balance to be struck between the 785nm and 1064nm excitation wavelengths. Multiple studies have suggested that the 1064nm excitation wavelength significantly reduces fluorescence and should therefore be used in bone analysis (France et al., 2014; Halcrow et al., 2014; Madden et al., 2018; McLaughlin & Lednev, 2011; Pestle et al., 2015). However, in Raman spectrometry, the intensity, and therefore resolution due to limitations of detectors, is proportional to  $\nu^4$ , where  $\nu$  is the frequency of the incident light (Keresztury, 2006). This suggests that at 1064nm the intensity of the scattered light is approximately a third of that at 785nm. While a third of the intensity might not be a significant difference in some contexts, it should be a consideration for future advancements in the applications of this technique. For the reasons of resolution and intensity, this project uses a 785nm excitation wavelength. To reduce fluorescence, then, a process of photobleaching is applied to the bone, which minimizes molecular changes to the sample while maintaining the ability to use the shorter wavelength, 785nm, to conduct the analysis. The process involves the use of a 532nm or 785nm laser with a power output of 100mW to irradiate the sample for 30-40 minutes or increasing the power output and irradiating the sample for a shorter period of time, approximately 3 minutes (Golcuk et al., 2006; Ortiz-Herrero et al., 2021; Shea & Morris, 2002). This protocol reduces fluorescence by approximately 80% in a dry bone sample and does not appear to impact the resulting spectra since it preserves the chemical and structural properties of the sample (Shea & Morris, 2002).

Whichever non-chemical approach is selected to reduce fluorescence, Raman spectrometry is completely non-destructive, allowing for the preservation of material and the replication of studies while being highly portable and providing accuracy similar to benchtop instruments to analyze remains *in situ* with portable instruments (France et al., 2014; Halcrow et

al., 2014; Madden et al., 2018; Pestle et al., 2015). Thus, researchers have frequently explored approaches to the analysis of bone diagenesis using Raman spectrometry and have more recently expanded applications of this technology.

When analyzing bone in Raman spectra, a few bands at particular wavelengths are most significant to most analyses (Table 1; Figure 3). These can be broadly separated into organic matter modes and mineral modes. The organic matter modes include the vibrational modes of Proline, Hydroxyproline, and Phenylalanine denoting collagen (Morris & Mandair, 2011), vibrational modes specifically related to amide bonds in proteins (Khan et al., 2013; McLaughlin & Lednev, 2011; Morris & Mandair, 2011; Penel, Leroy, Rey, et al., 1998), and those modes indicative of bonds between nitrogen and hydrogen (McLaughlin & Lednev, 2011) and between carbon and hydrogen (Khan et al., 2013; Morris & Mandair, 2011; Penel, Leroy, Rey, et al., 1998). The vibrational modes related to the mineral component in bone have been the subject of greater study and include the main stretching mode ( $\nu_1$ ) for  $\text{PO}_4$  (Awonusi, Morris, & Tecklenburg, 2007; Khan et al., 2013; McLaughlin & Lednev, 2011; Morris & Mandair, 2011; Penel, Leroy, Rey, et al., 1998), the main vibrational mode ( $\nu_1$ ) for  $\text{HPO}_4$  (Khan et al., 2013; Penel, Leroy, Rey, et al., 1998), the antisymmetric stretching mode ( $\nu_3$ ) of  $\text{PO}_4$  (Awonusi et al., 2007; Khan et al., 2013), and the stretching modes ( $\nu_1$ ) for  $\text{CO}_3$  at A-type substitutions (Penel, Leroy, Rey, et al., 1998) and B-type substitutions (Awonusi et al., 2007; Khan et al., 2013; Penel, Leroy, Rey, et al., 1998).

### ***Isotope Ratio Infrared Spectrometry (IRIS)***

Vibrational spectrometry depends on the frequency of the resulting radiation being proportional to the bond between the atoms in a molecule. This dependency of the resulting

Table 1. Raman band positions and assignments most often encountered in analyses of skeletal remains.

| Peak Position (cm <sup>-1</sup> ) | Assignment                     | References   |
|-----------------------------------|--------------------------------|--|
| 855-921                           | Proline                        | Morris and Mandair (2011)  |
| 876                               | Hydroxyproline                 | Morris and Mandair (2011)  |
| 960                               | $\nu_1$ PO <sub>4</sub>        | Awonusi et al. (2007); Khan et al. (2013); McLaughlin and Lednev (2011); Morris and Mandair (2011); Penel, Leroy, Rey, et al. (1998) |
| 1002                              | Phenylalanine                  | Morris and Mandair (2011)  |
| 1003-1005                         | $\nu_1$ HPO <sub>4</sub>       | Khan et al. (2013); Penel, Leroy, Rey, et al. (1998)   |
| 1006-1055                         | $\nu_3$ PO <sub>4</sub>        | Awonusi et al. (2007); Khan et al. (2013)  |
| 1060-1070                         | B-type $\nu_1$ CO <sub>3</sub> | Awonusi et al. (2007); Khan et al. (2013); Penel, Leroy, Rey, et al. (1998)  |
| 1102-1107                         | A-Type $\nu_1$ CO <sub>3</sub> | (Penel, Leroy, Rey, et al., 1998)  |
| 1217-1358                         | Amide III                      | Khan et al. (2013); McLaughlin and Lednev (2011); Morris and Mandair (2011); Penel, Leroy, Rey, et al. (1998)                        |
| 1415-1500                         | $\delta$ NH                    | McLaughlin and Lednev (2011)   |
| 1447-1452                         | C-H Bending                    | Khan et al. (2013); Morris and Mandair (2011); Penel, Leroy, Rey, et al. (1998)  |
| 1595-1720                         | Amide I                        | Khan et al. (2013); McLaughlin and Lednev (2011); Morris and Mandair (2011); Penel, Leroy, Rey, et al. (1998)                        |

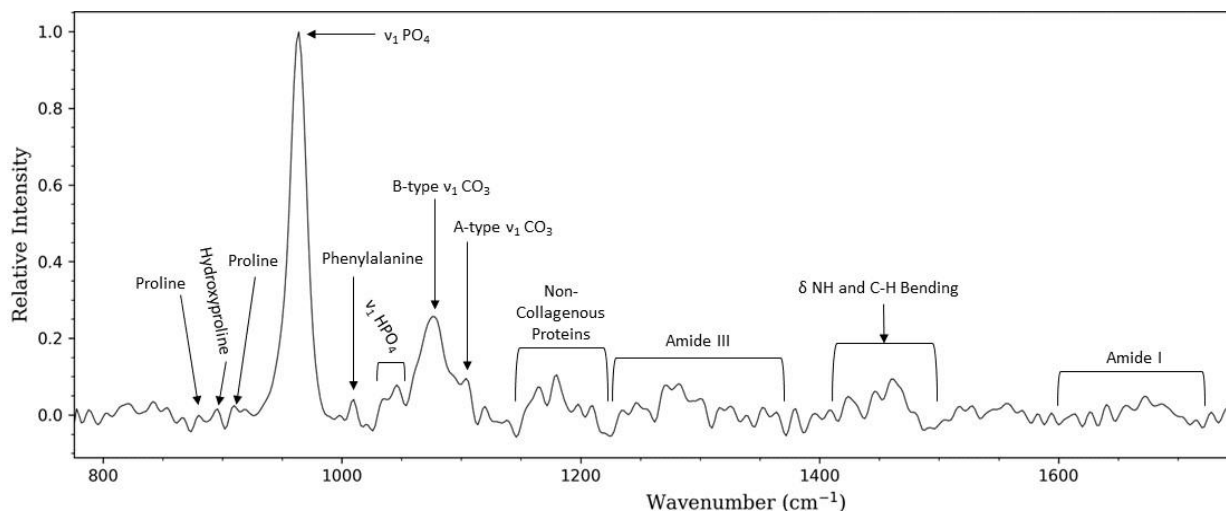


Figure 3. Sample Raman spectrum of unprocessed bone with complete baseline fluorescence removal. Vibrational modes and bands frequently encountered in bone samples are indicated.

frequency on the bond between atoms in vibrational spectrometry can be exploited to correlate spectrometric data with stable isotope ratio data. Following the physics of oscillating springs, the vibrational frequencies for absorption of energy and emission of energy for a given molecule will change. This means that as the mass of the atoms involved increases, the frequency of the energy absorbed and released decreases. This shifts the emitted wavelength resulting from different isotopes involved in a molecule and can thus be observed in the spectrum of a material as the peak intensity relates to the abundance of that corresponding molecule (Li et al., 2018). This application of Raman spectrometry has been supported in isotopic analyses of  $\delta^{13}\text{C}$  in  $\text{CO}_2$  gas (Li et al., 2018; Vitkin et al., 2020), its potential has been described for  $\delta^{13}\text{C}$  and  $\delta^{18}\text{O}$  analyses on mineral carbonates (McKay et al., 2013), and it has proven useful in the classification of organic matter using  $\delta^{13}\text{C}$  and  $\delta^{15}\text{N}$  values (Muhamadali et al., 2015), but has never been applied to human skeletal remains. The complexities of bone chemistry result in many “vibrational modes” from this slight change in isotopic composition of a molecule and a protocol for the use of this method in human skeletal remains is one of the goals of this study. The best approach to the creation of this protocol and predictive model, therefore, is to use dimensionality reduction methods to select the most well-correlated peaks to the traditional isotopic results found in bone, as described in the methods chapter of this work.

### **Summary**

In this chapter, I have explored the physical, biological, and chemical structure of bone and how an understanding of these structures can lead to less invasive data collection and more nuanced interpretations of isotopic data. From the microscopic to the macroscopic, I described the structures of bone and how these structures inform our understanding of bone remodeling. As

bone remodels, isotopes are incorporated into the tissues. This results in isotopic deposition that is not homogenous, especially as individuals may change diet, water source, or may move residence over relatively short periods of time. Biogeochemistry can help illuminate some of these changes, but these data must be interpreted through the lens of biomechanically mediated remodeling, as evidenced by the intraskeletal variation in isotopic ratios already demonstrated in the literature. Exploring intraskeletal variation in isotopic data can be problematic, as you will read in the following chapter. Therefore, a less destructive method may be available in the form of Raman spectrometry. While this technology is currently used in biological anthropology to assess diagenesis, explore patterns of burning, and even estimate postmortem interval, promising results may be found when collecting biogeochemical data using Isotope Ratio Infrared Spectrometry (IRIS). In the following chapter, I discuss the ethics of destructive analysis in biological anthropology and explain the need for a non-destructive method in the collection of isotopic data and in the exploration of intraskeletal and intra-element biogeochemical variation.

CHAPTER THREE  
A CRITICAL THEORY OF DESTRUCTIVE ANALYSES IN BIOLOGICAL  
ANTHROPOLOGY

In this chapter I discuss the ethics of destructive analyses, such as biogeochemical analyses as defined in Chapter Two, from a critical theory perspective. I present the concepts of biopower and necropower and coin a new term, necrodominance, that fits within these two realms, as foundational to an ethical treatment of human remains in biological anthropology.

Necrodominance represents the domination of deceased individuals and their descendants by the ideology of scientific supremacy and its arguments that scientific inquiry is for the benefit of society and can therefore exploit others in search of its goals. Necrodominance demonstrates that this argument of benefits to society is a fiction created to perpetuate scientific supremacy and continues to oppress marginalized communities. I present some solutions that have been suggested by various indigenous and non-indigenous scholars and argue that non-destructive analyses should be an additional tool to alleviate necrodominance when used in conjunction with cooperation/collaboration, informed consent for all steps in the analytical process, from research design and hypotheses to publication, and community control of the remains of their ancestors. Finally, I discuss how the current project fits within this framework and attempts to alleviate the problem of necrodominance through cooperation, collaboration, benefit sharing, and increasing the use of non-destructive analyses.

**Introduction**

In 1951, medical researchers at Johns Hopkins University obtained a sample of cells from a marginalized black woman undergoing treatment for cervical cancer. Those samples were

replicated *in vitro* by researchers at Johns Hopkins University, thus making Henrietta Lacks the source of the first immortal cell line in bioscience research (Skloot, 2010; Truog, Kesselheim, & Joffe, 2012). Her cell line, called HeLa, became extremely lucrative, both scientifically and financially, for any institution holding rights to replicate and use her biological sample in research and development, but Lacks herself died a poor woman without access to much-needed medical care (Skloot, 2010). These issues first came to light in 1976 (Rogers, 1976) but became more widely known for the general public after the publication of the book *The Immortal Life of Henrietta Lacks* in 2010 (Skloot, 2010). In response to protests of injustice and calls for posthumous compensation, physicians Truog et al. (2012) asserted that “the use of her residual clinical tissue, involving no additional risk or burden to her, does not demand any form of compensation.” Truog et al. (2012) claimed that intellectual effort rather than source material is the real creator of value for these cell lines, and therefore neither the patient nor their family should be compensated unless the procedure for removing said samples “imposes burdens over and above those required for indicated clinical care”. In a similar case brought before the California Supreme Court involving the replication of an immortal cell line from tissue removed without consent by UCLA scientists, the justices ruled that John Moore, the living plaintiff, did not have property rights over the cells that had been removed from his body, and that giving him those rights would “hinder research by restricting access to the necessary raw materials” (“Moore v. Regents of the University of California,” 1990). This case demonstrates that the courts and other institutions of authority support scientific dominance over *ex vivo* cells and tissues without regard to personal agency or bodily integrity.

These examples demonstrate the cultural and legal power that scientists have over biological material in the United States. The issue of social power in science has frequently been



discussed in both the medical and social sciences, and there is a long history of scientists disregarding the bodily rights of individuals in pursuit of scientific understanding (Highet, 2005; Tauber, 1999). The taking of biological samples is an action fraught with social problems like the decimation of bodily integrity, the general distrust of scientific conclusions from destructive analyses that cannot be replicated, questions over the ownership of the biological material, and the power relationships that are established between biological researchers and their test subjects (Campbell, 2003; Rabinow & Rose, 2006; Squires et al., 2019). Meaningful attempts to address some of the issues inherent to invasive biological sampling and data retention have been made by both anthropologists and bioscientists, but the solutions sometimes cannot completely address the social asymmetry intrinsic to such research (T. R. Turner, 2005, 2012; T. R. Turner et al., 2018). This is because the solutions frequently approach the problem using only professional ethical codes as their foundations for developing an ethical research design. A principalist approach, following a set of ethical principles that act as guidelines, is valid and valuable, providing significant improvements for unequal relationships and creating incentives for ethical behavior, but it may miss the broader implications of power asymmetry and the unintentionally biased foundations of professional ethical codes. For anthropology in particular, destructive analysis of biological material from individuals that have long since passed away presents a form of necropower (Mbembé, 2003), or exertion of control over the dead, that I here term necrodominance, since, as argued below, the mechanisms for the perpetuation of this necropower stem from those dominating the material, rather than the self-discipline described by biopower. I propose, therefore, that we step back and analyze the ethics of destructive analyses in biological anthropology with the lenses of biopower and critical theory, first understanding the dynamics of power and then evaluating solutions that address these root causes.

While the concepts of biopolitics (Foucault, 1984a; Pylypa, 1998), social capital (Bourdieu, 1990b), and agency theory (Campbell, 2003; Harper, 2010) are often used when discussing the living, these theoretical frameworks can also serve as the scaffolding upon which we examine the cultural and social relationships that are established through destructive analyses of biological material and the social and scientific life of that material after it has been removed from the individual or that individual has passed away. In this chapter, I also address some of the attempts at reconciliation between scientific goals and the problems of power dynamics inherent to the scientific inquiry of marginalized communities. Due to its history and aims, biological anthropology sits at the crux of the issues of power and marginalization for sampling and destructive analysis.

### **Biopower and Capital in Biological Sciences**

Biopower is defined by Michel Foucault as “what brought life and its mechanisms into the realm of explicit calculations and made knowledge-power an agent of transformation of human life” (Foucault, 1984b, p. 265). That is to say that biopower represents the non-judicial ways that human biology, and therefore sociality, have been administered and controlled. According to Pylypa (1998, p. 21), biopower “derives from its ability to function through ‘knowledge and desire’ — the production of scientific knowledge that results in a discourse of norms and normality, to which individuals desire to conform”. Thus, it works through self-discipline, self-regulation, and self-surveillance with an explicit and deliberate attempt by the oppressed to conform to the social norms. The relationship between external authority and the individual body is reversed, and, as Foucault explains, the rights of the individual are health, happiness, and life, but all are separate from the traditional right of sovereignty over one’s own

body. This separation of sovereignty places the body of the individual into a category that Agamben (1998) called a *homo sacer*, a middle ground in which the body is seen for its identity as a human but is not afforded the rights inherent to that identity. Those rights instead reside on figures of authority that exercise and benefit from biopower. Biopower is achieved through what Foucault calls disciplines, methods that allow authority to meticulously control the body and thus deploy constant subjugation (Foucault, 1984a). Discipline begins as active control and becomes internalized over time, transformed into the predominant mechanism through which biopower is asserted and maintained.

Foucault (1984a) describes the origin of discipline as explicitly different from slavery, service, or “vassalage,” but in the case of the sampling of biological material, regardless of for replicating cell lines or isotopic analysis, these forms of authority and power, as Foucault describes them, are evident. Slavery is described by Foucault as “based on a relation of appropriation of bodies” (Foucault, 1984a, p. 181), but nothing is more invasive and appropriative of the body than the deliberate removal of one or more portions of said body for the value of those in power, a practice that predominantly affects marginalized communities. Service, Foucault explains, “was a constant, total, massive, nonanalytical, unlimited relation of domination, established in the form of the individual will of the master” (Foucault, 1984a, p. 181). The relationship of service was perpetuated through a lack of recourse for the servant to change the behavior of the master. The example of the John Moore case at the beginning of this chapter demonstrates that in the society of the United States, the individuals converted into objects of study have little recourse, and whatever material is removed from their bodies no longer has rights afforded to the body of the individual and is therefore subject to the scientist’s “caprice” (Foucault, 1984a, p. 181). In vassalage, we see a “highly coded, but distant relation of

submission, which bore less on the operations of the body than on the products of labor and the ritual marks of allegiance” (Foucault, 1984a, p. 181). But here again we see a form of vassalage in the biological sciences where the “distant relation of submission” to the authority of the scientist controls the “products” of that body outside of the operations of the body itself. That is, that the authority of the scientist is not concerned with what the individual does with their body, but that the biological material taken is a product rightfully owned by the scientist, separate from said body and any rights therein granted. Reactions to the power of the bioscientist, in the form of denial of access, hostility, and litigation, are frequent and there is a notable lack of self-discipline and self-surveillance in the way that Foucault describes for biopower (Arbour & Cook, 2006; Colwell, 2018; Reardon & TallBear, 2012; Young, 2011).

So, while the power asymmetry between scientists and their objects of study is clearly a manifestation of biopower, discipline as defined by Foucault is not the mechanism that perpetuates this relationship. Instead, I propose that these structures of power are perpetuated through a *habitus*, conferring the scientist with social capital at the expense of the marginalized (Bourdieu, 1990a), and which must frequently be understood as a perpetuation of white supremacy in anthropological discourse (Blakey, 2020; DiGangi & Bethard, 2021). *Habitus* are “principles which generate and organize practices and representations” that are “[o]bjectively 'regulated' and 'regular' without being in any way the product of obedience to rules” (Bourdieu, 1990a, p. 53). The title of “scientist” as a profession in European and Euro-American society confers an authority that is not codified in law but is instead afforded cultural value for its own sake. This additional value is a form of social capital that increases the relational and symbolic power of the scientist in the social space (Bourdieu, 1989, p. 17). As in the example of Moore v. Regents of the University of California, social capital is extended through the courts to become

political capital and codified laws further extend the social capital of the scientists by providing them with additional power and so on in a perpetual cycle. An example of this additional political capital is in the original implementation of the Native American Graves Protection and Repatriation Act (NAGPRA) in which scientists, not tribal affiliates, made up at least half of the members of the committee that made decisions about ancestors of Native American communities (25 U.S.C. 3006(b)).

This is not to say that science should not be prioritized in our culture as a primary method of seeking empirical knowledge, but that the scientist as an ideal, not as the fallible human, is provided with social capital that is used in bioscience to pursue scientific goals without regard for the objects of study that, in this case, are human and rational subjects in themselves. While benefits may arise from biological research, those less likely to be granted access to scientifically generated knowledge are also those most likely to be the study subjects (Andrews & Nelkin, 1998; Hight, 2005; Rabinow & Rose, 2006). Rabinow and Rose (2006, p. 215) address the consequences of the expression of biopower in genomics research by demonstrating that molecular data can reshape the biopolitics of health and reconfigure “the relations of knowledge, power, and expertise” thus perpetuating the social capital of the scientist and increasing their power. Through genomics, elements of authority are finding new data to impose their biopower and the individual thus becomes a number to control through additional data (Rabinow & Rose, 2006, p. 213). The same can be said for isotopic analyses that requires expert knowledge to access and interpret, a knowledge that is often not accessible to the communities from whom the biological material originates.

The objectification of the individual as a biological material of study is in itself a mechanism of perpetuating biopower as it further removes social capital from the subject by

converting them from actors to objects. The discourse of biological material, even as it is defined in this essay, removes the humanity from the material. It is material, an object, with its former position as subject of its own inquiry and its former and existing relationships with descendants and related communities extinguished through our own use of language (Foucault, 1984b, p. 265). In European and Euro-American thought, this distinction also stems from the prominence of Cartesian dualism as it defines the body as a non-thinking object and the mind as non-physical thing (Descartes, 1984). This dualism, although frequently questioned after each of the mechanistic and ontological turns, has dominated European epistemology, and therefore positivist science, since the enlightenment, causing an objectification of the body as a separate entity from the soul/mind in bioscience (Robinson, 2017). In our current discourse within biological anthropology, isotopic samples are just that, objects and not people. Bone samples are reduced to their chemical composition or their observable traits and soft tissue and cells are separated and disconnected from the thinking individual. The question is then whether the discourse is shaped by the lack of sentience of the material as separated from the individual or if, in death, the individual becomes an object in Eurocentric scientific ontology.

### **Necropolitics and the Meaning of the Dead**

Biological anthropologists often interact with the remains of the dead rather than the bodies of the living. Although the broader concept of biopower works well in most bioscience contexts, the focus on the dead for biological anthropologists requires a corollary to this idea through the concept of *necropower*. Mbembé first presented the concept of *necropower* as the subjugation of life through the control of death and control of behavior through the terror of dying, physically and culturally (Mbembé, 2003). Through this form of power, authority has “the

capacity to define who matters and who does not, who is *disposable* and who is not” (Mbembé, 2003, p. 27). By using destructive analyses on biological material, the scientist is making a statement about which kind of body is disposable, thereby making a political statement, whether intentionally or unintentionally. In addition to direct bodily control, the concept of necropower has been extended to include the control over memories of the dead and the use of their bodies as tools for maintaining discipline and perpetuating power (Lesley, 2015; Perera, 2006). Thus, the remains of the dead represent symbols that can be variably interpreted and have powerful significance for currently living individuals through community identities regardless of the body’s personal identity.

Often the treatment of the remains, namely the burial, is more important for the relationship between the living and the dead than the symbolic meaning any individual person may embody (Verdery, 1999). The harmonious coexistence of the living and the ancestors is “about more than just getting along: it is part of an entire cosmology, part of maintaining order in the universe” and “[a]ll human groups have ideas and practices concerning what constitutes a ‘good death,’ how dead people should be treated, and what will happen if they are not properly cared for” (Verdery, 1999, p. 42). Although Verdery discusses historical Eastern Europe in particular, she is presenting a near universal aspect of human cultural life that transects time and space (see Isbell, 1997 for an ancient Andean example). Proper burial in many cultures often requires a posthumous bodily integrity (Young, 2011, p. 24), something that cannot be accomplished after the sampling of biological material and/or destructive analyses and so a conflict of values arises.

However, in the biomedical perspective, founded on Cartesian dualism and capitalism’s property rights, the body is made up of parts that are the property of the person rather than

representing an integral whole body (Campbell, 2003, p. 36). The discourse of biomedical research creates a self that is *dis-embodied*, creating a paradigm in which relations are the meeting of minds, and as such the body is incidental and external (Campbell, 2003, p. 40). In this paradigm, once the mind has passed away (brain death) the body becomes objectified and commodified as a mechanistic series of parts that no longer represent an individual (Sharp, 2000, p. 304). In organ donation, we see this dichotomy between the biomedical professionals and the living kin of the donor. The biomedical professionals take the perspective presented above, but the family members see those organs as embodying the individual that has passed away and may sometimes even create a “fictive kinship” with the recipients of the donated organs (Sharp, 2000, p. 304). Consequently, the donor lives on in the minds of the kin and their organs and tissues become a proxy for that person.

Although some philosophers and ethicists may argue that unethical behavior can harm someone after their death (Kreissl Lonfat et al., 2015; Levenbook, 1984), giving an important perspective especially in cases of “cultural harm” (Tsosie, 2007), this premise is not necessary to see how necropower and the use of the dead for personal or professional gain can harm those who are still living. As Verdery states, bodies have an “ineluctable self-referentiality as symbols: because all people have bodies, any manipulation of a corpse directly enables one’s identification with it through one’s own body” (Verdery, 1999, p. 32). Yet, the symbolic meaning of remains can shift depending on the positionality of the observer (Verdery, 1999, p. 28), and since they cannot speak for themselves, remains are imparted with meaning by interested parties (stakeholders). Through scientific discourse, the biological material gains significant value apart from its symbolic meaning as a “former” person. Within biological anthropology, the protection of the biological material, even in the proposal of destructive analyses, is paramount, thus, the



material transcends to the secularly sacred (Errickson et al., 2017; Kreissl Lonfat et al., 2015; Mays et al., 2013).

Authority always has a sacred component (Verdery, 1999, p. 37) and anthropology as a discipline exerting authority is no exception. From the purely “scientific” perspective, the material, divorced from its former humanity and the living people that claim a relationship, is a sacred object of “knowledge” and must therefore be protected from those who want to remove it from those who seek knowledge (Arnold, 2014; Parra, Anstett, Perich, & Buikstra, 2020). But the sacredness of that material outside of scientific, secular values becomes relegated to the “other,” the non-scientist who, according to the scientist, may have no knowledge of the “true” value of the material. And thus, the accepted meaning of the object in the social space, as imagined by the scientist, is constructed and imposed on to the remains, through a form of necrodominance, in spite of the wishes of those individuals who may have a bodily, emotional, or spiritual attachment to the remains.

### **The Agency of Biological Material**

Actor-Network Theory (ANT) opposes the idea that the meaning of the biological material is not inherent, and argues that all things, animate or inanimate, have agency. Bruno Latour, one of the foundational figures of ANT, suggests that objects have agency, and are therefore actors, because they “do things”, not voluntarily but still meaningfully, such that they shape the perceptions and behaviors of other actors (Latour, 2005, pp. 70-71). For example in the case of human remains in the presence of the general public, there is a visceral reaction, shaped by cultural context, but still wholly dependent on the presence of the body (Harper, 2010). Karen Barad (2003), pushes this idea further through the development of a discursive interaction

between the non-human and the human, collapsing the differences between these seemingly disparate categories that are created by our materialist perspective. What she means by this collapse is that the human and non-human actors affect each other through interaction and observation and are therefore both agents indistinguishable by their agency alone. While both Barad (2003) and Latour (2005) lament the emphasis on language in removing the agency of artifacts, they perpetuate this linguistic emphasis in their explanations for why objects are considered actors (Latour, 2005, p. 71). While biological anthropologists often claim that the “samples provide” some data, the reality is that scientists have extracted those data and have then interpreted them with their own theoretical framework of choice and from their own biases and expectations. Thus, biological material has actions done to it and is only collected, and thereby created as a sample, by the scientist with all of their expectations and purpose.

Biological material is not an actor as described in ANT, but to the scientist, it is often an object of study upon which actions are taken. Illies and Meijers (2009) provide a conceptual framework of ANT called the Action Scheme, that more closely resembles the relationship between actor and “artefact” in biological anthropology. The action scheme is the set of possible actions that can be ranked by “attractiveness” to the actor (Illies & Meijers, 2009, p. 428). The scheme is constructed from social, physical, and intentional frameworks within which an artefact can play a role depending on the perceptions and behaviors of the actor and how the artefact is constructed in the mind of said actor (Illies & Meijers, 2009, p. 430). For the scientist, biological material is likely to be found in the social framework such that the object affects the language used to describe and refer to the object and ownership of the material functions as symbolic status for the researcher. Through the acquisition of the biological material, inherently a creative endeavor, the scientist constructs a “sample” that becomes a part of the social framework that

affects the possible choices within the action scheme of the scientist, thus adding to the “attractiveness” of some of the possible choices. This action scheme approach can be a meaningful tool when approaching solutions to the ethical dilemmas of biological anthropology, but it does not imbue the material with inherent agency and, in fact, can explain the “agency” (more precisely pseudo-agency) of the material described by ANT. However, the material object still has no inherent agency or will-to-action. The object may shape the decision scheme, but it is continually dominated by the scientist through its creation and destruction.

### **Defining Necrodominance**

Due to the inability of the material object to act and create a self-discipline or be controlled through non-direct actions, I propose the term necrodominance to encompass the actions taken by scientists in the collection and analyses of biological material without regard for the meaning that the body may have to actors with less social capital. Biological material, as opposed to recognizable bodies or their proxies, has no inherent agency or meaning aside from that which is ascribed to them by stakeholders. Although this separation of body and sample is arbitrary and dependent on the perspective of the observer, it is frequently the perspective of the scientist when dealing with partial skeletal remains. Necrodominance is a dominance of the biological object perpetuated by any actor with power, whether juridical, social, cultural, or economic. Since the material has no inherent capital outside of the symbolic capital that it provides to interested parties, capital that shifts with the positionality of the individual, the object is constantly dominated by said parties. So, who has the right to material dominance over human remains and how should we treat data collected from those materials?

### *To Whom Belong the Data*

The question of who owns these biological materials and the resulting data collected from them parallels the epistemological questions of who owns any collected data and who has the authority, imparted by social capital, to interpret them. The answers to these questions rest on the symbolic power of the stakeholders. The social capital of the scientist, a privileged position relative to the subjects of study, provides them with the authority to define the identity of the material and the property rights for the material while simultaneously denying access to collected data to anyone outside of the scientific social space. From the perspective of the bioscientist, as per the mechanistic view of the body, the tissue is the property of an individual as long as that tissue can be identified as being a part of that individual while living (M. J. Allen, Powers, Gronowski, & Gronowski, 2010, p. 1676). If the biological material is anonymized, however, the material no longer is subject to legal protections for “human subject research” (M. J. Allen et al., 2010, p. 1677). According to the courts in the U.S., when tissue is harvested postmortem, there is no set protection for “human subject research,” and instead there is either a minimal property right or potentially no property interest for the living kin (M. J. Allen et al., 2010, pp. 1680-1681). This demonstrates the social capital of the bioscientists and the power of the courts to rule in favor of the scientist at the expense of the descendants. But what happens when direct descendancy, as defined by U.S. law and culture, cannot be established?

There is no law that protects this situation directly. One example in the U.S. is NAGPRA, which presents one possibility for such protections of ancient remains and their associated material culture. The law is written too broadly to specifically define what it means to prove a descendancy. To address this problem, Kaufmann and Rühli (2010) suggest the stakeholder

approach to such research. While their work specifically addresses mummy research, their methods and conclusions are generally applicable to biological anthropology. They identify five stakeholder categories: the ancient culture, researchers, tourism and museums, civil society, and cultural descendants. Necrodominance over biological sampling removes the first stakeholder, the ancient culture, as a subject of interest due to that culture's inability to assert dominance over their own remains, leaving four main stakeholders in the discussion. Of these four, the group that generally has the least amount of social capital are the cultural descendants and, therefore, any applicable ethical framework must take this disparity into consideration.

If we assert that the biological material is part of the individual, then it must be that data collected from these individuals, especially data that could be identifying such as DNA or isotopic analysis, must also belong to them. Privacy of personal data is a major conversation in modern U.S. politics, but this can also be a concern for ancient remains. Since no consent can be acquired from the remains, the concerns of all the stakeholders become primary. The institutional stakeholders (i.e., researchers, museums, and civil society) have little incentive to maintain data privacy since the sharing of data and publications is a major component of research, although recent ethical guidelines have made such privacy a requirement of access for many skeletal collections. However, as Kaufmann and Rühli (2010) state “[n]egative research results may act as prejudgements or prejudice against present-day descendants,” suggesting that descendants have a greater stake in the representation of their ancestors (610).

In medical research, personally identifying information is protected, but this can be difficult in genetics and biogeochemical research. While not all biological data can be personally identifying, many of the arguments for the collection of these data are based on the possibility of further understanding of life history by adding contextual information. As such, it has great

potential to be personally identifying. Thus, like the proverbial "big brother," the scientist knows more about you and your ancestors than yourself. In addition, Rebecca Tsosie (2007) explains that in U.S. constitutional law, often the protection of privacy is the only vehicle through which bodily integrity can be maintained through a reversal of the mechanistic perspective and a return to an embodiment perspective (399). Tsosie explains that "property" consists of a bundle of rights to the possession of the body while privacy "focuses on the right to include some individuals by joining with them in close personal relationships" that can only be constructed as personal by the individual. By maintaining control over the remains and preventing cultural descendants from accessing these data and their possible interpretations, the creation of a cultural story for the ancestors is left entirely up to those with greater social capital to perpetuate their necrodominance over the material.

### **Solutions**

So far, I have discussed the philosophical and theoretical implications of destructive biological sampling and the ethical implications of these perspectives. The purpose of this chapter is to find solutions that address these implications and may be employed in this and future research with improved ethical and philosophical grounding. First, we must acknowledge that the assumption that the analyses are necessary in all cases is flawed and stems from the perception of scientific supremacy. True collaboration with stakeholders must ultimately leave the decision of proceeding with any potential analyses to said stakeholders, with priority given to those stakeholders who have been historically marginalized. I am also not suggesting the complete rejection of all biological sampling or destructive analyses, clearly this project depends on our ability to sample the skeletal remains of individuals. Destructive biological analysis has

been an important tool for many of the advances we have in both the natural and social sciences. More recently, scholars have acknowledged the ethical challenges and have proposed various solutions to achieve a balance of acknowledging human rights while still achieving scientific goals. Most proposed solutions derive their guidelines from the Belmont Report in biological anthropology (T. R. Turner et al., 2018), and involve data sharing, benefit sharing, and non-destructive analyses. Some of the other proposed solutions take a broader approach and attempt to minimize the power asymmetries between marginalized communities and the researcher through dynamic informed consent, full collaboration with descendant communities, and indigenous control over the biological material.

Data sharing is based on the proposal that all data collected from individuals should belong to those individuals or their descendants. With that as the ideological foundation, all data collected, even if curated by the anthropologists, should be available to all members of the community and only be shared with individuals outside of that community with the consent of the community from whom these data derive (Arbour & Cook, 2006; T. R. Turner et al., 2018). However, this latter process to protect private data is not always followed by institutions charged with its conservation. For instance, a recent Freedom of Information Act (FOIA) request for a NAGPRA related case from an unknown individual repatriated by Indiana University led to the release of additional sensitive information on the location of Native remains, details of the new burial location, sites of cultural significance, and even sensitive ethnographic information that have now placed the sites at risk of looting and have risked the privacy of the descendant community (S. Ayers-Rigsby, personal communication, 2019; Lyons et al., 2019). While openly sharing data may seem beneficial, access that is too open can cause further harm.

One approach that can include many of the same benefits as data sharing but goes a step

further is benefit sharing. Often researchers take samples from the community and publish their work in academic journals without ever returning to the community to share their findings, forming an exploitative relationship rather than communicative one (Annas, 2006, p. 543; Riding In, 1992). Scholars have proposed that benefit sharing, in the form of sharing your acquired knowledge or providing accessible literature, demonstrates respect for the indigenous communities and can foster a more meaningful, collaborative, and long-lasting relationship between the researchers and the other stakeholders (Arbour & Cook, 2006; Riding In, 1992).

Kaufmann and Rühli (2010), similarly argue from a perspective of respect, but in this case, respect to the remains that are the subject of study. They assert that destructive analyses demonstrate a lack of respect of the individual regardless of their living status since “the more invasive a technology is the more it harms the concept of wholeness” (Kaufmann & Rühli, 2010, p. 611). Thus, they propose that non-invasive or non-destructive analyses be the primary form of investigation. However, Kaufmann and Rühli (2010) also note the problems of rigor with non-destructive analyses and the inability to access certain data without the destruction of a sample (e.g., DNA, biochemistry). Additionally, the reduced scientific prestige of non-invasive analyses also reduces the relative “attractiveness” of these behaviors within the action scheme, thus the actors have lesser social incentive to perform them. If the choice is made to collect non-invasive data, however, we still return to the position of the authoritative scientists collecting these biological data, even if through more respectful means. Without the addition of dynamic consent and benefit sharing, the non-destructive approach can still be exploited through the disparities in capital and lead to the silencing of opposing stakeholder voices.

The sharing of access to data and increased collaboration between researchers and the community create a collaborative anthropology, improving the interpretation of these data by



allowing a variety of perspectives to shape the discourse (T. R. Turner et al., 2018, p. 948). Dynamic informed consent is another vital part in this process of rectifying power imbalances. This approach seeks to foster “a long-term partnership” between communities and researchers by “promoting participant-centered approaches to research” and a revocable informed consent that is based on continuous communication (T. R. Turner et al., 2018). In this way, the power to accept or deny research lies in the community of origin rather than in an institution, thereby narrowing, but not eliminating, the divide of power between researcher and subject (T. R. Turner et al., 2018, p. 947). Similarly, but more radically, full collaboration with descendant communities appears to be an increasingly applicable approach. This entails the consultation with descendant communities beginning at the formation of research questions and continuing throughout the process in deciding methodologies and interpreting the results (Claw et al., 2017). While this process is ideal in all cases, difficulties lie in who speaks for the community at large. Political and internal conflicts in all communities can complicate the matter, but efforts must be made to gain some consensus, whether through community wide meetings or meetings with community selected representatives (Claw et al., 2017). This goes beyond consultation as defined by legal statutes in the U.S. and involves communication with the community throughout the entire research process.

Reardon and TallBear (2012) as well as Arbour and Cook (2006) present one of the more radical and promising approaches to alleviating the power disparities in biological research, namely the indigenous control of the biological material. In this model, biological material is maintained and housed by indigenous communities and can only be accessed through their permission for a single project. Arbour and Cook (2006) developed a concept that they called “DNA on loan,” in which the researcher only has temporary access to the material required for

their research, they act as stewards of the remains rather than as owners, and that material is then returned to the community who holds continuous ownership. Only the project originally proposed is permitted, and any secondary project must follow the procedures for approval. Even anonymized samples are maintained as the property of the community. According to Reardon and TallBear (2012), the “[DNA on loan] model encourages researchers to maintain regular communication and ongoing relationships with communities if they want to make use of samples as new questions and technologies of investigation arise” with the expectation of benefit sharing (S243). Another approach to indigenous control of sample is used by the Alaska Area Specimen Bank. To access these samples, research plans must be presented to the community whose samples they want to access, and the community must issue written consent (Reardon & TallBear, 2012, p. S243). This written consent is then submitted with the research design for additional approval by the Indian Health Services Institutional Review Board and the Alaska Native Tribal Health Consortium (Reardon & TallBear, 2012, p. S243). While this may seem like additional burden to some, these processes have allowed marginalized communities to maintain control over their biological samples while still allowing research to progress. By institutionalizing the beneficial actions, the relative “attractiveness” is reduced for projects that do not include them and increased for projects that include them, thus leading to deliberate action toward the more attractive options in the scheme. These models have yet to be implemented for the remains of the deceased, but further communication, stronger relationships between researchers and descendant communities, and options for less invasive methods must be the first steps in the process.

### *Solutions as Applied to this Project*

While the primary goal for this project is the development of non-destructive methods that can be selected in cases where the stakeholders would prefer non-invasive techniques, considerations of the wishes of the community were also at the forefront of the research design. The community of Patakfalva initiated contact with archaeological investigators to begin work at the site of Papdomb (Patakfalva-Papdomb throughout this thesis) (Zejdlik et al., 2020). Their desires to understand the site and the history of their community are what drives the project forward. For the region, local community and historical ethnicity are also highly valued due to the conflicts between Szekély and no-Szekély individuals throughout Transylvanian history. As such, it was important to the community and the archaeologists involved that the scientific directory of the project be part of the community, as is Zsolt Nyárádi, director of the Haáz Rezső Museum. The community and Nyárádi have given explicit permission for the isotopic analyses conducted for this and other biogeochemical studies at the site and it is the ultimate goal of this project to return skeletal remains that went unused for this project to the museum for curation unless explicitly asked not to do so. Thus, this project, although not including DNA analysis, is taking the “DNA on loan” approach such that any additional project proposed using these remains or the data collected from them must first request permission from Zsolt Nyárádi as a representative for the community of Patakfalva. To provide value for the community, a presentation of the results of this study will be planned for the summer of 2023.

For the remains in the University of Tennessee Skeletal Collection, no destructive or invasive analyses were conducted, thereby preserving the integrity of the remains of donors. To protect their privacy, all data have been anonymized and are only presented with project specific

donor identification. All analyses using individuals in the University of Tennessee Collection must seek permission from the director and undergo a panel review to assess the ethics and feasibility of the project while ensuring that donors' wishes are followed, especially if the project involves any invasive analytical technique. This project in particular ensured that no invasive analyses were conducted and that the wishes of the donors were followed.

In addition to these considerations, an important potential impact of this project is increasing the accessibility of isotopic analyses to underfunded institutions, especially those in the country of the site being investigated. By reducing the engineering and materials cost to collect isotopic data, the community stakeholders can increase their own agency and reduce their dependence on foreign scientists as they wish. While the instruments themselves can be relatively expensive for underfunded institutions, they cost less than the initial requirements for an isotope preparation laboratory and do not require the engineering of a new lab space, expensive consumables, shipping and extraditing of samples, or time-consuming processing. The hope is that this project will put the power of biogeochemical analyses in the hands of archaeological experts around the world that may previously have been unable to use these data for their own archaeological investigations.

### **Summary**

Biopower, as presented by Foucault, permeates bioscience research and can predominantly affect the ethical considerations of fields that focus on marginalized communities such as biological anthropology. In particular, destructive analysis of biological material from individuals that have passed away presents a form of necropower that I have termed necrodominance. But the traditional mechanisms for the perpetuation of this form of power are

not present with the inanimate object since it cannot practice self-discipline. Without agency, the biological material is an object that has actions imposed upon it and is dominated rather than it shaping the way researchers think about the individuals being studied. Who prevails in their dominance over the material is dependent on their level of capital, social, economic, and juridical, with scientists often prevailing due to their increased social capital over marginalized communities. Solutions to these power asymmetries have been proposed using codes of professional ethics to address the perceived problems. In this work, I have instead reviewed the philosophical implications of destructive analyses in biological anthropology and have examined the various ethical approaches through this lens.

The two main approaches to reduce the power asymmetries as presented in this work are dynamic informed consent and benefit sharing. Non-destructive analyses are an additional tool that can improve the relationship between the researcher and the biological material but improving the relationships between researchers and the community require the removal of exploitative relationship and the recognition that the disparities in social capital must constantly be addressed for truly informed consent. Lastly, indigenous control over biological material can provide a model going forward that will allow researchers to demonstrate their commitment to reducing power disparities and improving the relationship between researchers and communities to further create collaborative research. By implementing these three ethical models to research design and result dissemination, the implications of dominance can be reduced, and better collaborative relationships can be formed between researchers and stakeholder communities. As presented, this project seeks to implement many of the proposed solutions and provides a path by which local stakeholders can increase their agency over the remains and their biogeochemical analyses. In the following chapter, Chapter Three, I present the methods implemented in this

study that attempt to improve the accessibility of non-destructive analysis and the wider application of this tool to answer questions that may be of interest to both researchers and descendant communities.

## CHAPTER FOUR

### INDIVIDUALS ANALYZED AND METHODS

The individuals analyzed for this project originate from two main populations: individuals disinterred from the Patakfalva-Papdomb site in Transylvania and donors to the University of Tennessee Skeletal Collection. Isotopic ratio data of  $\delta^{13}\text{C}_{\text{vpdb}}$  and  $\delta^{18}\text{O}_{\text{vpdb}}$  from apatite were collected from the Patakfalva-Papdomb individuals using a Gas Bench Isotope Ratio Mass Spectrometer (IRMS) and Raman spectrometric data were collected using a dispersive Raman Spectrometer with an excitation wavelength of 785nm. Data from the contemporary donors to the University of Tennessee Skeletal collection were collected using only the dispersive Raman Spectrometer. Hypothesis one, on the use of Isotope Ratio Infrared Spectrometry (IRIS) as a proxy for IRMS values was tested using the IRMS data and Raman spectra collected from the Patakfalva-Papdomb individuals. Hypothesis two, on the effects of diagenesis on IRIS and IRMS derived values was examined using the indices of diagenesis calculated from Raman spectra of the Patakfalva-Papdomb individuals and the donors to the University of Tennessee skeletal collection. Hypothesis three, on the exploration of intra-element variation and the potential for biogeochemical reassociation of skeletal remains, was tested using the IRMS and IRIS derived isotopic values for the Patakfalva-Papdomb individuals, the IRIS derived isotopic values for the donors to the University of Tennessee Skeletal Collection, and the Raman spectra collected for individuals in both collections. All data processing and statistical analyses in hypothesis testing were completed using the Python (Python Software Foundation, 3.8.12) programming language and statistical packages found in the Anaconda software distribution for Python (Anaconda Software Distribution, 4.10.3). All code is available for

review on GitHub (<https://github.com/armandoanzellini/ANDSIA>).

### **Individuals Analyzed**

The individuals analyzed for this project originate from two separate populations. The first is a population from the Székelyföld region of Transylvania within the borders of modern Romania. The individuals were recovered from a churchyard cemetery dating to between 1100 and 1804 B.C.E. near the town of Patakfalva (Văleni) following requests by the local community for the excavation and analysis of the remains. The second population is from the University of Tennessee Skeletal Collection. The contemporary individuals in this collection have donated their remains since 1981 for the study of decomposition and further studies on their skeletonized remains, helping to advance forensic anthropology. Subsets of these collections of individuals were selected and permission for their analyses was requested from the appropriate sources, the Haáz Rezső Museum as representative of the community of Patakfalva for the individuals recovered from the site of Patakfalva-Papdomb and the director of the Forensic Anthropology Center for the donors to the University of Tennessee Skeletal Collection.

#### ***The Székelyfold and the Site of Patakfalva-Papdomb***

The Székelyfold is a region in modern day Romania located within the Carpathian Basin (Figure 4). This region has been inhabited by Hungarian-speaking peoples, self-identified as the Székely, since sometime between the fifth and ninth centuries C.E. (Brandstätter et al., 2007; Molnár, 2001). Within this region, the site of Patakfalva-Papdomb is located near the modern town of Patakfalva (Văleni), within the county of Harghita in modern day central Romania (Figure 4). The site is the location of a medieval Christian church (1100 – 1804 C.E.) with associated burials under the church floors and within, and outside, the surrounding churchyard.



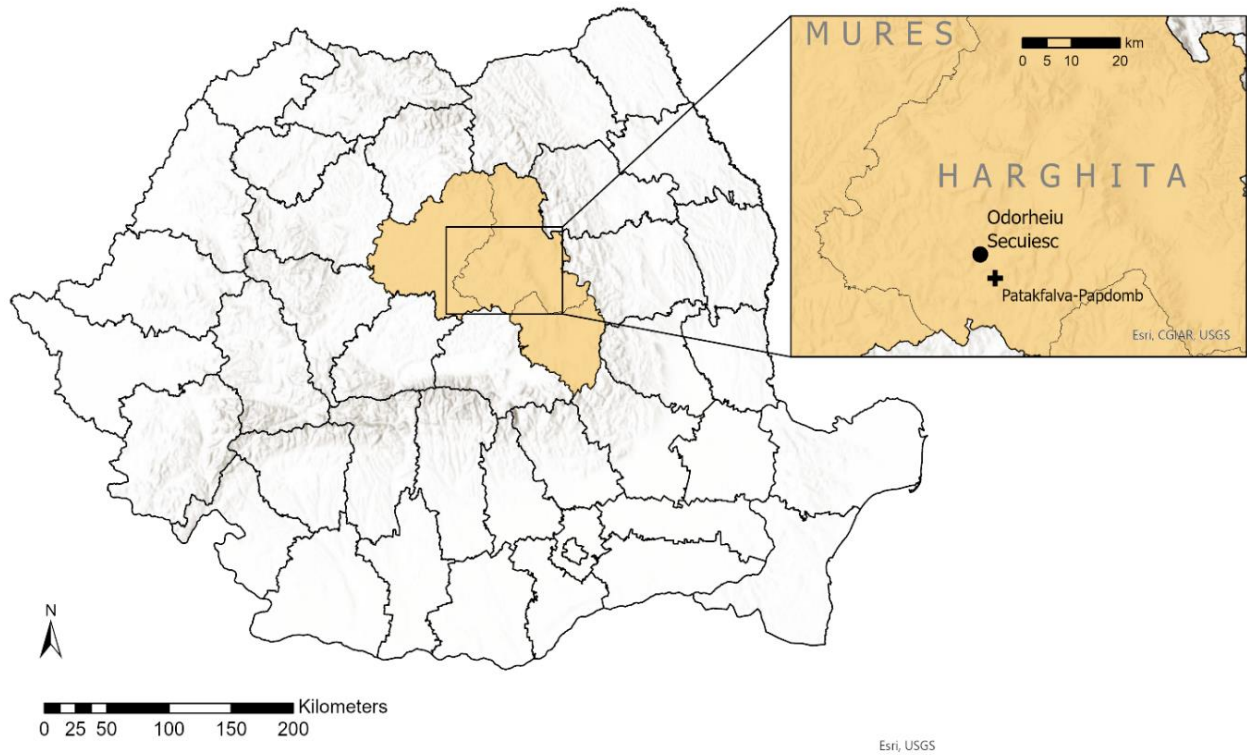


Figure 4. Map of the counties in Romania. Highlighted are the modern counties that encompass the area known as the Székelyfold. Inset shows the county of Harghita, the town of Székelyudhvarhely (Odorheiu Secuiesc), and the site of Patakfalva-Papdomb is marked with a cross.

During the Middle Ages, this site served three local communities, Văleni, Teleac, and Alexandrița, and became the resting place for many of the community members that lived nearby, regardless of socioeconomic status (Zejdlik et al., 2020). The site was being used as a contemporary burial ground until historical remains were discovered. The community of Patakfalva, through the mayor and local council, contacted the Székely run Haáz Rezső Museum in Székelyudvarhely (Odorheiu Secuiesc), Harghita County, Romania, for assistance in recovering the remains and learning more about the history of the site and community. The director of the Haáz Rezső Museum, Zsolt Nyárádi, has led the excavation of this site since 2014. The goal of the excavation is to recover archaeological material and human remains and understand the site's usage in the past while protecting the remains from further excavation for contemporary burials. Nyárádi and the community of Patakfalva invited ArcheoTek Canada, LLC, along with bioarchaeologists Katie Zejdlik and Jonathan Bethard to excavate and analyze the recovered remains. The site has been explored using over 47 trench excavations, each covering about 25 square meters and over 700 intact or mostly intact burials have been recovered as of 2021.

One of the main questions posed by the community and researchers for this site relates to the level of social differentiation in the community during the lifetime of the church and the life of non-elite individuals. Some interments at the site are more elaborate than others and their locations, either on the grounds or within the church walls, are hypothesized to correlate to social status (Zejdlik et al., 2020). This question has been explored primarily through the comparison of burial practice to collagen-derived isotopic data, which has demonstrated at least two individuals with more elaborate burials that also appeared to have greater access to animal protein compared to the primarily herbivorous diet of the local community (Trent et al., 2020). Other than the

perceived level of elaboration of individual burials, there are three main interment types present at the site. The first is traditional Christian burials with individuals placed in extended positions often directed east to west. As mentioned above, over 700 of these have been recovered as of 2021. The second interment type is an ossuary, located against the north wall of the church, measuring approximately 4 m by 2 m and bounded by stone walls abutting the wall of the church. Excavations of the ossuary are ongoing but the minimum number of individuals in this context surpasses 70 as of 2021. The third of the interment types is unassociated human skeletal remains that are mixed into the overburden covering the intact or semi-intact burials. As of 2021, no attempt has been made to enumerate the number of individuals represented by remains recovered from the fill. Evidence of medieval shovel marks present on these remains suggests that, once buried, these individuals were disinterred and then reinterred simultaneously with the overburden of a newly dug grave. The origin of these remains is unknown, but partially disturbed individual burials suggest that these may be the remains of traditionally buried individuals that were disturbed during the excavation of a more recent grave. Questions about the origin and possible status of these individuals, regardless of their interment type, can best be answered by comparing isotopic values to category of interment. Non-destructive reassociation of the remains that have been commingled or disassociated, such as those in the ossuary or overburden, along with the use of non-destructive isotopic analyses, will allow investigators to reconstruct some of the individuals present, potentially re-uniting partially disturbed burials and remains from the fill, and thereby further the aims of the investigation while protecting the integrity of the skeletal remains.

Previous isotopic analysis of individuals recovered from mostly intact burials included both apatite and collagen isotopic ratio values (Bethard et al., 2022; Trent et al., 2020), but for

the purposes of this study, I will focus on the apatite results since those will have the most direct comparison to the apatite-derived isotopic data for the individuals in this study. Analyses of bone apatite from individual burials found that, in adults, with the exception of two outliers,  $\delta^{13}\text{C}_{\text{apatite}}$  ranged between -14‰ and -10.5‰ while  $\delta^{18}\text{O}_{\text{vpdb}}$  ranged between -10.4‰ and -4.1‰ (Figure 5)(Bethard et al., 2022). Analyses of subadult bone apatite ranged from -14.5‰ to -10.8‰ in  $\delta^{13}\text{C}_{\text{apatite}}$ , with two outliers, and from -6.5‰ to -3.9‰ in  $\delta^{18}\text{O}_{\text{vpdb}}$ , with a single outlier (Figure 5)(Bethard et al., 2022). No significant difference in isotopic values can be observed between adults and subadults in this sample. These  $\delta^{13}\text{C}_{\text{apatite}}$  values, suggest a diet that was heavily  $\text{C}_3$  based, likely wheat or other cereal grains, but the outliers with  $\delta^{13}\text{C}_{\text{apatite}}$  values above -10.5‰ may suggest some inclusion of  $\text{C}_4$  plants either directly or through the consumption of animals that fed on  $\text{C}_4$  plants or domesticates like millet or other warm-season grasses for those individuals (Bethard et al., 2022; Reitsema & Kozłowski, 2013). Differences in the  $\delta^{18}\text{O}_{\text{vpdb}}$  values are within expected variation between individuals and likely signify a relatively local cohort as the topography of the region may have significantly affected the isotopic values of the local water sources (Berg et al., 2022; Bethard et al., 2022).

The remains analyzed in this study were recovered from the overburden covering intact burials. In conjunction with the analyses completed in this study, comparison to the previously collected isotopic values presented above present a more complete picture of mortuary practices in the region and the social selection of individuals for protected status within this burial space. The skeletal remains comprising this sample are fragmentary and represent several different skeletal elements, from both adults and subadults, including femora, tibiae, scapulae, humeri, radii, ulnae, ribs, crania, and mandibles. Approximately 67 individuals are represented by these skeletal elements, with 15 subadults and 52 adults (Table 2).

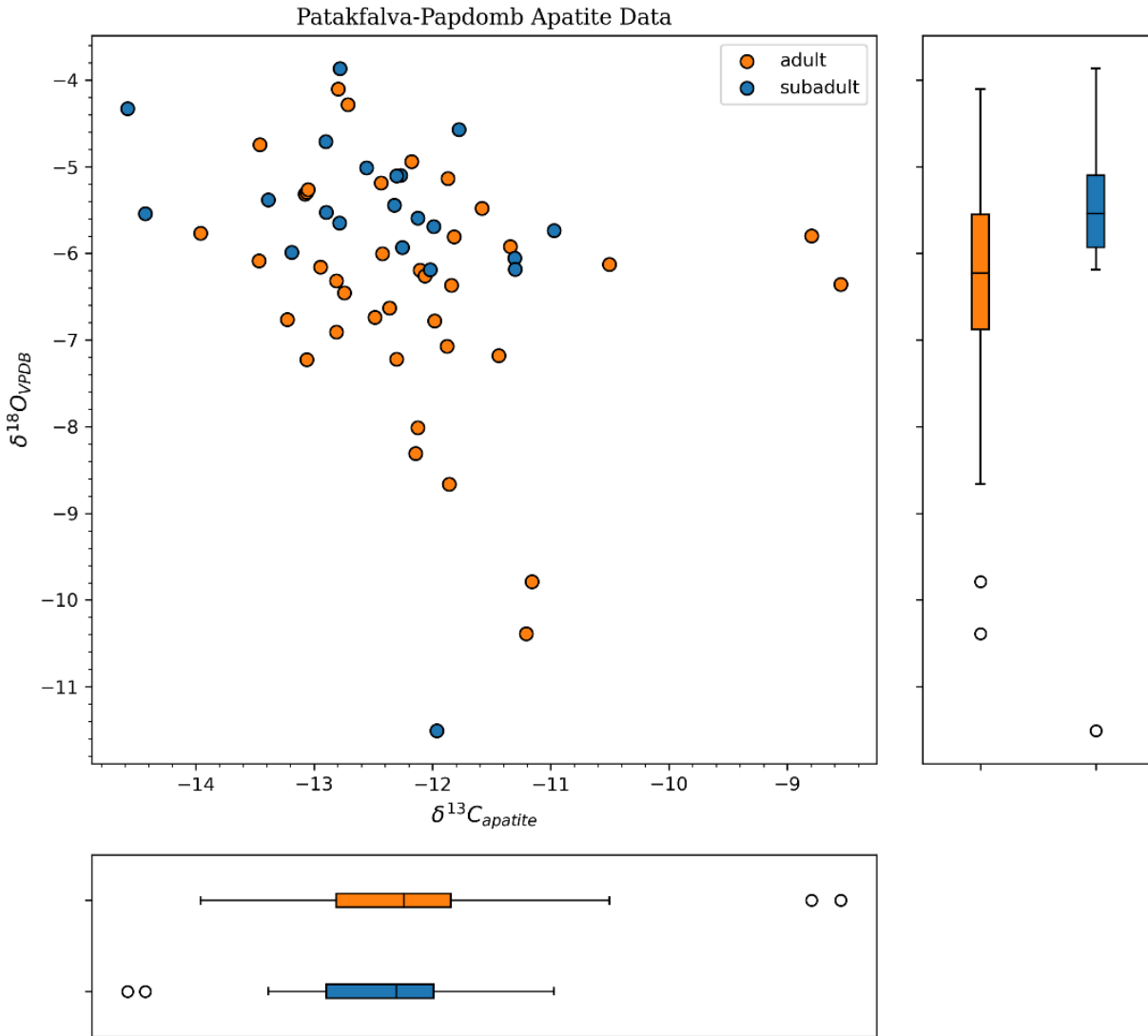


Figure 5. Scatter and marginal box plots of  $\delta^{18}O$  and  $\delta^{13}C$  isotopic data from bone apatite derived from individuals recovered from intact or almost intact graves at the site of Patakfalva-Papdomb. Data from Bethard, Zejdlik, Nyárádi, and Gonciar (2022).

Table 2. Summary table of skeletal elements of individuals from the Patakfalva-Papdomb site analyzed in this study. The N of elements represents the individual isolated skeletal elements while the N of samples represents the total number of samples representing each skeletal element.

|                        | Adult                          |                               | Subadult                       |                               |
|------------------------|--------------------------------|-------------------------------|--------------------------------|-------------------------------|
|                        | <i>N</i><br><i>of Elements</i> | <i>N</i><br><i>of Samples</i> | <i>N</i><br><i>of Elements</i> | <i>N</i><br><i>of Samples</i> |
| Cranial Vault          | 14                             | 14                            | 0                              | 0                             |
| Zygomatic              | 1                              | 1                             | 0                              | 0                             |
| Temporal               | 1                              | 1                             | 0                              | 0                             |
| Mandible               | 4                              | 4                             | 0                              | 0                             |
| Rib                    | 2                              | 3                             | 0                              | 0                             |
| Scapula                | 3                              | 3                             | 1                              | 1                             |
| Humerus                | 2                              | 4                             | 1                              | 1                             |
| Radius                 | 2                              | 2                             | 0                              | 0                             |
| Ulna                   | 1                              | 4                             | 2                              | 2                             |
| Ilium                  | 2                              | 3                             | 1                              | 1                             |
| Femur                  | 12                             | 23                            | 5                              | 8                             |
| Tibia                  | 3                              | 10                            | 3                              | 4                             |
| Fibula                 | 3                              | 7                             | 0                              | 0                             |
| Long Bone <sup>†</sup> | 2                              | 2                             | 2                              | 2                             |
| <i>Total</i>           | 52                             | 81                            | 15                             | 19                            |

<sup>†</sup> Unidentified long bone fragments

Elements were sectioned, sometimes into multiple portions, for analysis, representing proximal shaft versus midshaft or distal shaft on the same element, and a section was collected from each fragmentary skeletal element to compare non-destructive approaches to destructive approaches in isotopic ratio analyses (n = 100). In total, the collection of samples represents 19 subadults sampled with 8 originating from the same isolated skeletal element and 81 adults sampled with 29 originating from the same isolated skeletal element (Table 2). Appendix I provides an inventory of the Patakfalva-Papdomb skeletal elements and sampling location. Approximately 8% of the skeletal elements (n=8) were selected for duplication to ensure precision for the IRMS results and all samples had Raman spectra collected in duplicate to ensure the precision of those analyses. IRMS precision was measured by calculating absolute error scores between original and duplicated data and comparing those error values to the expected 1.2‰ minimum meaningful difference (MMD) for  $\delta^{13}\text{C}$  and the 3.2‰ MMD for  $\delta^{18}\text{O}$  values between labs for bone derived apatite (Chesson et al., 2019; Pestle, Crowley, et al., 2014). Precision for the Raman spectra was measured using Spearman's  $\rho$  rank correlation coefficient with an  $\alpha$  set to 0.05 (Henschel & van der Spoel, 2020; Samuel et al., 2021).

### ***The University of Tennessee Skeletal Collection***

The University of Tennessee Skeletal Collection was established in 1981 alongside the foundation of the Anthropological Research Facility (ARF) to curate the skeletal remains that resulted from the study of decomposition in a natural but partially controlled environment. Donors to the facility can either pre-enroll as donors or their families can enroll them in the program postmortem. Through this registration process, the donors or their families provide background information such as residential history, healthcare history, occupation, or any

additional information requested based on current study needs. Donors also allow for the curation of the remains after decomposition and for the use of the skeletal remains in other avenues of anthropological research.

Once individuals have fully decomposed at the ARF, the remains are brought into the laboratory space at the William M. Bass Forensic Anthropology Building for processing. Processing involves the cleaning of the skeletal remains with soft bristle brushes, water, and occasionally soap to remove particularly adhered lipids and remaining soft tissue. The skeletal remains of these donors are then allowed to dry and carefully packaged in acid-free curation boxes. They are then inventoried and accessioned into the University of Tennessee Skeletal Collection where they are carefully maintained at stable temperature and humidity. Destructive analysis of these individuals is discouraged, but donors are asked for permission for these analyses prior to enrollment in the program and any project requesting such analyses must undergo thorough evaluation. Donors allow all data to be available to researchers in an anonymized form to protect the privacy of the donors, and all investigations involving donors to the skeletal collection must be cleared by the director of the facility and undergo a panel review to ensure the feasibility of the project and ensure the ethics of each request. Currently, the University of Tennessee Skeletal Collection holds over 1,800 individuals, with approximately 100 additional donors being accepted every year. The extensive donation program, ethical considerations for the donors to the collection, and the wide range of residential locations for the individuals in this collection, as well as their well-documented residential histories, allow for precise, replicable, and ethical analyses and make this collection ideal for the current project.

To test intraskeletal variation using Raman spectrometry and IRIS, 30 individuals were selected from the University of Tennessee Skeletal Collection. Donors for this project were



selected by comparing their last known residence to an isoscape of known tap water oxygen values for the continental United States (Bowen et al., 2007) to ensure that final oxygen isotopic results were comparable to expected values and encompassed a wide range of variation. The relationship between drinking water and bone  $\delta^{18}\text{O}$  values was predicted from the isoscape values using the formula created by Daux et al. (2008) adjusted for calculation from carbonate derived oxygen isotopes:

$$\delta^{18}\text{O}_{\text{carb}} = \frac{\delta^{18}\text{O}_{\text{water}} + 46.81}{1.5092} \text{‰} \pm 2.85\text{‰}$$

Donors were selected for analyses only if they had a known last city of residence and were documented to have resided in that city for at least one year. Any individual with a residence time of less than one year is not expected to have fully incorporated oxygen isotopes in their skeleton, possibly adding a confounding factor when prior residential history is unknown. The 30 donors selected ranged in age from 27 to 94 with an average of 61 (sd = 13), with 19 self-identifying as male and 11 as female and the large majority identifying as having white ancestry (28) with one individual identifying as having black ancestry and one individual identifying as having Asian ancestry. Selected individuals, including their project-specific donor number, last known city of residence, length of residence, latitude and longitude of the city of residence, and predicted  $\delta^{18}\text{O}$  values for both tap water and carbonate apatite are presented in Appendix II. Summary data are presented in Table 3 and the isoscape used to predict the  $\delta^{18}\text{O}$  isotopic values is presented in Figure 6. The donors selected represent a range of predicted  $\delta^{18}\text{O}_{\text{water}}$  isotopic values from 0.05‰ to -15.98‰ ( $\bar{x}$  = -5.96‰, sd = 3.672; VSMOW), which, using the formula presented above, give isotopic carbonate values from 20.4‰ to 31.05‰ ( $\bar{x}$  = 27.07‰, sd = 2.433; VSMOW). While the  $\delta^{18}\text{O}$  results from the isoscape are in the VSMOW scale, all values

Table 3. Summary table of data from selected University of Tennessee Skeletal Collection donors.  $\delta^{18}\text{O}_{\text{water}}$  values have been estimated from an isoscape of tap water isotopic ratios across the United States and the  $\delta^{18}\text{O}_{\text{carbonate}}$  values have been estimated using the formula by Daux et al. (2008).  $\delta^{18}\text{O}$  values shown are in the VSMOW scale.

|              | N  | Age  |      |         | $\delta^{18}\text{O}_{\text{water}}$ |       |                | $\delta^{18}\text{O}_{\text{carbonate}}$ |       |               |
|--------------|----|------|------|---------|--------------------------------------|-------|----------------|--|-------|---------------|
|              |    | Mean | SD   | Range   | Mean                                 | SD    | Range          | Mean                                     | SD    | Range         |
| Male         | 19 | 59   | 12.8 | 27 – 76 | -5.32                                | 3.677 | -15.16 – 0.05  | 27.49                                    | 2.437 | 20.97 – 31.05 |
| Female       | 11 | 63   | 13.5 | 41 – 94 | -7.06                                | 3.557 | -15.98 – -3.68 | 26.34                                    | 2.357 | 20.43 – 28.57 |
| <i>Total</i> | 30 | 61   | 13   | 27 – 94 | -5.96                                | 3.672 | -15.98 – 0.05  | 27.07                                    | 2.433 | 20.43 – 31.05 |

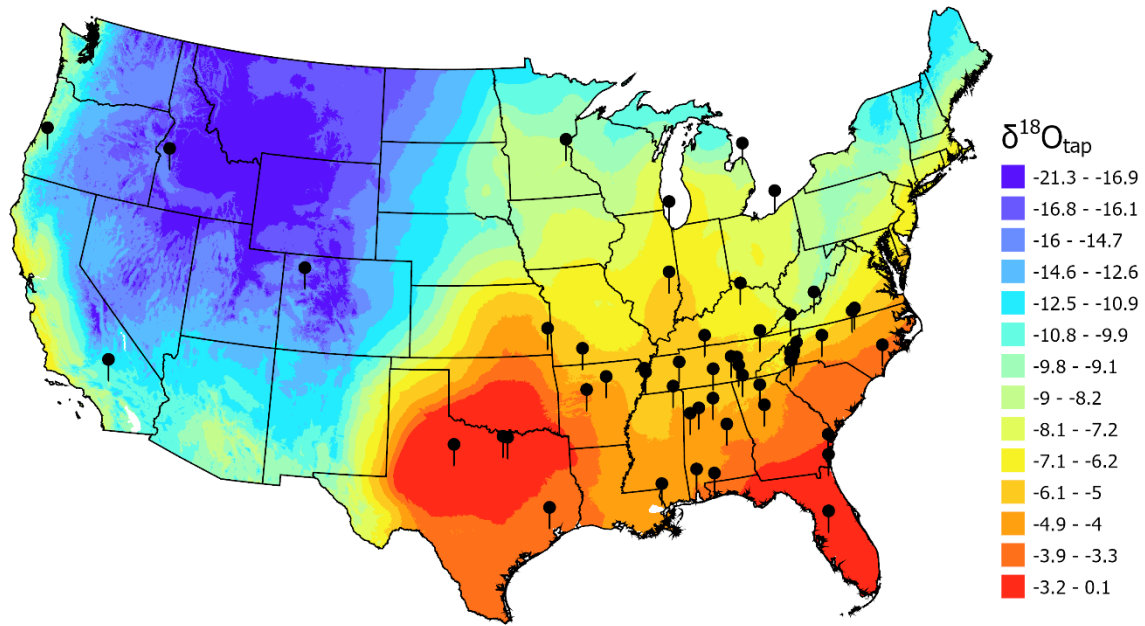


Figure 6. Map of tap water values for  $\delta^{18}\text{O}$  of the contiguous United States with pins denoting the residence location for selected donors from the University of Tennessee Skeletal Collection. All  $\delta^{18}\text{O}$  values are in reference to SMOW. Adapted from data by Bowen, Ehleringer, Chesson, Stange, and Cerling (2007).

were converted to VPDB prior to analyses for consistency with other bioarchaeological isotopic studies.

For consistency in the analysis of intraskeletal variation using Raman spectrometry, Raman spectra were collected from the humerus, radius, ulna, femur, tibia, fibula, and second rib on the right side for all individuals. These specific skeletal elements tend to be the most frequently recovered, are most often used in isotopic studies (Bartelink & Chesson, 2019; Jørkov et al., 2009), and have previously demonstrated differences in turnover rates between and within them (Jørkov et al., 2009) as well as potential isotopic differences between them within an individual (Berg et al., 2022). Each long bone had six total spectra collected, three anterior and three posterior, ranging from superior to inferior, while the second rib had Raman spectra taken at three locations ranging from vertebral to sternal (Figure 7). All spectra were collected from the diaphyses of the skeletal element, avoiding metaphyses and epiphyses that may affect the results due to their increased porosity and decreased cortical bone thickness. In total, 39 spectra were collected per individual, 1,170 spectra for the entire collection of 30 donors. Approximately 10% of the donors (n=3, number of spectra = 117) were randomly selected for duplication to ensure precision in the Raman spectra. Precision between the duplicate Raman spectra was measured using Spearman's  $\rho$ , like with the spectra from the Patakfalva-Papdomb individuals, with  $\alpha$  set to 0.05 (Henschel & van der Spoel, 2020; Samuel et al., 2021).

### **Raman Spectrometry**

Sample preparation for analysis in a Raman spectrometer was minimal since reduction in sample disturbance and preparation times is the ultimate intended purpose for the creation of this methodology. For the individuals from the Patakfalva-Papdomb site, the skeletal remains used in



Figure 7. Example of sampling locations for a left femur. Orange circles represent sampling locations. Only sampling locations visible in this anterior view are represented, but sampling occurred on anterior and posterior aspects of each element with the exception of rib 2 which was only sampled on the ventral surface.

this analysis were brushed thoroughly with water and were allowed to air dry. The donors to the University of Tennessee Skeletal Collection underwent no additional process prior to analyses with the Raman spectrometer.

The Raman spectrometer used in this study was housed in the Optical Spectrometry Laboratory, directed by Dr. Ngee Sing Chong, at Middle Tennessee State University. The instrument is an EnWave Optronics ProRaman-L complete system using a 785nm excitation wavelength with maximum power output of 500mW and a high sensitivity CCD detector cooled to -50°C. This instrument has a peak resolution of between 4.5 and 6.5cm<sup>-1</sup> dependent on the scattered wavelength. To reduce fluorescence, each sample was photobleached using the 785nm laser at a power output of 350mW at one second intervals with one second between excitations for 250 scans prior to data collection (Shea & Morris, 2002). This process was repeated multiple times if fluorescence continued to obscure the signal. Each sample was then analyzed with the optical probe approximately 10mm above the sample in a darkened enclosure with the laser set to a maximum power output of 350mW. Integration was set to 1 second and the results were averaged over 20 scans to reduce additional fluorescence noise not removed through photobleaching. Due to the reduced fluorescence presented by the individuals from the University of Tennessee Skeletal Collection, no photobleaching was needed for the collection of any of their Raman spectra and the parameter could be changed to 30 second integrations averaged over three scans. This increase in integration time provides a cleaner signal when fluorescence is less significant.

Raman spectra were collected for each of the bone segments used for IRMS analyses and, as a result of the short scan period and low effort, all bone segments representing individuals from Patakfalva-Papdomb were scanned twice. All spectra, both from University of Tennessee

donors and from Patakfalva-Papdomb individuals were cropped to the fingerprint region ( $400\text{cm}^{-1}$  to  $1900\text{cm}^{-1}$ ) prior to analyses. To remove any residual fluorescence, the collected spectra were then baseline corrected using the asymmetrically reweighted penalized least squares smoothing (arPLS) baseline method (Baek, Park, Ahn, & Choo, 2015), were smoothed to remove background noise using a Savitzky–Golay filtering algorithm (Barton et al., 2018), and were normalized to the highest peak value ( $\nu_1 \text{PO}_4$ ) to remove stochastic effects of Raman scattering on signal intensity. These processed spectra were then used for the proceeding steps in the analysis.

### **Isotope Ratio Mass Spectrometry (IRMS) and Correlation to Isotope Ratio Infrared Spectrometry (IRIS)**

In order to collect isotopic data from the bioapatite of Patakfalva-Papdomb individuals, the bone sections must be mechanically and then chemically prepared prior to IRMS analyses. Only the individuals from the Patakfalva-Papdomb collection were analyzed using the IRMS with permission for destructive sampling given by the Haáz Rezső Museum in Székelyudvarhely (Odorheiu Secuiesc) and the community of Patakfalva (Romanian: Văleni). Bone segments were removed from the individuals in the Patakfalva-Papdomb collection and were ultrasonically cleaned to remove adhered soil. Each bone segment was then fragmented and powdered to less than  $250\mu\text{m}$  using an agate mortar and pestle and approximately 20mg were collected for bioapatite carbonate analysis. Although some research has demonstrated that  $\delta^{18}\text{O}$  values from phosphate are more reliable than those derived from carbonate (Daux et al., 2008), phosphate extraction is labor intensive, sensitive to minor changes in the protocols, and, as a result, is infrequently used in forensic or bioarchaeological contexts (Chesson et al., 2017). Therefore,

carbonate analysis was chosen for this study.

To remove the organic matrix from each of the samples representing individuals from Patakfalva-Papdomb for bioapatite carbonate analysis, the collected powder was first saturated in a solution of 30% H<sub>2</sub>O<sub>2</sub> and allowed to react for 48 hours, with a replacement of the H<sub>2</sub>O<sub>2</sub> after 24 hours. After thorough rinsing using 18mΩ de-ionized water, the removal of labile carbonates was performed using a 0.1M solution of acetic acid (CH<sub>3</sub>COOH) buffered to a pH of 4.5 with 1M calcium acetate and the samples remained in that solution for approximately 4 hours. After another thorough rinsing of the acetic acid solution using the de-ionized water, the vials with sample powder were covered with permeable, low-lint wipes and placed in a dryer convection oven at 60°C overnight until no moisture remained. Approximately 10% of the samples (n = 8) were duplicated to verify the precision of the IRMS process by comparing the results to the MMD for each isotopic value (Pestle, Crowley, et al., 2014).

With these processes complete, the bioapatite samples were analyzed at the Stable Isotope Lab at the University of Tennessee, Knoxville. Bioapatite δ<sup>13</sup>C and δ<sup>18</sup>O values are reported from the lab in reference to VPDB, and although many forensic contexts will have values in references to VSMOW, for simplicity of the models and reliability of the results, all references will remain in reference to VPDB. To create a reliable and replicable protocol for Isotope Ratio Infrared Spectrometry (IRIS) of human skeletal remains, IRMS results must be correlated to IRIS results. In addition to the spectral peak height data, previous IRIS studies have found relevance for the frequency location of significant peaks along the spectrum (Dalou et al., 2018; Vitkin et al., 2020), therefore the locations for the PO<sub>4</sub> and CO<sub>3</sub> peaks along the spectrum were also included as potential variables. Due to the number of vibrational modes present in the Raman spectra of unprocessed bone, the best approach to creating the necessary linear regression

is to use a variable selection method of linear regression modeling on the spectral data, correlating the values at each wavelength in the spectrum to the scalar values of  $\delta^{13}\text{C}$  and  $\delta^{18}\text{O}$  (Ortiz-Herrero et al., 2021; Tapp & Kemsley, 2009). For this approach an 8-fold, 1000-repeat cross-validated Lasso algorithm was used for variable selection among all potential peaks in the Raman spectra (Filzmoser, Gschwandtner, & Todorov, 2012; Meinshausen & Bühlmann, 2006). The cross-validation was used to estimate the  $\lambda$  parameter that is used to select how many coefficients best fit the model. Using this cross-validated  $\lambda$ , the data were split into training and testing groups and the lasso model with the given  $\lambda$  value was fit and validated (Filzmoser et al., 2012). The Lasso variable selection linear regression approach also has the benefit of providing coefficients for the frequency wavenumber in the linear model that describe the strength of the relationship between the peak at that wavenumber and the dependent variable. This provided an opportunity to explore which Raman spectral bands correlate to isotopic values for a more detailed understanding of the interactions.

### **Calculating Diagenesis for Archaeologically Recovered Individuals**

Diagenesis, the process of ionic exchange and molecular bond breakdown, will affect all biochemical analyses of bone. As a result, stable isotopic analyses often require the screening of samples using vibrational spectrometry to assess the reliability of the collected biochemical data (Halcrow et al., 2014; Pestle et al., 2015; Sponheimer et al., 2019). The assessment, therefore, of diagenesis and its effects on the applications of the IRIS method must be examined. For this purpose, four main diagenetic indices from Raman spectra were calculated: Amide(I)/PO<sub>4</sub> ratio, the crystallinity index (CI), CO<sub>3</sub>/PO<sub>4</sub> ratio, and the ratio of fluorescence to signal (Bertoluzza et al., 1997; France et al., 2014; Halcrow et al., 2014; Pucéat, Reynard, & Lécuyer, 2004).



The usual approach to applying Raman spectrometry in the analysis of diagenesis involves the quantification of collagen content compared to mineral content. This is done through the analysis of molecular bonds that do not exist in bioapatite but do exist in collagen, such as amide bonds. The amide(I)/PO<sub>4</sub> ratio, between the amide I peak at 1636cm<sup>-1</sup> and the ν<sub>1</sub>PO<sub>4</sub> peak at 960cm<sup>-1</sup>, correlates closely with the percentage of collagen yield calculated from the demineralization of the samples studied (France et al., 2014). The threshold for defining “good” collagen preservation is a ratio of 19.4, below which bone is unlikely to have been altered and above which it is likely to have been diagenetically altered (France et al., 2014; Madden et al., 2018). By comparing the PO<sub>4</sub> content to the amide content in bone, researchers have demonstrated that increased diagenesis preferentially breaks down organic matter dependent on environmental conditions (France et al., 2014; Halcrow et al., 2014), but the mineral component also undergoes diagenesis.

The analysis of diagenesis for bioapatite has also been studied using Raman spectrometry. Pucéat et al. (2004) have created a crystallinity index for Raman spectra (CI<sub>raman</sub>) analogous to that used in FTIR, with an increase in crystallinity suggesting greater amount of recrystallization of the bioapatite and therefore the remains have suffered more diagenetic alteration. The CI<sub>raman</sub> is calculated by measuring the width of the peak at half of its total height, called the full width at half-maximum (FWHM) (Table 4). Results from the creation of the CI<sub>raman</sub> suggest that the values closely approximate the IRSF, but the accuracy of CI in the assessment of diagenesis is still debated (Pucéat et al., 2004; Trueman, Privat, & Field, 2008).

The CO<sub>3</sub>/PO<sub>4</sub> ratio (also known as the C/P ratio) takes advantage of the fact that recrystallization of the apatite preferentially nucleates PO<sub>4</sub> over CO<sub>3</sub> in the crystal matrix so that, as recrystallization occurs over the skeleton, the ratio approaches zero (Berna et al., 2004;

Leskovar, Zupanic Pajnic, Jerman, & Cresnar, 2020; Wright & Schwarcz, 1996). This ratio, however, can also be a measure of noise in the spectrum, as a ratio that exceeds 0.5 is unlikely to exist in even the best-preserved bioapatite due to the average replacement by CO<sub>3</sub> in human carbonated apatite (Beasley et al., 2014; Leskovar et al., 2020; Wright & Schwarcz, 1996).

Additionally, regardless of the photobleaching process, some fluorescence always remains when analyzing skeletal remains using a 785nm excitation wavelength (Ortiz-Herrero et al., 2021; Shea & Morris, 2002). Since fluorescence may affect the strength of the signal and add noise to the spectrum, a measure of the fluorescence present in the spectra of each skeletal element will also provide a measure of reliability. Since the most important measure of fluorescence is its occultation of signal in the spectrum, the ratio of fluorescence versus signal was calculated by dividing the total PO<sub>4</sub> peak height prior to baseline correction by the value of the baseline at the wavenumber of the peak. For this ratio, as the value approaches one, fluorescence is obscuring the signal almost entirely, while as it approaches zero it suggests almost no fluorescence present in the spectrum. This estimate, while unconventional (Golcuk et al., 2006; Shea & Morris, 2002), provides a measure of the percentage of the peak height that is fluorescence versus actual signal and avoids the pitfalls of the lack of understanding of the origins of fluorescence. All formulae for each of these indices can be found in Table 4.

Lastly, a quality control metric was created to ensure the quality of the spectra being used in all analyses. Raman spectra of human skeletal material should not have major signal bands between 800cm<sup>-1</sup> and 850cm<sup>-1</sup> or between 875cm<sup>-1</sup> and 930cm<sup>-1</sup> (McLaughlin & Lednev, 2011; Morris & Mandair, 2011; Penel, Leroy, Rey, et al., 1998). A quality control metric was, therefore, assessed using threshold values to select the best spectra free of artificial peaks in these regions. Spectra with either of these artificial bands reaching a relative intensity above 0.3

Table 4. Formulae for the calculation of the indices of diagenesis from Raman Spectrometry used in this study and their associated ranges for determining the extent of diagenetic alteration in bone.

| Index                            | Formula                                  | Fresh Bone  | Altered Bone | References                 |
|----------------------------------|--|-------------|--------------|----------------------------|
| Amide(I)/PO <sub>4</sub>         | $\frac{A_{960cm^{-1}}}{A_{1636cm^{-1}}}$ | < 19.4      | > 19.4       | France et al. (2014)       |
| CI <sub>Raman</sub>              | $\frac{4.9cm^{-1}}{\Gamma_{960cm^{-1}}}$ | < 0.5       | 0.5 - 1.4    | Puc at et al. (2004)       |
| CO <sub>3</sub> /PO <sub>4</sub> | $\frac{A_{1070cm^{-1}}}{A_{960cm^{-1}}}$ | 0.23 - 0.40 | < 0.23       | Wright and Schwarcz (1996) |
| Fluorescence Ratio               | $\frac{A_{960cm^{-1}}}{B_{960cm^{-1}}}$  | -           | -            | -                          |

A<sub>x</sub> is the absorbance (peak height), Γ<sub>x</sub> is the full width at half maximum, and B is the value of the baseline before subtraction at the given wavenumber (cm<sup>-1</sup>) of x. Fluorescence ratio is calculated before baseline correction, all others are calculated after baseline correction.

(more than 30% of the largest signal peak) or both artificial bands reaching a relative intensity above 0.15 were considered of “Bad” quality. Spectra that had one of these two artificial bands above 0.15 relative intensity were considered of “Fair” quality. If neither artificial band reached a relative intensity of 0.15 but did have a relative intensity of either of these artificial bands above 0.075 it was considered of “Good” quality, while anything better was categorized as “Great.” To confirm that this quality control metric correlated to real differences in the skeletal remains rather than stochastic differences between the spectra, boxplots were visually assessed and a Kendall’s  $\tau_c$  was calculated against all other indices of diagenesis to test for correlations to diagenetic alterations.

One of the benefits of using the IRIS approach is the ability to calculate these indices of diagenesis simultaneously with the isotopic ratios to estimate the reliability of the results. The given indices were tested for correlation with the IRIS-derived and IRMS-derived isotopic values to assess the reliability of both approaches on diagenetically altered bone. Prior to testing for correlation, the presence of outliers was assessed using a  $3.2\sigma$  threshold above which values were considered outliers (Bakar, Mohamad, Ahmad, & Deris, 2006). If outliers were detected, a non-parametric test of correlation, a Spearman’s  $\rho$  rank correlation coefficient, was applied, otherwise diagenetic alteration affecting isotopic results were tested by a Pearson’s  $r$  correlation coefficient. In the case of either test being applied, if the isotopic ratio values correlate with diagenetic indices, the data should be considered unreliable (Reitsema & Kozłowski, 2013).

### **Intra-element Variation in Biogeochemical Data**

Intra-element variation in isotopic values was explored in the IRMS derived isotopic values for the Patakfalva-Papdomb individuals while intraskeletal variation was explored using

the IRIS derived isotopic values and the Raman spectra of the donors from the University of Tennessee Skeletal Collection. For the IRMS derived values, approximately 22 skeletal elements were sampled at multiple locations and the isotopic values of each location were compared within the elements using mean absolute error and comparing those results with the MMD expected for each isotopic value (Pestle, Crowley, et al., 2014).

For the University of Tennessee donors, resulting spectra for the entire collection of study donors were compared using both IRIS derived isotopic ratios and the normalized spectra. For the IRIS derived isotopic values, four main comparisons were with an ANOVA analysis: 1) between individuals, 2) between sampling locations pooled by individual, 3) between skeletal elements, and 4) between sampling locations across all individuals. Since four total comparisons were made, a Bonferroni correction was applied, adjusting the level of significance from 0.05 to an  $\alpha$  of 0.0125. To satisfy the assumptions of the parametric ANOVA test, a Levene's test for equality of variance was applied to each of the distributions being compared. If the Levene's test was significant for heteroscedasticity, a non-parametric Welch's ANOVA was applied instead.

IRIS data were also compared using mean deviations and 95% confidence intervals (C.I.) (Gorard, 2005) in isotopic values within individuals and skeletal elements to explore the effects of sampling location on isotopic data. Deviations from the mean for each location were compared to the 95% C.I. of deviations across sampling locations for all individuals to explore if differences in sampling location exceed differences between or within individuals.

### **Reassociation of Individuals using Biogeochemical Data**

Previous work by (Berg et al., 2022) on reassociation using biogeochemical data utilized a threshold method to exclude individuals from potential reassociation. This method has two

main threshold levels: one at 95% confidence for which differences above 1.55‰ in isotopic values between samples indicate that they likely come from different individuals, and a second threshold at 99% confidence for which differences above 1.90‰ in isotopic values between samples indicate that they do come from different individuals. This approach was applied to both the Patakfalva-Papdomb individuals as well as the IRIS-derived isotopic values for the donors to the University of Tennessee Skeletal Collection. To examine the reliability of these thresholds, sensitivity, specificity, positive predictive value, and negative predictive value were calculated for the application of these thresholds on each collection of individuals separately. Another approach for increasing the nuance of reassociation is to use logistic regression, which provides a likelihood of association rather than exclusion as seen in threshold-based models; therefore, a logistic regression model was created using a 10-fold, 1000-repeat cross-validation approach on each of the collections of individuals separately. Predictive criteria were again calculated for each of these models to assess their reliability in comparison to the previously defined threshold approach.

To ensure the robusticity of the comparisons of variance and the use of intra-individual variance in reassociation using IRIS-derived values, Principal Component Analysis (PCA) was applied to the corrected and normalized spectra of the University of Tennessee donors after scaling to unit variance (Ortiz-Herrero et al., 2021). Each spectrum in this study is a two-dimensional array of wavenumber (frequency) and signal strength at the given frequency, and therefore includes 563 points per scan location. PCA was thus used to explore clustering and separation of individuals in the case where correlation between the scan and the individual are unknown (PCA). Lastly, to test the application of Raman spectra alone to reassociation in contexts where the number of individuals represented is unknown, I applied a Bayesian Gaussian

Mixture Model to the dataset of scans after being scaled to unit variance (Attias, 2000; Blei & Jordan, 2006). This model uses a Dirichlet process and Variational Inference to select the number of potential clusters with Gaussian distributions that describe the given data and maximize the log-likelihood of the model (Attias, 2000; Blei & Jordan, 2006). To simplify, this model assumes the multidimensional spectral data for a single individual derives from a Gaussian distribution. With this assumption, the model randomly selects a set of individuals and creates groups from those individuals, testing the likelihood that these groups represent the true groups in the dataset (Dirichlet process) and adjusting the groups to increase the likelihood, repeating this process 1000 times. The Dirichlet process is unbounded, meaning that the number of clusters is not previously known but the method seeks to optimize this parameter to estimate the number of individuals represented by the dataset. The Bayesian Gaussian Mixture Model was then compared to the true associations of the donors using an Adjusted Mutual Information score (AMI) that provides the accuracy of the model, with 0 being no correct classifications and 1 being perfect classifications (Vinh, Epps, & Bailey, 2010). All statistical analyses for reassociation, including Logistic Regression, PCA, and Bayesian Gaussian Mixture Model, were implemented using the Scikit-Learn package for Python (Pedregosa et al., 2011)

### **Summary**

The individuals analyzed in this study come from two main populations. The first is a collection of skeletal remains representing individuals interred without association to a single burial on the grounds of a medieval church in the Szekélyfold, Romania. These individuals were analyzed using a traditional Gas Bench IRMS for bioapatite derived isotopic ratios of  $\delta^{13}\text{C}$  and  $\delta^{18}\text{O}$  and Raman Spectrometry and form the foundation of the protocol for the IRIS protocol on

human skeletal remains. The second collection is a subset of donors to the University of Tennessee skeletal collection. These 30 individuals were analyzed using Raman spectrometry to calculate IRIS derived isotopic values and to explore the potential of using IRIS and Raman spectrometry to reassociate individuals. The effects of diagenesis on the isotopic data derived from both IRMS and IRIS methods were explored using measures of correlation between isotopic values and diagenetic indices. Raman spectra from the donors to the University of Tennessee collection were collected from a total of six sampling locations along long bones from superior to inferior and anterior to posterior and from three locations along the second rib. This distribution of sampling locations allowed the exploration of intra-element variation in biogeochemical data. Testing intra-element variation was accomplished through both parametric and non-parametric ANOVA analyses as well as deviations from the mean for each sampling location. Lastly, analyses of re-association were accomplished using both a threshold method and a logistic regression for isotopic data and through a Bayes Gaussian Mixture Model for Raman spectra without the application of IRIS. In the following chapter, I present the results from each of these analyses.



## CHAPTER FIVE

### RESULTS

In this chapter I present the results for each of the analyses conducted on the individuals from the site of Patakfalva-Papdomb and the donors from the University of Tennessee Skeletal Collection. First, I present the correlation between Raman spectrometry and isotopic data from apatite to evaluate whether Raman spectrometry can be successfully used as a proxy for traditional Isotope Ratio Mass Spectrometry (IRMS) isotopic analyses for human skeletal remains, as predicted in hypothesis one. The results of calculating diagenetic indices are presented as they correlate to isotopic data from both the IRMS and the IRIS techniques to explore the prediction of hypothesis two that IRIS and IRMS data are equally affected by diagenetic alteration. In testing of hypothesis three, on the application of intra-element variation to reassociation of skeletal remains, I present the results of testing intra-element variation in stable isotope data on the donors from the University of Tennessee Skeletal Collection, first exploring the IRMS- and IRIS-derived isotopic data distributions across sampling locations, skeletal elements, and individuals and then by calculating mean deviations for each sampling location. Finally, I examined the potential for using isotopic data in the re-association of skeletal remains using a previously defined threshold method and applying a logistic regression to isotopic value differences. This question is further explored through the use of variance maximization and clustering algorithms to test the possibility of using Raman spectrometry alone in the reassociation of skeletal remains of individuals. The replicability of the methodology at each step of the process is tested through duplicated analyses and presented along with the results.

## Raman Analysis and IRIS Protocol for Human Skeletal Remains

Results from the isotopic analysis of apatite from the remains of individuals representing the Patakfalva-Papdomb site fit within expected  $\delta^{13}\text{C}_{\text{apatite}}$  and  $\delta^{18}\text{O}_{\text{vpdb}}$  for their historical diet and region and demonstrate appropriate precision (Bethard et al., 2022; Trent et al., 2020)(Figure 8). Precision was estimated by duplicating eight of the samples and comparing their final isotopic values. The calculated mean absolute error (MAE) for the duplicated samples was 0.15‰ for  $\delta^{13}\text{C}_{\text{apatite}}$  and 0.25‰ for  $\delta^{18}\text{O}_{\text{vpdb}}$  demonstrating good correlation between original values and duplicate values and confirming the reliability of the results. The range for the  $\delta^{13}\text{C}_{\text{apatite}}$  values, between -15.15‰ and -11.64‰ ( $\bar{x} = -13.15\%$ ,  $\text{sd} = 0.646$ ), is consistent with these individuals having a mostly  $\text{C}_3$  plant diet, likely wheat. In fact, the values of the individuals not associated with an intact burial trend toward lower  $\delta^{13}\text{C}$  than the individuals from intact burials, but they remain well within the 1.2‰ MMD, and also seem to have reduced variation in  $\delta^{13}\text{C}_{\text{apatite}}$  values (Pestle, Crowley, et al., 2014)(Figure 8). The range in  $\delta^{18}\text{O}_{\text{vpdb}}$  values between -9.26‰ and -6.58‰ ( $\bar{x} = -8.08\%$ ,  $\text{sd} = 0.568$ ), while again slightly lower than values from individuals associated with a burial, are also well within the 3.2‰ MMD (Pestle, Crowley, et al., 2014)(Figure 8). For the unassociated individuals, the  $\pm 2.7\%$  in  $\delta^{18}\text{O}_{\text{vpdb}}$  cannot be interpreted as being significant variation, unlike the range in variation observed in the individuals from isolated burials. These isotopic values were then used as the basis for calibrating the IRIS method of isotopic analysis using Raman spectrometry from the individuals representing the Patakfalva-Papdomb site.

Although spectra were originally cropped to the fingerprint region ( $400\text{cm}^{-1}$  to  $1900\text{cm}^{-1}$ ), intense fluorescence in all of the samples led to unexpected fluorescence-based oscillations that

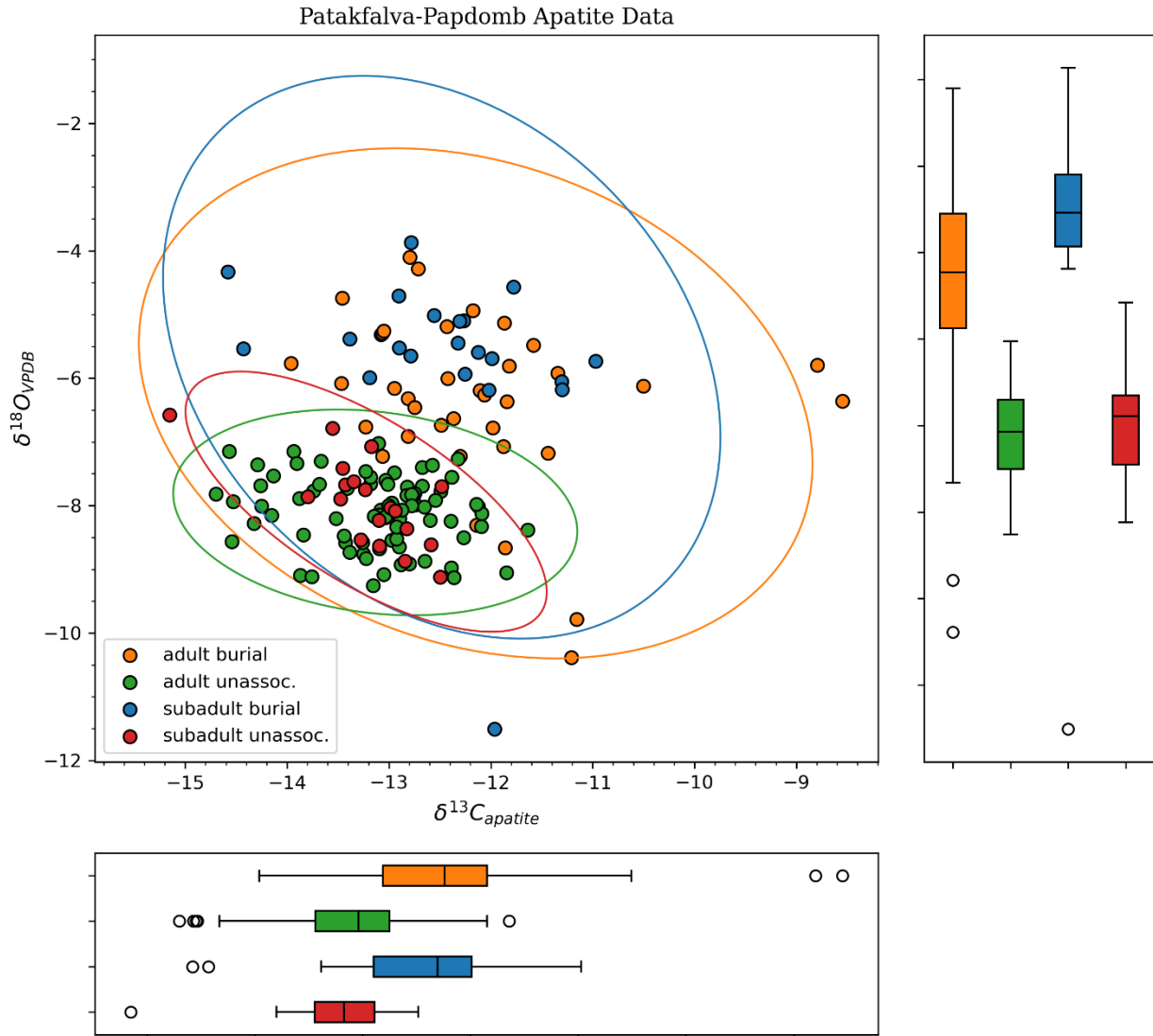


Figure 8. Scatter plot of the  $\delta^{13}C_{\text{apatite}}$  and  $\delta^{18}O_{\text{VPDB}}$  results from IRMS analysis of bone apatite. Results are grouped by mortuary context (burial or unassociated) and age category (adult or subadult). Burial apatite data from Bethard et al. (2022). Marginal scatter plots summarize the grouped data.

obscured all signal below  $775\text{ cm}^{-1}$ , therefore all spectra were cropped further to remove all signal below this frequency and avoid the noise. Spectra were then baseline corrected using the arPLS algorithm, smoothed to remove extrinsic noise using a Savitsky-Golay algorithm, and normalized to the highest peak ( $\nu_1\text{ PO}_4$ ). The quality control assessment detailed in the section on diagenesis in Chapter Four was applied to all spectra. This assessment is based on the finding of significant peaks around  $850\text{cm}^{-1}$  and  $930\text{cm}^{-1}$ , which are not expected in Raman spectra of human skeletal remains.

Using this quality control threshold assessment, all original and duplicate spectra were categorized into either “Great,” “Good,” “Fair,” or “Bad” using the criteria described in Chapter Four. Only scans qualifying as “Good” or “Great” in the quality control criteria, for both originals and duplicates, were selected for regression modeling. This reduced the sample size to 48 original scans and 32 duplicate scans, for a total sample size of 80 scans for the individuals from the Patakfalva-Papdomb site. Since random noise in a spectrum may inadvertently affect the Lasso linear regression model by keeping coefficients that may not actually describe the relationship between spectra and isotopic values, duplicate scans and original scans were combined into a single dataset and then split into randomly selected training and testing groups, with 90% of scans in the training group and 10% in the testing group, to validate the model.

Iterative testing for the selection of  $\lambda$  for the Lasso model estimated that the most appropriate  $\lambda$  for the  $\delta^{13}\text{C}_{\text{apatite}}$  model was 0.0889 leading to 25 variables selected for that model and  $\lambda$  for the  $\delta^{18}\text{O}_{\text{vpdb}}$  model was 0.16 leading to only three variables selected. The peak locations for  $\text{PO}_4$  and  $\text{CO}_3$  were found to not be significant in either linear regression model but instead the heights of various peak bands at particular frequencies were selected as independent variables for each model. Some of the bands selected are incidental since the model is only an approximation

of the real relationship between the spectrum and the isotopic values (all peak locations used in the linear model can be found in Appendix IV). However, some of these frequencies correlate to values that have significance in the molecular structure of bone (Table 5).

The  $\delta^{13}\text{C}_{\text{apatite}}$  model fits the training data moderately well ( $R^2 = 0.664$ ,  $\text{RMSE} = 0.64$ ,  $\text{MAE} = 0.47$ ) while the  $\delta^{18}\text{O}_{\text{vpdb}}$  model did not converge on a solution ( $R^2 = 0.081$ ,  $\text{RMSE} = 0.55$ ,  $\text{MAE} = 0.33$ ) (Figure 9). While the  $\delta^{18}\text{O}_{\text{vpdb}}$  model consistently had absolute error values below the MMD for the testing data, the model clearly does not demonstrate a good fit and cannot be used to estimate  $\delta^{18}\text{O}$  isotopic values (Figure 10). The low  $R^2$  result and the vertical relationship between IRIS- and RISM-derived values in Figure 9 demonstrate that for  $\delta^{18}\text{O}_{\text{vpdb}}$ , the model is using the mean of the reference sample as the primary regressor instead of attempting to fit the reference spectral data to the IRMS values. On the other hand, the  $\delta^{13}\text{C}_{\text{apatite}}$  model maintained absolute errors within the MMD for all data, and therefore was used in the exploration of intraskeletal biogeochemical variation (Figure 10).

### **Diagenesis, IRMS, and IRIS**

Indices of diagenesis were compared to isotopic values to explore correlations that inform the reliability of the results. Prior to sample-size reduction, all indices of diagenesis were calculated to test their relationship to the quality control measure for each spectrum. The Fluorescence Ratio index was calculated for all spectra, ranging from 0.74 to 0.96 ( $\bar{x} = 0.90$ ,  $\text{sd} = 0.033$ ) or between 74% and 96% of the spectral signal being obscured by fluorescence. After baseline correction and smoothing, the  $\text{CI}_{\text{raman}}$  ( $\bar{x} = 0.30$ ,  $\text{sd} = 0.022$ , [0.26 – 0.4]),  $\text{Amide(I)}\backslash\text{PO}_4$  ( $\bar{x} = 8.68$ ,  $\text{sd} = 2.718$ , [2.99 – 19.21]), and  $\text{CO}_3\backslash\text{PO}_4$  ( $\bar{x} = 0.43$ ,  $\text{sd} = 0.103$ , [0.22 – 0.81]) indices were also calculated (Table 6). All indices, with the exception of some higher values for

Table 5. Raman bands and their molecular assignment selected for the IRIS linear regression model. Their relationship and the strength of that relationship in the model are presented.

| Peak Band<br>Positions (cm <sup>-1</sup> ) | $\delta^{13}\text{C}_{\text{apatite}}$ |                          | $\delta^{18}\text{O}_{\text{vpdb}}$ |                          | Assignment                  |
|--|--|--------------------------|-------------------------------------|--------------------------|-----------------------------|
|  | Relationship                           | Strength of Relationship | Relationship                        | Strength of relationship |                             |
| 860-914                                    | Indirect                               | Weak                     |                                     |                          | Proline                     |
| 1002                                       | Direct                                 | Moderate                 |                                     |                          | Phenylalanine               |
| 1070                                       | Direct                                 | Moderate                 |                                     |                          | B-type v1 CO <sub>3</sub>   |
| 1252                                       |  |                          | Indirect                            | Strong                   | Amide III                   |
| 1410-1500                                  | Direct                                 | Strong                   |                                     |                          | $\delta$ NH, C-H<br>Bending |
| 1594-1734                                  | Indirect                               | Moderate                 |                                     |                          | Amide I                     |

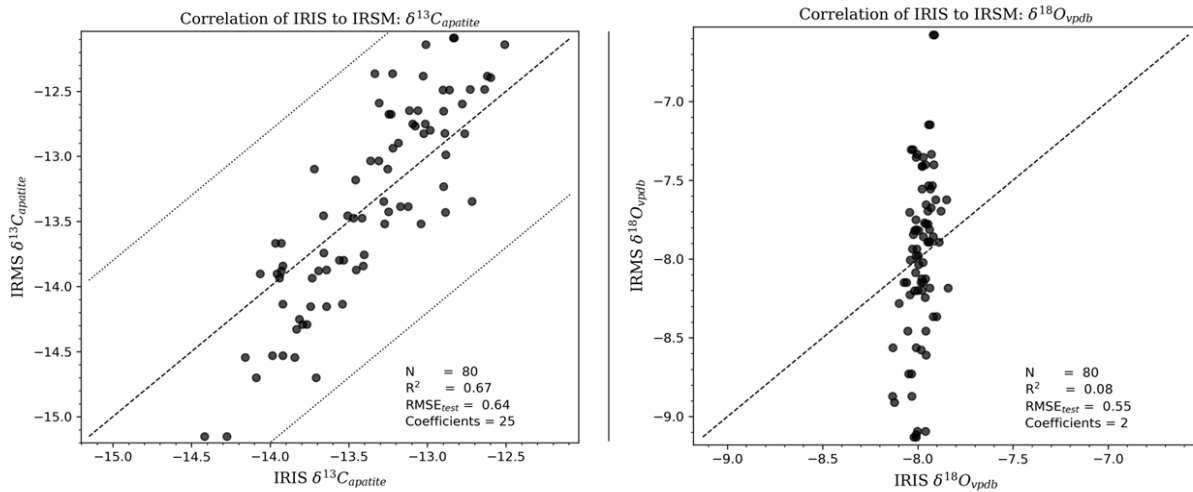


Figure 9. Correlation plots of IRIS derived and IRMS derived isotopic ratio values for  $\delta^{13}\text{C}_{\text{apatite}}$  (left) and  $\delta^{18}\text{O}_{\text{vpdb}}$  (right). Bands demonstrating the MMD (Pestle et al., 2014) are visible on the correlation plot for  $\delta^{13}\text{C}$  but the spread of original values for  $\delta^{18}\text{O}$  is too close for the MMD bands to be visible.

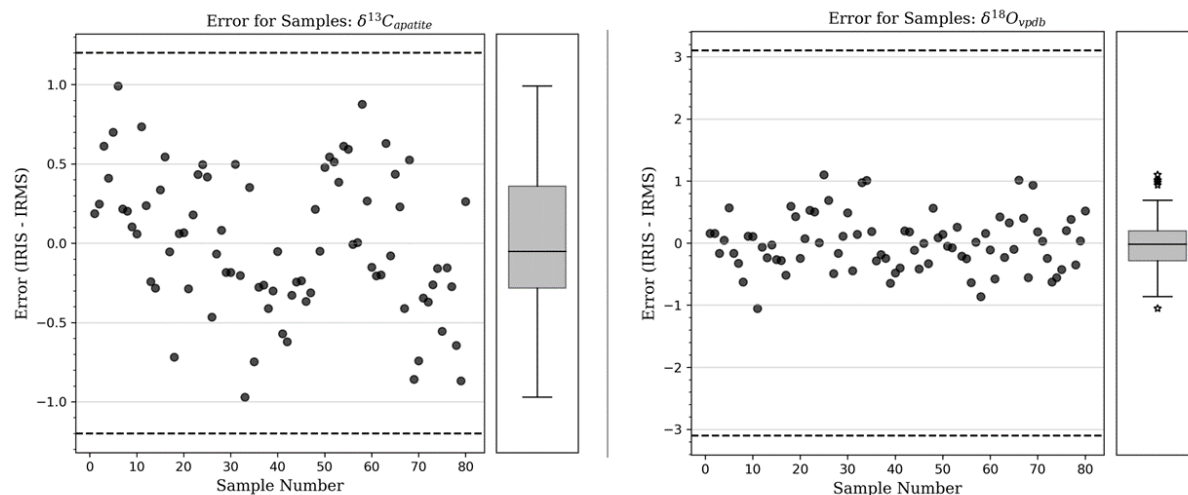


Figure 10. Error for the  $\delta^{13}\text{C}_{\text{apatite}}$  (left) and  $\delta^{18}\text{O}_{\text{vpdb}}$  (right) models for each sample spectrum in the testing dataset. Box plots on the right margin of each scatter plot show the distribution of the error and dashed lines in the error scatter plots show the MMD value (Pestle et al., 2014).

Table 6. Summary statistics for indices of diagenesis calculated from all Raman spectra.

|       | Fluorescence Ratio | $\text{CI}_{\text{raman}}$ | Amide(I)\PO <sub>4</sub> | CO <sub>3</sub> \PO <sub>4</sub> |
|-------|--------------------|----------------------------|--------------------------|----------------------------------|
| Mean  | 0.90               | 0.30                       | 8.68                     | 0.43                             |
| SD    | 0.033              | 0.022                      | 2.718                    | 0.103                            |
| Range | 0.74 – 0.96        | 0.26 – 0.4                 | 2.99 – 19.21             | 0.22 – 0.81                      |

CO<sub>3</sub>/PO<sub>4</sub>, fit within the expected ranges for bone that has not been significantly diagenetically altered. To ensure the quality control assessment was related to other indices of diagenesis rather than a stochastic difference between samples, a Kendall's  $\tau_c$  test was applied. The Kendall's  $\tau_c$  analysis showed significant correlations between the quality control assessment and the calculated indices, showing a moderate direct correlation with Amide(I)/PO<sub>4</sub> ( $\tau_c = 0.414$ ,  $p < 0.001$ ,  $\eta^2 = 0.37$ ) and strong indirect correlations for CO<sub>3</sub>/PO<sub>4</sub> ( $\tau_c = -0.567$ ,  $p < 0.001$ ,  $\eta^2 = 0.61$ ) and the Fluorescence Ratio ( $\tau_c = -0.655$ ,  $p < 0.001$ ,  $\eta^2 = 0.73$ ). No correlation was observed between the quality control assessment and the CI<sub>raman</sub> ( $\tau_c = 0.008$ ,  $p = 0.923$ ). Figure 11 demonstrates these correlations using boxplots.

For proceeding analyses, only indices of diagenesis calculated from Raman spectra classified as “good” or “great” using the quality control criteria were used. Indices of diagenesis from the selected spectra for the Patakfalva-Papdomb individuals showed no indication of diagenetic alteration with CI<sub>raman</sub> ( $\bar{x} = 0.31$ ,  $sd = 0.0195$ , [0.277 – 0.367]), Amide(I)/PO<sub>4</sub> ( $\bar{x} = 9.72$ ,  $sd = 2.981$ , [4.703 – 19.215]), and CO<sub>3</sub>/PO<sub>4</sub> ( $\bar{x} = 0.37$ ,  $sd = 0.083$ , [0.220 – 0.607]) values falling well within expected ranges for each index, with the exception of one outlier in the CO<sub>3</sub>/PO<sub>4</sub> index.. The majority of the spectra from the donors to the University of Tennessee skeletal collection also fell within the expected ranges for unaltered bone with CI<sub>raman</sub> ( $\bar{x} = 0.29$ ,  $sd = 0.011$ , [0.251 – 0.351]), Amide(I)/PO<sub>4</sub> ( $\bar{x} = 12.30$ ,  $sd = 4.457$ , [4.591 – 34.837]), and CO<sub>3</sub>/PO<sub>4</sub> ( $\bar{x} = 0.34$ ,  $sd = 0.060$ , [0.216 – 0.612]). However, some notable exceptions were present in the Amide(I)/PO<sub>4</sub> and the CO<sub>3</sub>/PO<sub>4</sub> indices. Approximately 5.9% of the donors ( $n = 42$ ) had Amide(I)/PO<sub>4</sub> values above the expected threshold and approximately 16.9% of the donors ( $n = 120$ ) had CO<sub>3</sub>/PO<sub>4</sub> values outside the expected range. While these range and threshold values provide a simple test of reliability, the best approach to explore isotope value



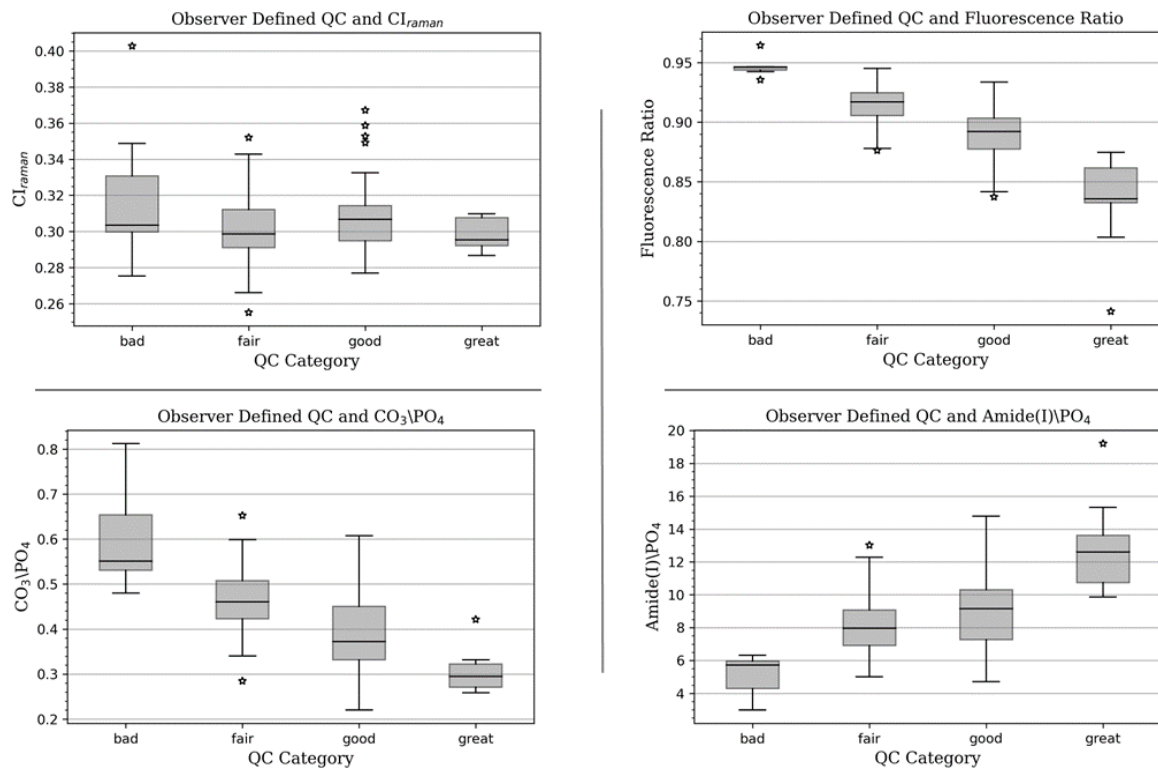


Figure 11. Boxplots showing the correlations between the calculated indices of diagenesis and the assessed quality control categories.

reliability is to test for potential correlations between the indices of diagenesis and the isotopic values. Since a single distribution is being compared to three other distributions, a Bonferroni correction for the  $\alpha$  was implemented, adjusting the significance level from 0.05 to 0.0167.

Prior to testing for correlation, the distributions must be checked for outliers following the assumptions required for a Pearson's  $r$  correlation coefficient analysis. The Patakfalva-Papdomb individuals included no outliers in any of the values while the University of Tennessee donors included a small number of outliers in all the distributions, requiring the use of a Spearman's  $\rho$  rank correlation coefficient analysis. The Patakfalva-Papdomb individuals showed no significant correlation for either  $\delta^{13}\text{C}_{\text{apatite}}$  for  $\text{CI}_{\text{raman}}$  ( $r = 0.115$ ,  $p = 0.437$ ), Amide(I)/ $\text{PO}_4$  ( $r = -0.193$ ,  $p = 0.188$ ), and  $\text{CO}_3/\text{PO}_4$  ( $r = 0.323$ ,  $p = 0.025$ ) or for  $\delta^{18}\text{O}_{\text{vpdb}}$  for  $\text{CI}_{\text{raman}}$  ( $r = -0.095$ ,  $p = 0.520$ ), Amide(I)/ $\text{PO}_4$  ( $r = -0.053$ ,  $p = 0.719$ ), and  $\text{CO}_3/\text{PO}_4$  ( $r = -0.146$ ,  $p = 0.321$ ). The University of Tennessee donors showed no significant correlation between  $\delta^{13}\text{C}_{\text{IRIS}}$  and  $\text{CI}_{\text{raman}}$  ( $\rho = -0.025$ ,  $p = 0.509$ ) or Amide(I)/ $\text{PO}_4$  ( $\rho = 0.011$ ,  $p = 0.769$ ) but did demonstrate a significant correlation between  $\delta^{13}\text{C}_{\text{IRIS}}$  and  $\text{CO}_3/\text{PO}_4$  ( $\rho = 0.137$ ,  $p < 0.001$ ). However, the effect size measured by  $\rho$  is small for a rank correlation.

Since the sample size for the University of Tennessee donors may obscure patterns in the correlation by having more numerous uncorrelated values overpower the underlying correlations, the donors whose indices of diagenesis were found to exceed the expected thresholds were separated and the correlations were again analyzed. For donors falling outside the expected range for Amide(I)/ $\text{PO}_4$ , the  $\text{CI}_{\text{raman}}$  ( $\rho = 0.46$ ,  $p = 0.002$ ) and  $\text{CO}_3/\text{PO}_4$  ( $\rho = 0.43$ ,  $p = 0.004$ ) results showed significant correlations with  $\delta^{13}\text{C}_{\text{IRIS}}$  values with moderate effect sizes while the Amide(I)/ $\text{PO}_4$  ( $\rho = -0.348$ ,  $p = 0.02$ ) results had no such correlation to  $\delta^{13}\text{C}_{\text{IRIS}}$ . For those donors whose Amide(I)/ $\text{PO}_4$  values were within expected ranges for unaltered bone, no correlations

were observed for either  $CI_{\text{raman}}$  ( $\rho = -0.049$ ,  $p = 0.21$ ) or Amide(I)/ $PO_4$  ( $\rho = 0.028$ ,  $p = 0.46$ ) values, but a significant correlation was found for  $CO_3/PO_4$  values ( $\rho = 0.126$ ,  $p = 0.0011$ ) when compared to  $\delta^{13}C_{\text{IRIS}}$ , although the effect size was again small. For donors falling outside the expected range of  $CO_3/PO_4$  values, no significant correlations were found between any of the indices and  $\delta^{13}C_{\text{IRIS}}$  values (all  $\rho < 0.2$ , all  $p > 0.01$ ), while for those donors whose  $CO_3/PO_4$  values fell within the expected ranges for unaltered bone only the  $CO_3/PO_4$  values ( $\rho = 0.122$ ,  $p = 0.003$ ) showed any significant correlation with  $\delta^{13}C_{\text{IRIS}}$  values, but again with a small effect size, while Amide(I)/ $PO_4$  and  $CI_{\text{raman}}$  had non-significant correlations (all  $\rho < 0.04$ , all  $p > 0.3$ ).

### **Intra-element Variation in Biogeochemical Data**

The first exploration of intra-element variation used the IRMS derived isotopic values from the samples representing individuals from the site of Patakfalva-Papdomb. Twenty-two elements from this collection had at least two sites sampled along the length of the element. These included an ilium, a rib, ulnae, humeri, femora, and tibiae. On average, isotopic values between sampling locations of a single element were consistent and maintained a mean absolute error (MAE) below the duplication precision results and well below the expected results for intraskeletal variation. MAE for  $\delta^{13}C_{\text{apatite}}$  values within skeletal elements was 0.139‰ ( $\bar{x} = -0.021$ ,  $sd = 0.311$ , 95% C.I. [-0.64 – 0.6]) while MAE for  $\delta^{18}O_{\text{vpdb}}$  values 0.206‰ ( $\bar{x} = -0.101$ ,  $sd = 0.474$ , 95% C.I. [-1.05 – 0.85]). Comparing these to the IRMS duplication results for the same location on the same skeletal element,  $\delta^{13}C_{\text{apatite}}$  duplication values varied slightly more at 0.15‰ MAE and similarly  $\delta^{18}O_{\text{vpdb}}$  duplication values also varied slightly more at 0.25‰ MAE, suggesting no significant difference between sampling locations along a single skeletal element.

For the analysis of the donors to the University of Tennessee Skeletal Collection, all

Raman scans underwent baseline correction, smoothing, and normalization following the same protocols as those used for the Patakfalva-Papdomb individuals. Since Raman scans had been duplicated for three donors, those duplicated scans were also baseline corrected and smoothed and were compared to the corresponding original data using a Spearman's  $\rho$  rank correlation. As expected for duplications, all duplicate scans were strongly correlated ( $p < 0.001$ ,  $\rho > 0.7$ ).

Raman spectra of the donors from the University of Tennessee collection also underwent the quality control categorization to remove spectra that may have had abundant fluorescence prior to further analyses.

Of the total 1,170 scans (39 scans for 30 individuals), 461 scans were classified as “Bad” or “Fair” (~39.4%) while 709 were classified as “Good” or “Great” (~60.6%). Only those classified as “Good” or “Great” were selected for further analysis. Total sample size decreased to 29 individuals and the number of scans for each sample location also decreased (Table 7). The Lasso linear regression model for  $\delta^{13}\text{C}_{\text{apatite}}$  was then applied to each of the spectra and the resulting isotopic values of  $\delta^{13}\text{C}_{\text{IRIS}}$  were used to explore the intra-element variation across the complete individuals. Isotopic results for the donors were internally consistent but appear to be significantly different from expected  $\delta^{13}\text{C}_{\text{apatite}}$  values for contemporary residents of North America. Average  $\delta^{13}\text{C}_{\text{IRIS}}$  value for these individuals was -13.64‰ (sd = 0.366, [-14.80 – -11.10]), approximately 2.61‰ depleted in  $^{13}\text{C}$  on average than expected for a contemporary American population ( $\bar{x} = -11.04\text{‰}$ ), but having a similar expected range for that population of approximately 3.98‰ (Berg et al., 2022).

To explore intra-element isotopic variation, four differences in the isotopic distributions were tested: 1) differences between individuals at the total isotopic distribution level, 2) differences between sampling locations across the entire individual, 3) differences between

skeletal elements, and 4) differences between sampling locations among any of the bones to test for patterns that may arise anterior to posterior or superior to inferior. To compare differences between individuals to differences within individuals, the  $\delta^{13}\text{C}_{\text{IRIS}}$  values of the donors were first grouped by individual and analyzed. A Levene's test for heteroscedasticity demonstrated that variance was significantly different between individuals ( $W = 2.10$ ,  $p < 0.001$ ), therefore a non-parametric Welch's ANOVA was conducted and demonstrated significant differences in isotopic values between individuals with a moderate effect size ( $F = 6.803$ ,  $p < 0.001$ ,  $\omega^2 = 0.19$ ) (Delacre, Leys, Mora, & Lakens, 2019; Moder, 2016; Tomczak & Tomczak, 2014).

The next two tests, comparing individuals by sampling location and comparing skeletal elements both passed the Levene's test ( $W = 0.937$ ,  $p = 0.58$ ;  $W = 1.12$ ,  $p = 0.35$ , respectively), therefore a classical ANOVA was conducted for each and found no significant difference ( $F = 1.117$ ,  $p = 0.29$ ,  $\eta^2 = 0.06$ ;  $F = 2.008$ ,  $p = 0.06$ ,  $\eta^2 = 0.016$ , respectively). Since the ANOVA were conducted on samples from the same individuals, repeated measures may reinforce the mean and reduce the variance such that the ANOVA results may be affected, so interpretations must be made with this potential bias in mind. Lastly, differences stemming from the location sampled, either more proximally or more distally or anterior to posterior regardless of individual, also passed the Levene's test ( $W = 1.27$ ,  $p = 0.28$ ) and, similarly, a classical ANOVA found no significant difference between sampling locations ( $F = 1.26$ ,  $p = 0.28$ ,  $\eta^2 = 0.009$ ).

To further explore differences within skeletal elements, their mean deviation was explored. Mean deviation across locations for all individuals averaged approximately  $-0.0026\%$  ( $sd = 0.0678$ , 95% C.I.  $[-0.1383 - 0.1535]$ ). All mean deviations were below the standard deviation of the distribution of  $\delta^{13}\text{C}_{\text{IRIS}}$  at each location and well below the 95% C.I. for each location, suggesting that differences between individuals and between skeletal elements far

supersede deviations from the mean at each location (Table 7). Figure 12 through Figure 14 visually demonstrate these mean deviations and their significance when compared to the standard deviation for each sampling location along a skeletal element.

### **Reassociation of Skeletal Remains using Biogeochemistry**

The threshold model for reassociation using isotopic values created by Berg et al. (2022) was applied to the samples representing the Patakfalva-Papdomb individuals to explore the possibilities of reassociation. For  $\delta^{13}\text{C}_{\text{apatite}}$ , the thresholds created by Berg et al. (2022) are 1.55‰ at the 95% confidence level that the samples are probably from different individuals and 1.90‰ at the 99% confidence level that the samples are from different individuals. The assumption is that all samples coming from different elements in this collection of individuals are from different individuals. Although this is debatable, it is highly likely considering the number of individuals excavated from Patakfalva-Papdomb and the unassociated nature of the remains here represented. For this collection, since no false negatives were detected (i.e., no value exceeded the threshold when originating from the same individual), the specificity and positive predictive value (PPV) were both 100%. However, the threshold system has sensitivity and negative predictive values (NPV) that are concerning when using this approach. The 95% threshold had a sensitivity of 9.78% and a negative predictive value of 1.12%, while the 99% threshold did slightly worse with a sensitivity of 4.36% and a negative predictive value of 1.06%.

The threshold approach was also applied to the University of Tennessee donors using the  $\delta^{13}\text{C}_{\text{IRIS}}$  values. This larger sample gave predictive values closer to the expectations set forth by Berg et al. (2022). At the 95% confidence threshold, the specificity and positive predictive value were high at approximately 99.4% and 97.3% respectively. As before, the sensitivity and

Table 7. Mean deviation table for skeletal element and location demonstrating that no sampling location deviates by more than the 95% C.I. of the distribution of  $\delta^{13}\text{C}_{\text{IRIS}}$  values.

| Skeletal Element | Location  | N     | $\delta^{13}\text{C}_{\text{IRIS}}$ mean for location | Individual mean $\delta^{13}\text{C}_{\text{IRIS}}$ S.D. | Mean deviation at location | 95% C.I. for $\delta^{13}\text{C}_{\text{IRIS}}$ |
|------------------|-----------|-------|---|--|----------------------------|--|
| Rib              | Vertebral | 14    | -13.8   | 0.361  | -0.0468                    | $\pm 0.721$                                      |
|                  | Midshaft  | 16    | -13.7   | 0.347  | 0.0560                     | $\pm 0.693$                                      |
|                  | Sternal   | 9     | -13.7   | 0.298  | -0.0268                    | $\pm 0.595$                                      |
| Humerus          | Anterior  |       |   |  |                            |  |
|                  | Superior  | 12    | -13.6   | 0.319  | 0.0231                     | $\pm 0.638$                                      |
|                  | Midshaft  | 21    | -13.6   | 0.280  | 0.1213                     | $\pm 0.560$                                      |
|                  | Inferior  | 21    | -13.8   | 0.285  | -0.1299                    | $\pm 0.569$                                      |
|                  | Posterior |       |   |  |                            |  |
|                  | Inferior  | 23    | -13.7   | 0.261  | -0.0367                    | $\pm 0.523$                                      |
|                  | Midshaft  | 17    | -13.7   | 0.281  | -0.0474                    | $\pm 0.562$                                      |
| Radius           | Anterior  |       |   |  |                            |  |
|                  | Superior  | 22    | -13.6   | 0.240  | 0.0664                     | $\pm 0.480$                                      |
|                  | Midshaft  | 25    | -13.7   | 0.236  | -0.0238                    | $\pm 0.472$                                      |
|                  | Inferior  | 23    | -13.6   | 0.229  | 0.0457                     | $\pm 0.457$                                      |
|                  | Posterior |       |   |  |                            |  |
|                  | Inferior  | 20    | -13.7   | 0.210  | 0.0014                     | $\pm 0.420$                                      |
|                  | Midshaft  | 23    | -13.8   | 0.227  | -0.0306                    | $\pm 0.453$                                      |
| Ulna             | Anterior  |       |   |  |                            |  |
|                  | Superior  | 22    | -13.5   | 0.275  | 0.1535                     | $\pm 0.551$                                      |
|                  | Midshaft  | 22    | -13.7   | 0.298  | -0.0371                    | $\pm 0.597$                                      |
|                  | Inferior  | 19    | -13.7   | 0.309  | -0.0999                    | $\pm 0.618$                                      |
|                  | Posterior |       |   |  |                            |  |
|                  | Inferior  | 18    | -13.7   | 0.308  | -0.0462                    | $\pm 0.616$                                      |
|                  | Midshaft  | 20    | -13.6   | 0.298  | 0.0276                     | $\pm 0.595$                                      |
| Femur            | Anterior  |       |   |  |                            |  |
|                  | Superior  | 19    | -13.7   | 0.248  | 0.0009                     | $\pm 0.495$                                      |
|                  | Midshaft  | 15    | -13.7   | 0.249  | -0.0602                    | $\pm 0.499$                                      |
|                  | Inferior  | 13    | -13.7   | 0.243  | -0.0266                    | $\pm 0.486$                                      |
|                  | Posterior |       |   |  |                            |  |
|                  | Inferior  | 16    | -13.6   | 0.284  | 0.0831                     | $\pm 0.568$                                      |
|                  | Midshaft  | 17    | -13.6   | 0.273  | -0.0006                    | $\pm 0.546$                                      |
| Superior         | 19        | -13.7 | 0.286   | -0.0047  | $\pm 0.573$                |  |

Table 7. Continued.

| Skeletal Element | Location  | N        | $\delta^{13}\text{C}_{\text{IRIS}}$ mean for location | Individual mean $\delta^{13}\text{C}_{\text{IRIS}}$ S.D. | Mean deviation at location | 95% C.I. for $\delta^{13}\text{C}_{\text{IRIS}}$ |             |
|------------------|-----------|----------|---|--|----------------------------|--|-------------|
| Tibia            | Anterior  | Superior | 21  | -13.5  | 0.285                      | 0.0324   | $\pm 0.57$  |
|                  |           | Midshaft | 23  | -13.4  | 0.278                      | 0.0764   | $\pm 0.556$ |
|                  |           | Inferior | 14  | -13.6  | 0.290                      | 0.0146   | $\pm 0.579$ |
|                  | Posterior | Inferior | 19  | -13.7  | 0.275                      | -0.0413  | $\pm 0.55$  |
|                  |           | Midshaft | 15  | -13.6  | 0.284                      | 0.0111   | $\pm 0.569$ |
|                  |           | Superior | 15  | -13.7  | 0.267                      | -0.1350  | $\pm 0.535$ |
| Fibula           | Anterior  | Superior | 16  | -13.5  | 0.275                      | 0.1535   | $\pm 0.551$ |
|                  |           | Midshaft | 19  | -13.7  | 0.298                      | -0.0371  | $\pm 0.597$ |
|                  |           | Inferior | 15  | -13.7  | 0.309                      | -0.0999  | $\pm 0.618$ |
|                  | Posterior | Inferior | 16  | -13.7  | 0.308                      | -0.0462  | $\pm 0.616$ |
|                  |           | Midshaft | 18  | -13.6  | 0.298                      | 0.0276   | $\pm 0.595$ |
|                  |           | Superior | 15  | -13.6  | 0.319                      | -0.0203  | $\pm 0.637$ |

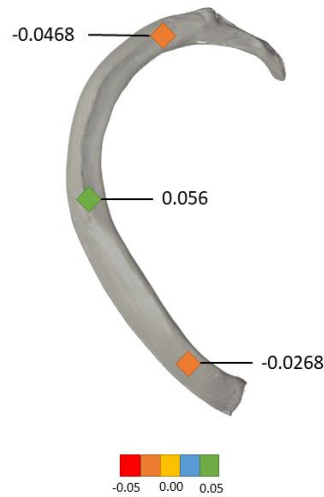


Figure 12. Visual representation of the mean deviation of  $\delta^{13}\text{C}_{\text{IRIS}}$  for the right second rib. View is superior. Colors represent magnitude and sign of deviation. Adapted from Šavlovskis and Raits (2021).



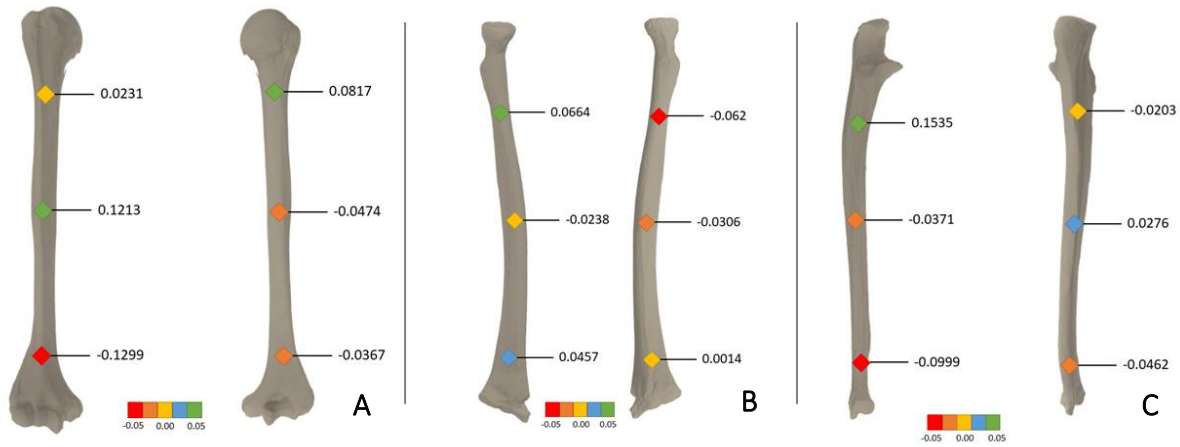


Figure 13. Visual representation of mean deviation of  $\delta^{13}\text{C}_{\text{IRIS}}$  for the right upper limbs: (A) humerus, (B) radius, and (C) ulna on both the anterior (left) and posterior (right) views. Colors represent the magnitude and sign of the deviation. Adapted from (Bauer, 2016).

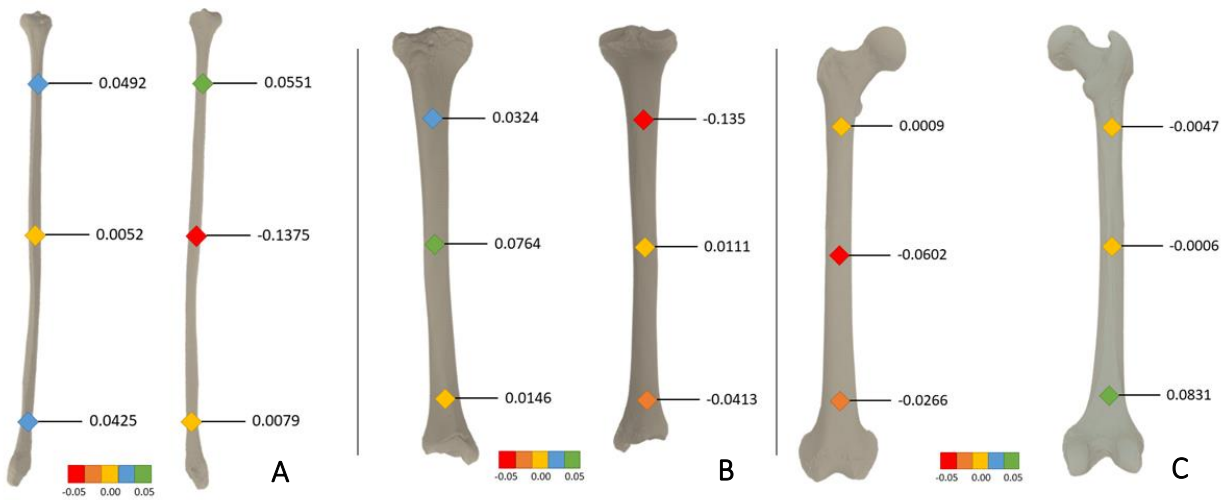


Figure 14. Visual representation of mean deviation of  $\delta^{13}\text{C}_{\text{IRIS}}$  for the right lower limbs: (A) fibula, (B) tibia, and (C) femur on both the anterior (left) and posterior (right) views. Colors represent the magnitude and sign of the deviation. Adapted from (Bauer, 2016).

negative predictive value were much lower at 0.84% and 3.82% respectively. There is no significant difference in the predictive power of the threshold approach at the 99% confidence level for the University of Tennessee donors, with specificity and positive predictive value at 99.7% and 96.3% respectively while the sensitivity and negative predictive value similarly had trivial reductions to 0.38% and 3.80% respectively. These results are exactly as expected when applying an exclusionary threshold approach.

While exclusionary threshold approaches are beneficial to assign a qualitative likelihood of two isotopic values belonging to different individuals, the application of a probabilistic model can often provide a more nuanced understanding and a probability value for association as well as exclusion. For this purpose, a logistic regression was fit to the data from the University of Tennessee donors and the Patakfalva-Papdomb individuals separately using a 10-fold, 1000-repeat cross-validation. The data from these collections were kept separate due to potential differences due to their differently derived isotopic values, namely IRMS derived and IRIS derived  $\delta^{13}\text{C}_{\text{vpdb}}$  values, and their potential to add a confounding factor. Logistic regression models showed high positive predictive values for both the Patakfalva-Papdomb individuals (99.1%) and the University of Tennessee donors (96.2%), however this is an artifact of the imbalance of the datasets. The logistic regression model ultimately created a threshold value larger than any observed variation within individuals. This is clearly observed in the specificity (0%) and negative predictive value (0%) for both sets of comparisons.

To increase the robusticity of the results from reassociation using both the threshold method and the logistic regression method, and to test the ability of spectral rather isotopic data in the reassociation of individuals, clustering based on Raman spectra was tested using complete spectral data and dimensionality reduction methods. PCA results demonstrated poor separation

between individuals based on maximized variance. The first six components only accounted for 59% of the variance in the collection of donors, but this is to be expected for the large number of independent variables in spectral data. An attempt at unsupervised clustering of the spectral data using a Bayesian Gaussian Mixture Model with a Dirichlet process led to poor results in estimating association between sampling locations (AMI = 0.220) but had a relatively good estimate of the number of individuals represented by creating 36 clusters, when 29 individuals were represented, but performed no better than a simple estimate of the minimum number of individuals based on repeated skeletal elements.

### **Summary**

In this chapter, I have presented the results of analyses for each of the three hypotheses outlined in Chapter One. These include the ability to use Raman spectrometry as a proxy to IRMS derived isotopic values, the effects of diagenesis on using IRIS derived values as a proxy for IRMS derived isotopic data, and the accuracy of using isotopic data to reassociate individuals by understanding intraskeletal and intra-element variation in isotopic values. The first hypothesis, on the application of IRIS as a proxy for IRMS isotopic values, was tested using IRMS analyses on the Patakfalva-Papdomb individuals and then testing of an IRIS protocol for the estimation of isotopic data from Raman spectra of human skeletal remain. Results demonstrated that IRIS is applicable for  $\delta^{13}\text{C}$  but is more problematic for  $\delta^{18}\text{O}$ . The second hypothesis, on the effects of diagenesis on IRMS and IRIS isotopic data, was tested through comparisons between indices of diagenesis and IRMS and IRIS derived isotopic values using parametric and non-parametric correlation coefficients. Results suggest that IRIS and IRMS derived isotopic values are equally susceptible to diagenetic effects, with neither being more

reliable than the other. The third hypothesis, on the use of intra-element isotopic variation in the reassociation of skeletal remains, was explored through intraskeletal and intra-element variation in isotopic data using both IRMS and IRIS approaches and the testing of reassociation of individuals using isotopic data applying both a threshold method and a logistic regression based on differences in isotopic values. Intra-element variation was far below intra-skeletal variation in both IRMS and IRIS derived isotopic values. Reassociation using a threshold method for exclusion was successful within its constraints but an attempt at logistic regression modeling was unsuccessful. In the following chapter, I contextualize these results within the existing literature of stable isotope analysis, necrodominance, bone remodeling, and diagenesis.

## CHAPTER SIX

### DISCUSSION

In this chapter I explore the significance of the results of each analysis as they relate to the outlined hypotheses on 1) Isotope Ratio Infrared Spectrometry (IRIS) as a proxy for Isotope Ratio Mass Spectrometry (IRMS), 2) the effects of diagenesis on IRMS and IRIS derived values, and 3) intraskeletal and intra-element variation in isotopic data and the potential for isotopic data to be used in the reassociation of skeletal remains. First, I contextualize the results of the comparison between IRMS and IRIS and outline the preliminary nature of the IRIS methodology but demonstrate the potential for the future offered by these results. Then, I explore the results of the effects of diagenesis on both IRMS and IRIS derived isotopic values and compare these methods as they correlate to indices of diagenesis. This is then followed by an exploration of the results of testing intra-element isotopic variation in bioapatite using both IRMS and IRIS methods and the implications of these results to future isotopic analyses. Lastly, that exploration of intra-element and intraskeletal variation forms the foundation for the exploration of reassociation of commingled skeletal elements using isotopic data, using both the previously created method for reassociation of skeletal remains employing an exclusionary threshold (Berg et al., 2022) and the results from the exploration of logistic regression as a potential method for reassociation. Lastly, I contextualize this project and its results within necrodominance and outline ways that this project could have better served the needs of the communities represented by the remains being studied.

## **IRMS, IRIS, and the Future of Isotopic Analysis of Human Skeletal Remains**

The protocols for the collection of isotopic data from bioapatite using the traditional Isotope Ratio Mass Spectrometry (IRMS) method are, by now, well established (Berg et al., 2022; Chesson et al., 2019; Crowley & Wheatley, 2014; Pellegrini & Snoeck, 2016; Snoeck & Pellegrini, 2015) since the reliability of these methods has been standardized and generalized over a significant number of datasets with great variation in expected  $\delta^{13}\text{C}_{\text{apatite}}$  and  $\delta^{18}\text{O}_{\text{carbonate}}$  values. The results, therefore, of isotopic analyses of apatite from the individuals representing the site of Patakfalva-Papdomb using a traditional IRMS method fit well within previously identified  $\delta^{13}\text{C}_{\text{apatite}}$  and  $\delta^{18}\text{O}_{\text{vpdb}}$  ranges, even if slightly shifted due to minor differences between laboratories for the preparation and the mass spectrometry protocols. These IRMS results identify a mostly C<sub>3</sub>, as previously characterized (Bethard et al., 2022). The variation of  $\delta^{18}\text{O}_{\text{vpdb}}$  values for the individuals from the overburden is small, approximately  $\pm 2\%$ , suggesting a relatively local cohort of individuals. However, this is in contrast to the  $\delta^{18}\text{O}_{\text{vpdb}}$  values for the individual burials that extend approximately  $\pm 6\%$ , suggesting a much broader geographic range for those individuals. This much broader geographic range may be related to residential mobility in the region, or it may be related to shifts in the source of water over time. These differences are unlikely to be the result of seasonal variation due to the contrast between the unassociated and associated individuals. They are also unlikely to represent differences related to social status since the  $\delta^{13}\text{C}_{\text{apatite}}$  values suggest a similar diet across the site. Therefore, these differences may relate to temporal shifts if the hypothesis that unassociated individuals were buried earlier and then disturbed to inter more recent individuals is supported. This hypothesis of disturbance, however, requires further study. With IRMS results fitting within expected values, I explored the

potential of applying Isotope Ratio Infrared Spectrometry (IRIS) from Raman spectrometry to the question of apatite isotopic analysis.

Fluorescence for all the Raman spectra, both from the donors to the University of Tennessee Skeletal Collection and from the Patakfalva-Papdomb individuals, significantly obscured the signal. The photobleaching process improved many of the spectra collected, but a significant amount of fluorescence remained. The origins of this fluorescence are unknown, but the Fluorescence Ratio correlated well with measures of the amount of organic matter remaining in the sample (Amide(I)/PO<sub>4</sub>) (see section on Diagenesis, Isotopes, and IRIS). The obscuring of the signal is likely a major factor in the difficulty of correlating Raman spectra to isotopic data from the human skeletal remains since those remains are likely to preserve collagen as well as other non-collagenous proteins that significantly fluoresce, as has previously been found in both Raman and FTIR (Golcuk et al., 2006; Pestle, Ahmad, Vesper, Cordell, & Colvard, 2014; Shea & Morris, 2002). As we learn more about the factors that cause fluorescence in Raman spectrometry, we may better account for these effects, especially when using a 785nm excitation wavelength. Algorithmic corrections may also be able to fix this issue as it relates to the oscillations observed in all spectra below 775cm<sup>-1</sup>, but further research must be conducted to support this approach. The use of 1064nm excitation wavelength may in fact improve the IRIS model by avoiding some of the fluorescence and noise even if the resolution is less refined, as other studies have found success in the application of this excitation wavelength (France et al., 2014; Madden et al., 2018; Pestle, Ahmad, et al., 2014). The trade-off of using 1064nm over 785nm is the lack of resolution, especially for smaller peaks, but the Lasso linear correlation appears to have selected larger peaks for correlation rather than the smaller peaks that require better resolution to assess.

Results from the IRIS protocol, when compared to the IRMS values, are promising but preliminary. For  $\delta^{13}\text{C}_{\text{apatite}}$ , the cross-validated model led to a moderate correlation for the Lasso linear model, with an  $R^2$  of 0.66, but a high root mean square of the error (RMSE), at approximately 0.64, as compared to the standard deviation of the sample, also approximately 0.64. This is potentially the result of a limited amount of variation in the  $\delta^{13}\text{C}$  values in the sample and may be improved by increasing the variance of the  $\delta^{13}\text{C}$  of the sample used for training the model. Absolute errors between IRMS-derived and IRIS derived isotopic values are well within interlaboratory deviations (Pestle, Crowley, et al., 2014), but are similarly skewed by the currently existing training data for  $\delta^{13}\text{C}$ . IRIS-derived  $\delta^{13}\text{C}$  values are approximately  $\pm 1\%$  from the IRMS derived values. While this precision is acceptable in whole-diet explorations comparing  $\text{C}_4$  and  $\text{C}_3$  diets, more nuanced questions will require the more precise IRMS methodology. This deviation between IRMS and IRIS may also be related to the superficial nature of the Raman spectrometry which cannot scan the intra-cortical envelope. However, with the current dataset,  $\delta^{18}\text{O}_{\text{carbonate}}$  values cannot be estimated using the IRIS methodology. Although mean absolute error (MAE) was low for the  $\delta^{18}\text{O}_{\text{carbonate}}$  Lasso linear regression, again the RMSE was high, approximating the standard deviation of 0.56, and ultimately the model had a very low  $R^2$  around 0.08, suggesting the mean of the sample alone was a better predictor than any regressor. This again may be related to the limited variation in  $\delta^{18}\text{O}$  in the sample, but regardless these results are less promising than the  $\delta^{13}\text{C}$  regression results.

One factor that may explain this discrepancy is elucidated by exploring the peak bands the Lasso model selected. When exploring  $\delta^{13}\text{C}_{\text{apatite}}$  and  $\delta^{18}\text{O}_{\text{carbonate}}$ , the peak bands that should have the strongest relationship should include B-type and A-type  $\nu_1 \text{CO}_3$  and their potential shifts related to the increased atomic weight of  $^{13}\text{C}$  (McKay et al., 2013; Vitkin et al., 2020). However,



the model found no such correlation between these peak bands and  $\delta^{18}\text{O}_{\text{carbonate}}$  and found only a moderate correlation to B-type  $\nu_1 \text{CO}_3$  for  $\delta^{13}\text{C}_{\text{apatite}}$ . The strongest direct correlation in the  $\delta^{13}\text{C}_{\text{IRIS}}$  model was with the CH bending band, while the strongest indirect correlation for the  $\delta^{18}\text{O}_{\text{IRIS}}$  model was with the Amide III band. Neither of these relate to carbonate replacement in the apatite lattice and instead relate to organic matter in the skeletal material. This fact explains the lack of correlation to the  $\delta^{18}\text{O}_{\text{carbonate}}$  values, since oxygen is a very small part of the Amide III vibrational mode and of all other potential organic peaks, only hydroxyproline potentially has one oxygen atom outside the amide bond. The only question, if the correlations are occurring with organic molecules instead of the crystal lattice, is why  $\delta^{18}\text{O}_{\text{carbonate}}$  does not relate to the Amide I peak band, which has a strong oxygen component. Potentially the reason is that carbonate oxygen and amide bond oxygen originate from different isotopic pools.

The Lasso model found good correlation between the Raman spectra and the  $\delta^{13}\text{C}_{\text{apatite}}$  values. However, the strongest relationships occurred with the organic component bands rather than the carbonate bands. Strong or moderately strong direct correlations occurred with phenylalanine and CH bending bands. Carbon in their molecular structure is very important and therefore these peak bands are likely to show significant differences based on isotopic replacement. The Amide I peak band also has a moderately strong correlation but its indirect in this case, potentially an attempt by the model to correct for the organic components affecting the correlation to  $\delta^{13}\text{C}_{\text{apatite}}$ . Isotopic pools for carbon in skeletal material are relatively the equivalent between collagen and apatite, with the main differences stemming from the processes of transamination (in the case of collagen-based carbon isotope values) and complete recreation of the carbonate molecule (in the case of  $\text{CO}_3$  replacements in the apatite lattice), often leading to an apatite-collagen spacing that is useful in isotopic interpretations when using IRMS (France &

Owsley, 2015; Hedges, 2003; Lee-Thorp et al., 1989). This spacing may explain the moderate correlation such that the IRIS model from Raman spectra is relying on the potential  $\delta^{13}\text{C}_{\text{collagen}}$  values to approximate the  $\delta^{13}\text{C}_{\text{apatite}}$  values. This can only be tested further with fitting the model to  $\delta^{13}\text{C}_{\text{collagen}}$  values. A good correlation with the same model between  $\delta^{13}\text{C}_{\text{collagen}}$  values and  $\delta^{13}\text{C}_{\text{IRIS}}$  values would suggest that the IRIS model fit to the organic content rather than the apatite, as originally intended in this study.

Despite these potentially confounding factors, the IRIS model was applied to the University of Tennessee donors to explore its application to an unknown set of individuals. When applied to the University of Tennessee donors, the range of isotopic values for  $\delta^{13}\text{C}_{\text{IRIS}}$  derived from IRIS approximated the expected variation for contemporary Americans (Berg et al., 2022). The range of isotopic values is not expected to be very large since overall contemporary American diets combine  $\text{C}_3$  and  $\text{C}_4$  plants, with a slightly higher proportion of  $\text{C}_4$  plants, what has been called a “supermarket” diet (Chesson, Podlesak, Thompson, Cerling, & Ehleringer, 2008; Schoeller, Minagawa, Slater, & Kaplan, 1986). However, the mean of the  $\delta^{13}\text{C}_{\text{apatite}}$  values was shifted by more than the MMD.

There are two potential explanations for this apparent shift. The simplest explanation is that the model could be overfitting to the training data and, while giving a proper variance, maybe be fitting too closely to the mean of the training data. The second possibility could be that isotopic fractionation is significantly different enough between bulk sampling used in IRMS and the periosteal focus of the Raman spectrometric analysis. The first potential problem of overfitting was mitigated through the use of 8-fold, 1000-repeat cross-validation, a process that ensures the model does not fit the training data alone by segmenting said training data and fitting the model over multiple iterations. While this mitigates the risk of overfitting, a dataset limited in

variance may still fall victim to this common problem. Only a more varied dataset can clarify the problem of overfitting. The potential for the latter, that a physiological difference may exist between the envelopes of bone, has a foundation in our understanding of these “envelopes” of bone, namely periosteal, haversian, and endosteal, and how these differ in remodeling rates, biomechanics, and physiology (Eriksen, 1986; Gosman, Stout, & Larsen, 2011; Robling et al., 2006). In fact, Maggiano et al. (2019) found a slightly different  $\delta^{18}\text{O}$  value in the intracortical envelope than the endosteal envelope, even when accounting for seasonally-derived variation. This question can only be further explored by segmenting samples into corresponding envelopes and using traditional IRMS to explore their potential variation in isotopic values. Due to the amount of sample required for each part of the biogeochemical preparation process, targeted bulk sampling must extend across the surface more than is currently standard, further increasing the destructive nature of the methodology. Such a destructive approach can only be justified from a biogeochemical standpoint, through support of the hypothesis that intra-element variation is lower than the MMD. While the results of this study cannot be used to support the replacement of IRMS by IRIS, they demonstrate a potential avenue for non-destructive isotopic methods that we must be compelled to explore in the future.

### **Diagenesis, Isotopes, and IRIS**

While the current IRIS models are not sufficiently precise to completely replace the traditional and well-established IRMS method, the effects of diagenesis are equivalent for each approach. The first step to exploring diagenesis was the use of the quality control criteria defined for this study. Using our understanding of Raman spectra for bone, the criteria were defined to exclude spectra that demonstrated artificial peaks related to fluorescence. These criteria were

then compared to the indices of diagenesis to examine their reliability for selecting spectra and explore the potential reasoning for the presence of fluorescence-based oscillations obscuring the Raman signal.

The fluorescence ratio defined for this study correlated well with the quality control criteria. Since the fluorescence ratio determined the percentage of signal that was obscured by the fluorescence, this correlation was to be expected if the criteria did in fact estimate the quality of the signal. These criteria, and therefore the fluorescence ratio, correlated well with the Amide(I)/PO<sub>4</sub> index, suggesting that fluorescence, and thereby the quality of the spectra, may be the result of all organic matter present in the remains, including collagenous and non-collagenous proteins. The relationship between CO<sub>3</sub>/PO<sub>4</sub> and the quality control criteria may be more closely related to the potential effects of fluorescence-based oscillations on the height of the CO<sub>3</sub> peak band rather than any direct correlation to the molecular structure. One example that suggests this may be the case is the CI<sub>raman</sub>, which, of all the indices of diagenesis, does not correlate at all with the quality criteria. This is because CI<sub>raman</sub> is based on the full width at half-maximum (FWHM) of the PO<sub>4</sub> peak rather than the peak height. Peak height may be affected by fluorescence oscillations, but FWHM would not be affected. However, the lack of correlation between quality and CI<sub>raman</sub> may also relate to the current debate on the applicability of CI<sub>raman</sub> to the question of diagenesis. While CI<sub>raman</sub> is frequently used in isotopic studies to estimate extent of diagenesis (Beasley et al., 2014; Ortiz-Herrero et al., 2021; Wright & Schwarcz, 1996) some scholars have cast doubt on its reliability as a measure of diagenesis (Puc at et al., 2004; Trueman et al., 2008) and suggest that CO<sub>3</sub>/PO<sub>4</sub> and Amide(I)/PO<sub>4</sub> are more reliable measures.

When exploring the indices of diagenesis and their relationship to IRIS and IRMS, the Amide(I)/PO<sub>4</sub> and CI<sub>raman</sub> indices showed no correlation to  $\delta^{13}\text{C}_{\text{apatite}}$  or  $\delta^{13}\text{C}_{\text{IRIS}}$  values when

within the expected ranges for bone that has not been diagenetically altered (France et al., 2014; Madden et al., 2018; Ortiz-Herrero et al., 2021). The  $\text{CO}_3/\text{PO}_4$  index, on the other hand, consistently shows a correlation to  $\delta^{13}\text{C}_{\text{apatite}}$  and  $\delta^{13}\text{C}_{\text{IRIS}}$  even for diagenetically unaltered bone identified using the  $\text{CO}_3/\text{PO}_4$  and Amide(I)/ $\text{PO}_4$  index values. Since no correlation should be expected in unaltered bone, the correlation with the  $\text{CO}_3/\text{PO}_4$  index is concerning (France et al., 2014; Madden et al., 2018; Ortiz-Herrero et al., 2021). If the IRIS derived values alone had showed this correlation, then that may have been an indication of unreliable results from the model; however, even the IRMS-derived isotopic values correlated with  $\text{CO}_3/\text{PO}_4$ . The reason for this is unknown, and more work is required to explore this correlation. This correlation either suggests a misinterpretation of the  $\text{CO}_3/\text{PO}_4$  ratio in Raman spectra, such that the ratios given work for FTIR but not for Raman spectrometry, or that noise may be causing Raman indices of diagenesis to be miscalculated. The latter is unlikely to be the correct explanation since the correlation increased when outliers in  $\text{CO}_3/\text{PO}_4$  and Amide(I)/ $\text{PO}_4$  ratios were removed, suggesting that the correlation is likely real. Therefore, the most parsimonious explanation is that, while these ratios have been developed and thoroughly studied for FTIR, they are less often studied in Raman spectrometry and thus the range of what is considered unaltered bone may be larger due to differences between the techniques.

Ultimately, IRMS-derived and IRIS-derived isotopic values had similar relationships to the diagenetic indices tested, having no significant bias in one method over the other. Therefore, the hypothesis of diagenesis affecting IRIS and IRMS equally is supported, suggesting that with improved methodology for IRIS, it may be a useful alternative to IRMS in the near future. For this reason, both methods were applied in the exploration of intra-element isotopic variation.

## Intra-Element Isotopic Variation

Understanding intra-element and intraskeletal variation is essential in our applications of biogeochemistry in bioarchaeology and forensic anthropology. While intraskeletal variation, those differences in isotopic values between skeletal elements in the same individual, has been studied, although not extensively, (Berg et al., 2022; Fahy et al., 2017; Jørkov et al., 2009; Olsen et al., 2014), intra-element variation, those differences in isotopic values between sampling locations on the same skeletal element, in bulk sampling for biogeochemical analyses has not been previously explored. The current study, therefore, explored this intra-element variation in both study populations. The intra-element variation in the individuals from the Patakfalva-Papdomb site was explored using the IRMS derived  $\delta^{13}\text{C}_{\text{apatite}}$  and  $\delta^{18}\text{O}_{\text{vpdb}}$  values, while the intra-element variation in the donors to the University of Tennessee collection was explored using the IRIS derived  $\delta^{13}\text{C}_{\text{apatite}}$  values as well as the Raman spectra as proxies for the molecular and chemical composition of bone affecting isotopic data, as had been previously explored using FTIR (Gonçalves et al., 2018). When testing intra-element variation in the individuals from Patakfalva-Papdomb, mean deviations between the sampling locations were lower than the precision estimates from duplication, which used the same sampling location as a duplicate. This suggests that deviation from the mean isotopic value of the skeletal element is lower than instrument or protocol precision. Some of these sampling locations were in close proximity to each other along the diaphysis while other sample locations segmented both proximal and distal portion of the diaphyses of long bones. Neither the sampling locations in close proximity nor those further apart showed significant differences in isotopic values.

Intra-element variation in the donors to the University of Tennessee was examined

through both  $\delta^{13}\text{C}_{\text{IRIS}}$  and complete Raman spectra with dimensionality reduction methods. Using ANOVA on the  $\delta^{13}\text{C}_{\text{IRIS}}$  values, no significant differences were found within individuals between skeletal elements or between sampling locations, and significant differences were found only between individuals. This suggests that the differences between individuals are much greater than intraskeletal or intra-element differences. With intraskeletal variation currently established at approximately 1.55‰ at the 95% confidence interval (Berg et al., 2022) and inter-laboratory differences approximating the 1.2‰ range at the 95% confidence interval (Pestle, Crowley, et al., 2014), it appears that minor differences between sampling locations may well fall within these standard errors. Our understanding of the minimum meaningful difference (MMD) between laboratories, for  $\delta^{13}\text{C}_{\text{apatite}}$  at least, suggests that the precision is sufficient to potentially observe remodeling related differences within skeletal elements, but bulk sampling may be too coarse to tease apart these differences. Carbonate derived  $\delta^{18}\text{O}$ , however, appears highly unreliable for such small differences to emerge in the data, since inter-laboratory MMD are approximately 3.1‰ (Pestle, Crowley, et al., 2014), and while previous work has demonstrated  $\delta^{18}\text{O}$  differences within a skeletal element (Maggiano et al., 2019), the poor reliability of these  $\delta^{18}\text{O}_{\text{carbonate}}$  values and their susceptibility to diagenesis (Berg et al., 2022; Daux et al., 2008) make it a less than ideal approach to the exploration of remodeling based differences.

Exploring the mean deviation of the sampling locations per skeletal element clarifies the ANOVA results. While it was hypothesized that remodeling patterns would affect isotopic values along a skeletal element, no such pattern is observable in the data. Remodeling rates are faster near epiphyses than along midshafts and are significantly different anterior to posterior (Hsieh et al., 2001; Lanyon et al., 1982). If the results followed expectations based on

remodeling, midshaft values would trend towards the mean while the extremities of the diaphyses would be expected to deviate to a greater extent. Similarly, isotopic values should cluster into anterior and posterior values based on mean deviation. No such pattern is observed. When exploring the differences using Raman spectra, variation maximizing PCA was used to explore the biogeochemical clustering that may occur. PCA does not attempt to match categories, merely just to find the linear transformation that maximizes variance. If maximum variance was to be found between individuals, then individuals should tend to cluster among themselves and separate from each other in the PCA analyses. If maximum variance was to be found between sampling locations or skeletal elements, on the other hand, then those would cluster regardless of individual association and would suggest significant intra-element variation in Raman spectra. However, PCA results showed no clustering in any of these patterns when variance was maximized. Although the number of variables in Raman spectra is large enough to potentially confound the analysis, only 59% of the variance is explained with 6 components, these results nevertheless support the much simpler and more direct isotopic results that suggest a negligible variance for both intra-element and intraskeletal isotopic values.

These results demonstrating a lack of intra-element isotopic variation, therefore, may be explained in one of two ways. While diet was dependent on seasonality in the past, that is no longer the case in the contemporary U.S., with diets remaining relatively stable over enough time to stabilize isotopic incorporation (Bartelink & Chesson, 2019; Chesson et al., 2008; Chesson et al., 2017). The second explanation may be related to the comparison of surface-to-surface data rather than bulk sampling or depth dependent sampling, as has been previously explored (Bell et al., 2001; Fahy et al., 2017; Maggiano et al., 2019). Surfaces are more mechanoresponsive and therefore are more likely to quickly remodel under biomechanical stress (Birkhold et al., 2016).



This could result in more homogenous isotopic values across the periosteal surface while there may be unidentified differences between the envelopes (Eriksen, 1986; Gosman et al., 2011; Robling et al., 2006).

The first possibility, that the lack of seasonal dietary changes in a contemporary population would affect isotopic data is unsupported when comparing the results of the donors to the University of Tennessee to the individuals from Patakfalva-Papdomb. Intra-element variation in both the Patakfalva-Papdomb individuals and the donors to the University of Tennessee skeletal collection falls within the maximum expected intraskeletal variation, without major deviations within elements or between elements of the same individual. A medieval population would not have access to the so-called “supermarket” diet that generalizes isotopic values regardless of location or season. Since results of intra-element variation are similar for the contemporary and medieval populations, an alternative explanation is needed.

While differences may exist in the incorporation of isotopes into bone, most contemporary methods of isotopic analysis have too much error to account for the potentially minute differences between sampling locations on a single individual. Remodeling rates would only affect isotopic values if there were significant differences in seasonal residential location (for  $\delta^{18}\text{O}$ ) or in diet (for  $\delta^{13}\text{C}$ ). Minimum meaningful differences (MMD) between IRIS and bulk IRMS values, and between laboratories analyzing IRMS samples, are still higher than intra-element variation expected for small seasonal changes in diet or residential location. At maximum, intra-element variation in previous research appears to deviate approximately  $\pm 1.5\%$  from bulk sampling average value in  $\delta^{18}\text{O}$  (Maggiano et al., 2019), less than half of the 3.1% MMD for  $\delta^{18}\text{O}_{\text{carbonate}}$  (Pestle, Crowley, et al., 2014). Intra-element variation for  $\delta^{13}\text{C}_{\text{apatite}}$  would be highly dependent on a seasonal change in diet from  $\text{C}_3$  plants to  $\text{C}_4$  plants over a two or three

month period, which is possible given the geographical distribution of these types of plants (O'Leary, 1988; Still et al., 2003), but could not be observed with bulk sampling techniques. Therefore, it is likely that intra-element variation will be insignificant in most isotopic studies, but the potential of these differences, if found, could be create a more nuanced interpretation

### **Commingling and Isotopic Reassociation**

By laying the foundation of intraskeletal and intra-element variation in isotopic data, I can examine the reassociation of individuals using isotopic analysis. For reassociation, the threshold protocol presented by Berg et al. (2022), shows great exclusionary potential but does a poor job at actual reassociation, as it was not intended to be used in that manner. A positive test for the threshold method, meaning differences are greater than the given threshold, suggests the two isotopic values originate from different individuals, while a negative test has no interpretive value. An exclusionary method like this can only suggest that two individuals are different but has no predictive value in suggesting that two isotopic values originate from the same individual. Therefore, when using this method, the specificity, or the concordance of the test to real exclusion, and the positive predictive value, or the successful identification of values that are outside the range of being form the same individual, are both very high, above even the 95% and 99% expectations set forth by Berg et al. (2022). But, as the threshold method is not intended for reassociation but rather exclusion, the sensitivity, the concordance of the test to real association, and the negative predictive value, or the successful identification of two isotopic values being from the same individual, are both very low, as is to be expected. To try improving this aspect of the approach, a logistic regression function for association was fit to the differences in isotopic values in all the data collected form the individuals in this study.

A logistic regression method, however, did not provide better results than the threshold method, at least with the current dataset. While the collection of values belonging to the same individual seemed to cluster within the 99% confidence interval suggested by Berg et al. (2022), the logistic regression encountered too many values within that threshold to appropriately estimate probability of reassociation with any better precision than the threshold method. Two possible interpretations arise from these results; 1) that differences between and within individuals with similar diets are too narrow, or 2) that a more balanced dataset with equal numbers of associated and unassociated isotopic values may improve the prediction. The first interpretation is that differences in isotopic values between individuals sharing the same diet and originating from the same location are too narrow to appropriately reassociate. While remodeling has been explored through biogeochemistry, suggesting significant intra-element differences may exist in isotopic values (Babraj et al., 2002; Brady et al., 2008; Cerling et al., 2007), these differences may fall within the MMD and intraskeletal variation of the isotopic value. Therefore, bulk sampling for isotopic analyses would obscure some of the potential differences. The second is more methodological in nature and is based on the fact that, to attain a significant sample size, the number of isotopic values from the same individual is grossly outnumbered by the number of isotopic values originating from different individuals. This imbalance affects the logistic regression model and skews the results toward exclusion rather than association.

Neither interpretation precludes the future application of these methods to reassociation, only that the methods as they are currently applied, namely using bulk sampling and net differences in a single isotopic value, do not have the predictive power necessary for reassociation of individuals that may be from the same region and shared similar diets. Increasing the number of isotopic values used, for example using differences in  $\delta^{13}\text{C}_{\text{apatite}}$ ,

$\delta^{13}\text{C}_{\text{collagen}}$ ,  $\delta^{18}\text{O}$ , and  $\delta^{15}\text{N}$  together as predictor values may significantly improve the method. Additionally, a greater number of individuals as the foundational dataset, balancing out the number of isotopic differences between associated and unassociated skeletal remains and increasing the variation in diet and region of origin, may allow future studies to create logistic regression that provide a posterior probability of reassociation, and improve on the exclusionary thresholds already presented.

IRIS methodology is too imprecise at the moment to attempt to use it in the same way as IRMS values. However, a non-destructive approach was thought possible using only the Raman spectra. This study used the complete spectra in a Bayesian Gaussian Mixture Model, attempting association and clustering to explore the application of this method when the minimum number of individuals is estimated. This model takes a prior value of expected number of clusters, in this case it would take the estimated minimum number of individuals, and then attempt to discover Gaussian shaped clusters in the dataset. While the model did a relatively good job when estimating the number of potential clusters, the categorization of isotopic values into individuals was less successful. The number of clusters estimated by the method were 36 when 29 individuals were represented, a slight overestimation, but the accuracy of the model was only 0.22 using the Adjusted Mutual Information Score (AMI). While disappointing, this result is to be expected when taking into account the previously discussed results on intraskeletal and inter-individual variation in isotopic values. The biogeochemical differences between individuals, although significant when explored using ANOVA, may not be great enough to model clustering, mostly related to the amount of overlap that exists in individuals that have relatively equivalent diets and location of residence. Additionally, with the individuals that had vastly different residences, namely the donors to the University of Tennessee, the lack of correlation

between Raman spectra and  $\delta^{18}\text{O}$  values suggests that using Raman spectra may not be a good proxy for residential location in this situation of attempting to reassociate individuals.

### **The Context of Necrodominance**

When stakeholders desire to use biogeochemical methods to explore the past to which they feel connected, two potential methods are now available, IRIS and IRMS. The results for a non-destructive isotopic analysis through IRIS suggest the method is in its infancy and cannot yet completely replace traditional IRMS analyses in certain situations. Clear explanations of the costs and benefits of each method should be presented to the stakeholders prior to research design. This allows informed consent from stakeholders for all analyses and continues to empower communities of origin in the analyses of their past. In the case of this study, the potential for the use of isotopic analyses in studying individuals from Patakfalva-Papdomb site had been discussed with the community and the archaeological director. Research design, however, was not discussed with the community of Patakfalva, and this is an oversight to be remedied in future studies and prior to the publication of results from this study. Benefits sharing is a primary goal for this project, and the results of these analyses will be presented to the community, in consultation with that community and with museum director Zsolt Nyárádi, in the summer of 2023. The history of biological anthropology is fraught with the misuse and marginalization of communities, especially those communities already marginalized by society at large (Claw et al., 2017; Deloria Jr., 1992; Highet, 2005; Sadongei & Cash Cash, 2007), and the misuse of biological anthropology research in the subjugation of communities (Deloria Jr., 1992; DiGangi & Bethard, 2021; Kaufmann & Rühli, 2010; Riding In, 1992; Walker, 2008). The imposition and domination of skeletal material by outside authorities, such as scientist, can only

really be addressed by those in positions of authority. As bioarchaeologists and forensic anthropologists have become more aware of these imbalances in power, many attempts have been made to improve the sensitivity of the discipline (Arnold, 2014; Geller & Suri, 2014; Kaufmann & Rühli, 2010; Kreissl Lonfat et al., 2015; Parra et al., 2020; Squires et al., 2019). This emphasis on the ethical treatment of human remains and the recognition of stakeholders and communities of origin as having all agency over the remains of their ancestors must continue.

### **Summary**

In this chapter I contextualized the results of this study within the existing literature. First, I explained why the results of the IRIS method are currently unreliable but present a promising avenue for future investigations of non-destructive methods. Then, I explained the effects of diagenesis on both the IRIS and IRMS method and demonstrate that diagenesis affects both approaches equally. In this section I also suggest that further study is needed in understanding some of these indices as calculated using Raman spectrometry. I then examined the results of intra-element and intraskeletal isotopic variation and suggested that bulk sampling of the remains may be too gross to identify the minute differences related to remodeling. Additionally, I explained that similar diets and residential locations may be obscuring potential intra-element differences since a change in the isotopic pool is required for a noticeable difference to occur based on remodeling. I then explored the approaches to reassociation using isotopic analyses, describing the benefits and pitfalls of the threshold exclusion method and describing the inefficacy of a logistic regression model for reassociation. Lastly, I explain that while the goal of a reliable non-destructive method may not yet have been reached, the lessons from an exploration of necrodominance must be brought into all future work in biological

anthropology. In the following chapter I will provide some concluding remarks, present the limitations of the current study, and provide some future considerations for isotopic analyses.

## CHAPTER SEVEN

### CONCLUSION

Stable isotope analyses have been applied in biological anthropology for decades to assess dietary preferences and residential history in the past as well as explore patterns of remodeling in the human skeleton. Isotope incorporation in the skeleton occurs over time and is related to the rate of remodeling of bone in living individuals. While remodeling differences between skeletal elements have been assumed in bulk sampling for isotopic analyses, and therefore intraskeletal differences have been examined, remodeling differences exist within skeletal elements, and these have yet to be thoroughly examined. The current study, therefore, explored these differences using both a traditional Isotope Ratio Mass Spectrometry (IRMS) method, which is destructive, and an alternative, non-destructive method using Isotope Ratio Infrared Spectrometry (IRIS) based on Raman spectrometry for  $\delta^{13}\text{C}_{\text{apatite}}$  and  $\delta^{18}\text{O}_{\text{carbonate}}$ . The application of IRIS to unprocessed human skeletal remains showed promising results but are still preliminary and cannot be relied upon at this time to replace traditional IRMS. One benefit of IRIS is the ability to simultaneously estimate indices of diagenesis and explore the reliability of the isotopic results since no major differences appeared in the reliability of the application of the methods based on diagenetic indices. While preliminary, the application of IRIS as an indirect proxy for IRMS helped explore intraskeletal and intra-element variation in isotopic ratios for the individuals in this study. Intra-element variation in  $\delta^{13}\text{C}$  and  $\delta^{18}\text{O}$  was negligible when compared to intraskeletal variation in the same values, suggesting that current bulk sampling techniques are too coarse to tease apart differences in isotopic values related to remodeling and that these differences may only exist with drastic changes of diet or residential location. Knowing this lack



of significant variation, the use of the previously defined thresholds for reassociation by exclusion (Berg et al., 2022), were successful in their goals of exclusion but could not be reliably used to reassociate individuals. A use of a logistic regression for reassociation was not any more successful, however, and it appears that inter-individual variation is less pronounced than necessary for an isotopic method of reassociation. The complex interactions between diet, residential location, and patterns of remodeling have not yet been fully explored, but this study can form the foundation upon which further study can proceed.

### **Research and Limitations**

Hypothesis one predicted that IRIS would be a valuable proxy for traditional IRMS analyses for both  $\delta^{13}\text{C}$  and  $\delta^{18}\text{O}$  if the IRIS derived values fit within the minimum meaningful differences for each, 1.2‰ and 3.1‰ respectively (Pestle, Crowley, et al., 2014). The results suggest that at this time  $\delta^{13}\text{C}$  from IRIS may be reliable but requires a better reference sample while  $\delta^{18}\text{O}$  values from IRIS are unreliable, and thus the hypothesis must be rejected. While promising, the creation of the linear regression model is based on the baseline isotopic data, and with data that are not highly varied there is a problem of overfitting for the model. Correlations between the isotopic ratios in collagen and apatite are also causing the model to fit on peaks in the spectrum that are related to organic matter rather than apatite. This may suggest that the model is fitting the relationship between  $\delta^{13}\text{C}_{\text{apatite}}$  and  $\delta^{13}\text{C}_{\text{collagen}}$  rather than directly estimating  $\delta^{13}\text{C}_{\text{apatite}}$ .

Hypothesis two predicted that diagenesis would affect IRIS and IRMS derived isotopic values equally. While the results of IRIS application may be preliminary, IRIS and IRMS seem to be equally reliable, with diagenesis affecting IRIS derived isotopic data as much as the IRMS

derived isotopic data, therefore this hypothesis can be supported. One of the many benefits of using IRIS for isotopic analysis is the ability to calculate indices of diagenesis using the same instrument and the same analysis, allowing for the immediate exploration of diagenetic alterations.

Hypothesis three predicted that, with knowledge of intra-element and intraskeletal variation, skeletal remains may be reassociated through biogeochemistry with better specificity than osteometric methods. With the current approaches to reassociation using spectral data, the hypothesis must be rejected. While previous studies on the exploration of isotopic variation within individual skeletal elements suggested some potential differences, these differences appear to be related to variation in remodeling between endosteal/periosteal and intracortical (Birkhold et al., 2016; Maggiano et al., 2019) or between newer and older osteons within intracortical bone (Bell et al., 2001; Fahy et al., 2017; Gosman et al., 2011; Schulte et al., 2013; van Oers, Ruimerman, van Rietbergen, et al., 2008), the use of bulk sampling in IRMS does not discriminate between these envelopes. The lack of variation across a skeletal element when using bulk sampling supports previous analyses on remodeling rates having differences between envelopes (Eriksen, 1986; Gosman et al., 2011; Maggiano et al., 2019) or by osteon (Fahy et al., 2017; van Oers, Ruimerman, van Rietbergen, et al., 2008) and suggest that differences between anterior and posterior or distal and proximal portions of the skeletal remains, as had been found in studies on biomechanics and remodeling (Lanyon et al., 1982), are less common in daily experience. This, of course, is partially the limitation of bulk sampling, the reasoning behind studies exploring osteonal differences (Bell et al., 2001; Fahy et al., 2017) as well as amino-acid specific differences in collagen-derived isotopes (Fogel & Tuross, 2003; Howland et al., 2003) to achieve a more nuanced understanding. However, neither of these methods is frequently

available to most researchers and both are destructive.

As IRIS results are based on bulk sampling, that method is unlikely to provide a more nuanced exploration. This is one of its limitations. However, as the ethics of destructive and invasive analyses in biological anthropology are being questioned, a new approach of non-destructive and non-invasive methods is necessary. That is what IRIS provides, but only when properly calibrated and methodologically sound. As it is now in its infancy, IRIS cannot be used to replace the invasive methodology that has had over 30 years of adjustment and improvement. That does not suggest the impossibility of using the method, especially since the results of this study have suggested promising returns.

### **Future Considerations**

This study was a preliminary step in approaching the problem of destructive analyses in biological anthropology and the exploration of intra-element variation. Clearly, this study has demonstrated that intra-element variation should not be a concern in most isotopic analyses, since the variation of individuals on steady diets will not change significantly when using bulk sampling. However, more concerted efforts to reduce the destructive and invasive nature of many of our analytical methods in biological anthropology should be at the forefront of our field.

The results from this study on applying IRIS to isotopic values focus on isotopic ratios from bioapatite rather than collagen. However, collagen results can add significant data and are more often applied in bioarchaeological contexts. Therefore, future work must explore the application of the IRIS protocols for the assessment of collagen isotopic data as well as improve the application of IRIS to apatite isotopic values. Additionally, while most biogeochemical studies work in biological anthropology explore  $\delta^{18}\text{O}$  values from carbonate, many studies have

demonstrated the potential concerns for its continued use as a marker of residential history (Berg et al., 2022; Daux et al., 2008). Therefore, I suggest that future work should focus on phosphate  $\delta^{18}\text{O}$  values and correlate those to Raman spectrometry, improving reliability and interpretability of the results in both bioarchaeological and forensic contexts. As IRIS is in its infancy for human skeletal remains, future work must also address the issues of fluorescence and noise as they relate to IRIS protocols. Previous work has used chemical processing to reduce fluorescence, this defeats one of the benefits of Raman spectrometry in biogeochemical studies. Attempts at using 1064nm excitation for Raman spectrometry and the algorithmic reduction of fluorescence can be explored in the short term while improving and generalizing the approach, but these require more thorough collaborations outside of our own field. These approaches may take greater effort but could result in more robust approximations for all applications of IRIS and a significant step toward a less invasive biological anthropology.

A less invasive biological anthropology is also one of the foci of reducing necrodominance. The proposed solutions to necrodominance must be used in conjunction to conduct ethical research. For this reason, I propose the following recommendations to alleviate this in biological anthropology:

1. Avoid the assumption that any analyses are necessary over and above the wishes of the stakeholders and descendant communities.
2. Complete collaboration with descendant communities, beginning at the research design stage, to ensure that the needs and desires of the community are being met by the project.
3. Data privacy and a stewardship model of both data and samples collected from individuals, ensuring that any future research is beholden to suggestion number one.

4. All material or remains collected and used for any project must therefore be owned solely by the descendant community and they should decide the ultimate fate of remains and material.
5. All research projects should attempt to give back to the descendant community, either through accessible knowledge in the form of public lectures or through generally applicable results.
6. Future methodological advancements should place an emphasis on discovering non-invasive and non-destructive methods for all analyses in biological anthropology. As technology improves in all scientific fields, so will the potential for non-destructive methods to be discovered.

This study has demonstrated the potential for non-destructive methods and can lay the foundation for further improvements in this approach. Additionally, while intra-skeletal variation in stable isotopes had been previously studied, this project demonstrated that bulk sampling is unlikely to discover intra-element variation in isotopic values, suggesting that sampling location is not as important in the biogeochemical study of human skeletal remains as the skeletal element from which the results are derived.

## REFERENCES

- Agamben, G. (1998). *Homo Sacer: Sovereign Power and Bare Life* (D. Heller-Roazen, Trans.). Stanford, CA: Stanford University Press.
- Allen, M. J., Powers, M. L., Gronowski, K. S., & Gronowski, A. M. (2010). Human tissue ownership and use in research: what laboratorians and researchers should know. *Clinical Chemistry*, 56(11), 1675-1682. doi:10.1373/clinchem.2010.150672
- Allen, M. R., & Burr, D. B. (2019). Bone Growth, Modeling, and Remodeling. In D. B. Burr & M. R. Allen (Eds.), *Basic and Applied Bone Biology* (2nd ed., pp. 85-100). San Diego: Academic Press.
- Allori, A. C., Sillon, A. M., Pan, J. H., & Warren, S. M. (2008). Biological basis of bone formation, remodeling, and repair-part III: biomechanical forces. *Tissue Engineering: Part B*, 14(3), 285-293. doi:10.1089/ten.teb.2008.0084
- Andrews, L., & Nelkin, D. (1998). Whose body is it anyway? Disputes over body tissue in a biotechnology age. *The Lancet*, 351(9095), 53-57. doi:10.1016/S0140-6736(05)78066-1
- Annas, G. J. (2006). Anthropology, IRBs, and Human Rights. *American Ethnologist*, 33(4), 541-544.
- Arbour, L., & Cook, D. (2006). DNA on loan: issues to consider when carrying out genetic research with aboriginal families and communities. *Community Genet*, 9(3), 153-160. doi:10.1159/000092651

- Arnold, B. (2014). Life After Life: Bioarchaeology and Post-mortem Agency. *Cambridge Archaeological Journal*, 24(3), 523-529. doi:10.1017/s0959774314000572
- Attias, H. (2000). A Variational Bayesian Framework for Graphical Models. *Advances in Neural Information Processing Systems*, 12.
- Awonusi, A., Morris, M. D., & Tecklenburg, M. M. J. (2007). Carbonate assignment and calibration in the Raman spectrum of apatite. *Calcified Tissue International*, 81(1), 46-52. doi:10.1007/s00223-007-9034-0
- Babraj, J., Cuthbertson, D. J., Rickhuss, P., Meier-Augenstein, W., Smith, K., Bohé, J., . . . Rennie, M. J. (2002). Sequential extracts of human bone show differing collagen synthetic rates. *Biochemical Society Transactions*, 30(2), 61-65. doi:10.1042/bst0300061
- Baek, S.-J., Park, A., Ahn, Y.-J., & Choo, J. (2015). Baseline correction using asymmetrically reweighted penalized least squares smoothing. *Analyst*, 140(1), 250-257. doi:10.1039/c4an01061b
- Bakar, Z. A., Mohamad, R., Ahmad, A., & Deris, M. M. (2006, 7-9 June 2006). *A Comparative Study for Outlier Detection Techniques in Data Mining*. Paper presented at the 2006 IEEE Conference on Cybernetics and Intelligent Systems.
- Balasse, M., Ambrose, S. H., Smith, A. B., & Price, T. D. (2002). The Seasonal Mobility Model for Prehistoric Herders in the South-western Cape of South Africa Assessed by Isotopic Analysis of Sheep Tooth Enamel. *Journal of Archaeological Science*, 29(9), 917-932. doi:10.1006/jasc.2001.0787

- Balasse, M., Bocherens, H., & Mariotti, A. (1999). Intra-bone Variability of Collagen and Apatite Isotopic Composition Used as Evidence of a Change of Diet. *Journal of Archaeological Science*, 26(6), 593-598. doi:10.1006/jasc.1998.0376
- Barad, K. (2003). Posthumanist Performativity: Toward an Understanding of How Matter Comes to Matter. *Signs: Journal of Women in Culture and Society*, 28(3), 801-831. doi:10.1086/345321
- Bartelink, E. J., & Chesson, L. A. (2019). Recent applications of isotope analysis to forensic anthropology. *Forensic Sciences Research*, 4(1), 29-44. doi:10.1080/20961790.2018.1549527
- Barton, S. J., Ward, T. E., & Hennelly, Bryan M. (2018). Algorithm for optimal denoising of Raman spectra. *Analytical Methods*, 10(30), 3759-3769. doi:10.1039/c8ay01089g
- Bauer, E. (Producer). (2016). Human Bones: 3D Models Collection.
- Beasley, M. M., Bartelink, E. J., Taylor, L., & Miller, R. M. (2014). Comparison of transmission FTIR, ATR, and DRIFT spectra: implications for assessment of bone bioapatite diagenesis. *Journal of Archaeological Science*, 46, 16-22. doi:10.1016/j.jas.2014.03.008
- Beaumont, J., Atkins, E. C., Buckberry, J., Haydock, H., Horne, P., Howcroft, R., . . . Montgomery, J. (2018). Comparing apples and oranges: Why infant bone collagen may not reflect dietary intake in the same way as dentine collagen. *American Journal of Physical Anthropology*, 167(3), 524-540. doi:10.1002/ajpa.23682
- Bell, L. S., Cox, G., & Sealy, J. (2001). Determining isotopic life history trajectories using bone



- density fractionation and stable isotope measurements: A new approach. *American Journal of Physical Anthropology*, 116(1), 66-79. doi:10.1002/ajpa.1103
- Bentley, R. A. (2006). Strontium Isotopes from the Earth to the Archaeological Skeleton: A Review. *Journal of Archaeological Method and Theory*, 13(3), 135-187. doi:10.1007/s10816-006-9009-x
- Berg, G. E., Chesson, L. A., Yuryang, J., Youngsoon, S., & Bartelink, E. J. (2022). A Large-Scale Evaluation of Intraperson Isotopic Variation Within Human Bone Collagen and Bioapatite. *Forensic Science International*, 111319. doi:10.1016/j.forsciint.2022.111319
- Berna, F., Matthews, A., & Weiner, S. (2004). Solubilities of bone mineral from archaeological sites: the recrystallization window. *Journal of Archaeological Science*, 31(7), 867-882. doi:10.1016/j.jas.2003.12.003
- Bertoluzza, A., Brasili, P., Castrì, L., Facchini, F., Fagnano, C., & Tinti, A. (1997). Preliminary Results in Dating Human Skeletal Remains by Raman Spectroscopy. *Journal of Raman Spectroscopy*, 28(2-3), 185-188. doi:10.1002/(sici)1097-4555(199702)28:2/3<185::aid-jrs69>3.0.co;2-6
- Bethard, J. D. (2013). Isotopes. In E. DiGangi, A. & M. K. Moore (Eds.), *Research Methods in Human Skeletal Biology* (pp. 425-447). Waltham, MA: Academic Press.
- Bethard, J. D., Zejdlik, K., Nyárádi, Z., & Gonciar, A. (2022). *Székely Subsistence and Social Stratification Revealed through Stable Isotope Analysis*. Paper presented at the European Association of Archaeologists Annual Meeting, Budapest, Hungary

- Birkhold, A. I., Razi, H., Duda, G. N., Weinkamer, R., Checa, S., & Willie, B. M. (2016). The Periosteal Bone Surface is Less Mechano-Responsive than the Endocortical. *Scientific Reports*, 6, 23480. doi:10.1038/srep23480
- Blakey, M. L. (2020). Archaeology under the Blinding Light of Race. *Current Anthropology*, 61(S22), S183-S197. doi:10.1086/710357
- Blei, D. M., & Jordan, M. I. (2006). Variational inference for Dirichlet process mixtures. *Bayesian Analysis*, 1(1). doi:10.1214/06-ba104
- Bourdieu, P. (1989). Social Space and Symbolic Power. *Sociological Theory*, 7(1), 14-25.
- Bourdieu, P. (1990a). Structures, Habitus, Practices. In *The Logic of Practice* (pp. 52-65). Stanford: Stanford University Press.
- Bourdieu, P. (1990b). Symbolic Capital. In *The Logic of Practice* (pp. 112-121). Stanford: Stanford University Press.
- Bowen, G. J., Ehleringer, J. R., Chesson, L. A., Stange, E., & Cerling, T. E. (2007). Stable isotope ratios of tap water in the contiguous United States. *Water Resources Research*, 43(3). doi:10.1029/2006wr005186
- Bower, N. W., Getty, S. R., Smith, C. P., Simpson, Z. R., & Hoffman, J. M. (2005). Lead isotope analysis of intra-skeletal variation in a 19th century mental asylum cemetery: diagenesis versus migration. *International Journal of Osteoarchaeology*, 15(5), 360-370. doi:10.1002/oa.796

- Brady, A. L., White, C. D., Longstaffe, F. J., & Southam, G. (2008). Investigating intra-bone isotopic variations in bioapatite using IR-laser ablation and micromilling: Implications for identifying diagenesis? *Palaeogeography, Palaeoclimatology, Palaeoecology*, 266(3), 190-199. doi:10.1016/j.palaeo.2008.03.031
- Brandstätter, A., Egyed, B., Zimmermann, B., Duftner, N., Padar, Z., & Parson, W. (2007). Migration rates and genetic structure of two Hungarian ethnic groups in Transylvania, Romania. *Annals of Human Genetics*, 71(Pt 6), 791-803. doi:10.1111/j.1469-1809.2007.00371.x
- Brätter, P., Gawlik, D., Lausch, J., & Rösick, U. (1977). On the distribution of trace elements in human skeletons. *Journal of Radioanalytical Chemistry*, 37(1), 393-403. doi:10.1007/bf02520545
- Burr, D. B. (2019). Bone Morphology and Organization. In D. B. Burr & M. R. Allen (Eds.), *Basic and Applied Bone Biology* (2nd ed., pp. 3-26). San Diego: Academic Press.
- Burt, N. M. (2013). Stable isotope ratio analysis of breastfeeding and weaning practices of children from medieval Fishergate House York, UK. *American Journal of Physical Anthropology*, 152(3), 407-416. doi:10.1002/ajpa.22370
- Campbell, C. S. (2003). Body, Self, and the Property Paradigm. *The Hastings Center Report*, 22(5), 34-42.
- Cerling, T. E., Ayliffe, L. K., Dearing, M. D., Ehleringer, J. R., Passey, B. H., Podlesak, D. W., . . . West, A. G. (2007). Determining biological tissue turnover using stable isotopes: the

- reaction progress variable. *Oecologia*, 151(2), 175-189. doi:10.1007/s00442-006-0571-4
- Chesson, L. A., Kenyhercz, M. W., Regan, L. A., & Berg, G. E. (2019). Addressing data comparability in the creation of combined data sets of bioapatite carbon and oxygen isotopic compositions. *Archaeometry*, 61(5), 1193-1206. doi:10.1111/arc.12480
- Chesson, L. A., Podlesak, D. W., Thompson, A. H., Cerling, T. E., & Ehleringer, J. R. (2008). Variation of hydrogen, carbon, nitrogen, and oxygen stable isotope ratios in an American diet: fast food meals. *Journal of Agricultural and Food Chemistry*, 56(11), 4084-4091. doi:10.1021/jf0733618
- Chesson, L. A., Tipple, B. J., Ehleringer, J. R., Park, T., & Bartelink, E. J. (2017). Forensic applications of isotope landscapes (“isoscapescapes”). In C. C. Boyd Jr. & D. C. Boyd (Eds.), *Forensic Anthropology: Theoretical Framework and Scientific Basis* (pp. 127-148). Hoboken, NJ: John Wiley & Sons.
- Christen, P., Ito, K., Ellouz, R., Boutroy, S., Sornay-Rendu, E., Chapurlat, R. D., & van Rietbergen, B. (2014). Bone remodelling in humans is load-driven but not lazy. *Nature Communications*, 5, 4855. doi:10.1038/ncomms5855
- Claw, K. G., Lippert, D., Bardill, J., Cordova, A., Fox, K., Yracheta, J. M., . . . Garrison, N. A. (2017). Chaco Canyon Dig Unearths Ethical Concerns. *Human Biology*, 89(3), 177-180. doi:10.13110/humanbiology.89.3.01
- Colwell, C. (2018). Rights of the dead and the living clash when scientists extract DNA from human remains. *The Conversation*. Retrieved from <https://theconversation.com/rights-of->

the-dead-and-the-living-clash-when-scientists-extract-dna-from-human-remains-94284

Cooper, C. G., Lupo, K. D., Zena, A. G., Schmitt, D. N., & Richards, M. P. (2018). Stable isotope ratio analysis (C, N, S) of hair from modern humans in Ethiopia shows clear differences related to subsistence regimes. *Archaeological and Anthropological Sciences*, 1-11. doi:10.1007/s12520-018-0740-5

Crowley, B. E., & Wheatley, P. V. (2014). To bleach or not to bleach? Comparing treatment methods for isolating biogenic carbonate. *Chemical Geology*, 381, 234-242. doi:10.1016/j.chemgeo.2014.05.006

Dalou, C., Füre, E., Caumon, M.-C., & Laumonier, M. (2018). *Determination of 15N/14N ratios in reduced silicate glasses using Raman spectroscopy*. Paper presented at the Japan Geosciences Union Meeting, Chiba, Japan.

Daux, V., Lecuyer, C., Heran, M.-A., Amiot, R., Simon, L., Fourel, F., . . . Escarguel, G. (2008). Oxygen isotope fractionation between human phosphate and water revisited. *Journal of Human Evolution*, 55(6), 1138-1147. doi:10.1016/j.jhevol.2008.06.006

Delacre, M., Leys, C., Mora, Y. L., & Lakens, D. (2019). Taking Parametric Assumptions Seriously: Arguments for the Use of Welch's *F*-test instead of the Classical *F*-test in One-Way ANOVA. *International Review of Social Psychology*, 32(1), 13-25. doi:10.5334/irsp.198

Deloria Jr., V. (1992). Indians, Archaeologists, and the Future. *American Antiquity*, 57(4), 595-598. doi:10.1017/S000273160005472X

- DeNiro, M. J., & Schoeniger, M. J. (1983). Stable carbon and nitrogen isotope ratios of bone collagen: variations within individuals, between sexes, and within populations raised on monotonous diets. *Journal of Archaeological Science*, *10*(3), 199-203.
- Descartes, R. (1984). Meditations on First Philosophy. In J. Cottingham, R. Stoothoff, & D. Murdoch (Eds.), *The Philosophical Writings of René Descartes* (Vol. 2, pp. 1-62). Cambridge: Cambridge University Press.
- DiGangi, E. A., & Bethard, J. D. (2021). Uncloaking a Lost Cause: Decolonizing ancestry estimation in the United States. *American Journal of Physical Anthropology*. doi:10.1002/ajpa.24212
- Dupras, T. L., & Tocheri, M. W. (2007). Reconstructing infant weaning histories at Roman period Kellis, Egypt using stable isotope analysis of dentition. *American Journal of Physical Anthropology*, *134*(1), 63-74.
- Eriksen, E. F. (1986). Normal and Pathological Remodeling of Human Trabecular Bone: Three Dimensional Reconstruction of the Remodeling Sequence in Normals and in Metabolic Bone Disease\*. *Endocrine Reviews*, *7*(4), 379-408. doi:10.1210/edrv-7-4-379
- Errickson, D., Grueso, I., Griffith, S. J., Setchell, J. M., Thompson, T. J. U., Thompson, C. E. L., & Gowland, R. L. (2017). Towards a Best Practice for the Use of Active Non-contact Surface Scanning to Record Human Skeletal Remains from Archaeological Contexts. *International Journal of Osteoarchaeology*, *27*(4), 650-661. doi:10.1002/oa.2587
- Fahy, G. E., Deter, C., Pitfield, R., Miskiewicz, J. J., & Mahoney, P. (2017). Bone deep:

- Variation in stable isotope ratios and histomorphometric measurements of bone remodelling within adult humans. *Journal of Archaeological Science*, 87, 10-16.  
doi:10.1016/j.jas.2017.09.009
- Filzmoser, P., Gschwandtner, M., & Todorov, V. (2012). Review of sparse methods in regression and classification with application to chemometrics. *Journal of Chemometrics*, 26(3-4), 42-51. doi:<https://doi.org/10.1002/cem.1418>
- Fogel, M. L., & Tuross, N. (2003). Extending the limits of paleodietary studies of humans with compound specific carbon isotope analysis of amino acids. *Journal of Archaeological Science*, 30(5), 535-545. doi:10.1016/s0305-4403(02)00199-1
- Foucault, M. (1984a). Docile Bodies. In P. Rabinow (Ed.), *The Foucault Reader*. New York: Pantheon Books.
- Foucault, M. (1984b). Right of Death and Power over Life. In P. Rabinow (Ed.), *The Foucault Reader* (pp. 258-289). New York: Pantheon Books.
- Fox, K., & Hawks, J. (2019). Use ancient remains more wisely. *Nature*, 572(7771), 581-583.  
doi:10.1038/d41586-019-02516-5
- France, C. A. M., & Owsley, D. W. (2015). Stable Carbon and Oxygen Isotope Spacing Between Bone and Tooth Collagen and Hydroxyapatite in Human Archaeological Remains. *International Journal of Osteoarchaeology*, 25(3), 299-312. doi:10.1002/oa.2300
- France, C. A. M., Thomas, D. B., Doney, C. R., & Madden, O. (2014). FT-Raman spectroscopy as a method for screening collagen diagenesis in bone. *Journal of Archaeological*

*Science*, 42, 346-355. doi:10.1016/j.jas.2013.11.020

Frost, H. M. (1987). Bone “mass” and the “mechanostat”: A proposal. *The Anatomical Record*, 219(1), 1-9. doi:10.1002/ar.1092190104

Frost, H. M. (2000). The Utah paradigm of skeletal physiology: an overview of its insights for bone, cartilage and collagenous tissue organs. *Journal of Bone and Mineral Metabolism*, 18(6), 305-316. doi:10.1007/s007740070001

Geller, P. L., & Suri, M. S. (2014). Relationality, Corporeality and Bioarchaeology: Bodies qua Bodies, Bodies in Context. *Cambridge Archaeological Journal*, 24(3), 499-512. doi:10.1017/s0959774314000523

Golcuk, K., Mandair, G. S., Callender, A. F., Sahar, N., Kohn, D. H., & Morris, M. D. (2006). Is photobleaching necessary for Raman imaging of bone tissue using a green laser? *Biochimica et Biophysica Acta*, 1758(7), 868-873. doi:10.1016/j.bbamem.2006.02.022

Gold, E. R. (1996). *Body parts: Property rights and the ownership of human biological materials*. Washington, D.C.: Georgetown University Press.

Gonçalves, D., Vassalo, A. R., Mamede, A. P., Makhoul, C., Piga, G., Cunha, E., . . . Batista de Carvalho, L. A. E. (2018). Crystal clear: Vibrational spectroscopy reveals intrabone, intraskeleton, and interskeleton variation in human bones. *American Journal of Physical Anthropology*, 166(2), 296-312. doi:10.1002/ajpa.23430

Gorard, S. (2005). Revisiting a 90-Year-Old Debate: The Advantages of the Mean Deviation. *British Journal of Educational Studies*, 53(4), 417-430. doi:10.1111/j.1467-



8527.2005.00304.x

Gosman, J. H., Stout, S. D., & Larsen, C. S. (2011). Skeletal biology over the life span: a view from the surfaces. *American Journal of Physical Anthropology*, *146*(S53), 86-98.

doi:10.1002/ajpa.21612

Groves, S. E., Roberts, C. A., Lucy, S., Pearson, G., Gröcke, D. R., Nowell, G., . . . Young, G. (2013). Mobility histories of 7th-9th century AD people buried at early medieval

Bamburgh, Northumberland, England. *American Journal of Physical Anthropology*,

*151*(3), 462-476. doi:10.1002/ajpa.22290

Halcrow, S. E., Rooney, J., Beavan, N., Gordon, K. C., Tayles, N., & Gray, A. (2014). Assessing Raman Spectroscopy as a Prescreening Tool for the Selection of Archaeological Bone for

Stable Isotopic Analysis. *PloS One*, *9*(7), e98462. doi:10.1371/journal.pone.0098462

Harper, S. (2010). The social agency of dead bodies. *Mortality*, *15*(4), 308-322.

doi:10.1080/13576275.2010.513163

Heaton, T. H. E., Vogel, J. C., von la Chevallerie, G., & Collett, G. (1986). Climatic influence on the isotopic composition of bone nitrogen. *Nature*, *322*(6082), 822-823.

doi:10.1038/322822a0

Hedges, R. E. M. (2002). Bone diagenesis: an overview of processes. *Archaeometry*, *44*(3), 319-

328. doi:10.1111/1475-4754.00064

Hedges, R. E. M. (2003). On bone collagen—apatite-carbonate isotopic relationships.

*International Journal of Osteoarchaeology*, *13*(1-2), 66-79. doi:10.1002/oa.660

- Hedges, R. E. M., Clement, J. G., Thomas, C. D. L., & O'Connell, T. C. (2007). Collagen turnover in the adult femoral mid-shaft: modeled from anthropogenic radiocarbon tracer measurements. *American Journal of Physical Anthropology*, *133*(2), 808-816.  
doi:10.1002/ajpa.20598
- Henschel, H., & van der Spoel, D. (2020). An Intuitively Understandable Quality Measure for Theoretical Vibrational Spectra. *The Journal of Physical Chemistry Letters*, *11*(14), 5471-5475. doi:10.1021/acs.jpcclett.0c01655
- Hight, M. J. (2005). Body Snatching & Grave Robbing: Bodies for Science. *History and Anthropology*, *16*(4), 415-440.
- Howland, M. R., Corr, L. T., Young, S. M. M., Jones, V., Jim, S., Van Der Merwe, N. J., . . . Evershed, R. P. (2003). Expression of the dietary isotope signal in the compound-specific  $\delta^{13}\text{C}$  values of pig bone lipids and amino acids. *International Journal of Osteoarchaeology*, *13*(1-2), 54-65. doi:10.1002/oa.658
- Hsieh, Y. F., Robling, A. G., Ambrosius, W. T., Burr, D. B., & Turner, C. H. (2001). Mechanical Loading of Diaphyseal Bone In Vivo: The Strain Threshold for an Osteogenic Response Varies with Location. *Journal of Bone and Mineral Research*, *16*(12), 2291-2297.  
doi:10.1359/jbmr.2001.16.12.2291
- Hufthammer, A. K., Høie, H., Folkvord, A., Geffen, A. J., Andersson, C., & Ninnemann, U. S. (2010). Seasonality of human site occupation based on stable oxygen isotope ratios of cod otoliths. *Journal of Archaeological Science*, *37*(1), 78-83.  
doi:10.1016/j.jas.2009.09.001

- Illies, C., & Meijers, A. (2009). Artefacts Without Agency. *The Monist*, 92(3), 420-440.  
doi:10.5840/monist200992324
- Isbell, W. H. (1997). *Mummies and Mortuary Monuments: A Post-processual Prehistory of Central Andean Social Organization*. Austin: University of Texas Press.
- Jaouen, K., & Pons, M.-L. (2016). Potential of non-traditional isotope studies for bioarchaeology. *Archaeological and Anthropological Sciences*, 9(7), 1389-1404.  
doi:10.1007/s12520-016-0426-9
- Jørkov, M. L. S., Heinemeier, J., & Lynnerup, N. (2009). The petrous bone—A new sampling site for identifying early dietary patterns in stable isotopic studies. *American Journal of Physical Anthropology*, 138(2), 199-209. doi:10.1002/ajpa.20919
- Katzenberg, M. A. (2008). Stable Isotope Analysis: A Tool for Studying Past Diet, Demography, and Life History. In M. A. Katzenberg & S. R. Saunders (Eds.), *Biological Anthropology of the Human Skeleton* (2nd ed., pp. 413-441). Hoboken: John Wiley & Sons Ltd.
- Katzenberg, M. A., & Lovell, N. C. (1999). Stable isotope variation in pathological bone. *International Journal of Osteoarchaeology*, 9(5), 316-324. doi:10.1002/(SICI)1099-1212(199909/10)9:5<316::AID-OA500>3.0.CO;2-D
- Kaufmann, I. M., & Rühli, F. J. (2010). Without 'informed consent'? Ethics and ancient mummy research. *Journal of Medical Ethics*, 36(10), 608-613. doi:10.1136/jme.2010.036608
- Keenan, S. W., & Engel, A. S. (2017). Early diagenesis and recrystallization of bone. *Geochimica et Cosmochimica Acta*, 196, 209-223. doi:10.1016/j.gca.2016.09.033

- Keresztury, G. (2006). Raman Spectroscopy: Theory. In J. M. Chalmers & P. R. Griffiths (Eds.), *Handbook of Vibrational Spectroscopy* (Vol. 1, pp. 71-87). New York: John Wiley & Sons.
- Kerstel, E. (2004). Isotope ratio infrared spectrometry. In P. A. de Groote (Ed.), *Handbook of Stable Isotope Analytical Techniques* (Vol. I, pp. 759-787). Amsterdam: Elsevier Science.
- Khan, A. F., Awais, M., Khan, A. S., Tabassum, S., Chaudhry, A. A., & Rehman, I. U. (2013). Raman Spectroscopy of Natural Bone and Synthetic Apatites. *Applied Spectroscopy Reviews*, 48(4), 329-355. doi:10.1080/05704928.2012.721107
- Kimura-Suda, H., Kajiwara, M., Sakamoto, N., Kobayashi, S., Ijio, K., Yurimoto, H., & Yamato, H. (2013). Studies on bone metabolism by using isotope microscopy, FTIR imaging, and micro-Raman spectroscopy. *Journal of Oral Biosciences*, 55(2), 61-65. doi:10.1016/j.job.2013.04.006
- Knudson, K. J., & Price, T. D. (2007). Utility of multiple chemical techniques in archaeological residential mobility studies: Case studies from Tiwanaku- and Chiribaya-affiliated sites in the Andes. *American Journal of Physical Anthropology*, 132(1), 25-39. doi:10.1002/ajpa.20480
- Kreissl Lonfat, B. M., Kaufmann, I. M., & Rühli, F. (2015). A Code of Ethics for Evidence-Based Research With Ancient Human Remains. *The Anatomical Record*, 298(6), 1175-1181. doi:10.1002/ar.23126

Lanyon, L. E., Goodship, A. E., Pye, C. J., & MacFie, J. H. (1982). Mechanically adaptive bone remodelling. *Journal of Biomechanics*, *15*(3), 141-154. doi:10.1016/0021-9290(82)90246-9

Latour, B. (2005). *Reassembling the Social – An Introduction to Actor-Network-Theory*. Oxford: Oxford University Press.

Le Huray, J. D., & Schutkowski, H. (2005). Diet and Social Status during the La Tène Period in Bohemia: Carbon and Nitrogen Stable Isotope Analysis of Bone Collagen from Kutná Hora-Karlovy and Radošovice. *Journal of Anthropological Archaeology*, *24*(2), 135-147. doi:10.1016/j.jaa.2004.09.002

Lee-Thorp, J. A., Sealy, J. C., & van der Merwe, N. J. (1989). Stable carbon isotope ratio differences between bone collagen and bone apatite, and their relationship to diet. *Journal of Archaeological Science*, *16*(6), 585-599. doi:10.1016/0305-4403(89)90024-1

Leskovaar, T., Zupanic Pajnic, I., Jerman, I., & Cresnar, M. (2020). Separating forensic, WWII, and archaeological human skeletal remains using ATR-FTIR spectra. *International Journal of Legal Medicine*, *134*(2), 811-821. doi:10.1007/s00414-019-02079-0

Lesley, E. (2015). Death on Display: Bones and Bodies in Cambodia and Rwanda. In F. Ferrándiz & A. C. G. M. Robben (Eds.), *Necropolitics: Mass Graves and Exhumations in the Age of Human Rights* (pp. 213-239). Philadelphia: University of Pennsylvania Press.

Levenbook, B. B. (1984). Harming Someone after His Death. *Ethics*, *94*(3), 407-419.

Li, J., Li, R., Zhao, B., Guo, H., Zhang, S., Cheng, J., & Wu, X. (2018). Quantitative

- measurement of carbon isotopic composition in CO<sub>2</sub> gas reservoir by Micro-Laser Raman spectroscopy. *Spectrochimica Acta. Part A: Molecular and Biomolecular Spectroscopy*, 195, 191-198. doi:10.1016/j.saa.2018.01.082
- López-Costas, O., Lantes-Suárez, Ó., & Martínez Cortizas, A. (2016). Chemical compositional changes in archaeological human bones due to diagenesis: Type of bone vs soil environment. *Journal of Archaeological Science*, 67, 43-51. doi:10.1016/j.jas.2016.02.001
- Lynch, J. J. (2018). The Automation of Regression Modeling in Osteometric Sorting: An Ordination Approach. *Journal of Forensic Sciences*, 63(3), 798-804. doi:10.1111/1556-4029.13597
- Native American Graves Protection and Repatriation Review Committee Meeting*, (2019).
- Madden, O., Chan, D. M. W., Dundon, M., & France, C. A. M. (2018). Quantifying collagen quality in archaeological bone: Improving data accuracy with benchtop and handheld Raman spectrometers. *Journal of Archaeological Science: Reports*, 18, 596-605. doi:10.1016/j.jasrep.2017.11.034
- Maggianno, C. M., White, C. D., Stern, R. A., Peralta, J. S., & Longstaffe, F. J. (2019). Focus: Oxygen isotope microanalysis across incremental layers of human bone: Exploring archaeological reconstruction of short term mobility and seasonal climate change. *Journal of Archaeological Science*, 111, 105028. doi:10.1016/j.jas.2019.105028
- Manolagas, S. C. (2000). Birth and death of bone cells: basic regulatory mechanisms and

- implications for the pathogenesis and treatment of osteoporosis. *Endocrine Reviews*, 21(2), 115-137. doi:10.1210/edrv.21.2.0395
- Matsubayashi, J., & Tayasu, I. (2019). Collagen turnover and isotopic records in cortical bone. *Journal of Archaeological Science*, 106, 37-44. doi:10.1016/j.jas.2019.03.010
- Mays, S., Elders, J., Humphrey, L., White, W., & Marshall, P. (2013). *Science and the Dead: A guideline for the destructive sampling of archaeological human remains for scientific analysis*. Retrieved from London:
- Mbembé, A. (2003). Necropolitics. *Public Culture*, 15(1), 11-40.
- McKay, N. P., Dettman, D. L., Downs, R. T., & Overpeck, J. T. (2013). On the potential of Raman-spectroscopy-based carbonate mass spectrometry. *Journal of Raman Spectroscopy*, 44(3), 469-474. doi:10.1002/jrs.4218
- McLaughlin, G., & Lednev, I. K. (2011). Potential application of Raman spectroscopy for determining burial duration of skeletal remains. *Analytical and Bioanalytical Chemistry*, 401(8), 2511-2518. doi:10.1007/s00216-011-5338-z
- McLaughlin, G., & Lednev, I. K. (2012). Spectroscopic Discrimination of Bone Samples from Various Species. *American Journal of Analytical Chemistry*, 03(02), 161-167. doi:10.4236/ajac.2012.32023
- Meinshausen, N., & Bühlmann, P. (2006). High-dimensional graphs and variable selection with the Lasso. *The Annals of Statistics*, 34(3), 1436-1462. doi:10.1214/009053606000000281

- Moder, K. (2016). How to keep the Type I Error Rate in ANOVA if Variances are Heteroscedastic. *Austrian Journal of Statistics*, 36(3), 179-188.  
doi:10.17713/ajs.v36i3.329
- Molnár, M. (2001). *A Concise History of Hungary*. Cambridge: Cambridge University Press.
- Momma, K., & Izumi, F. (2008). VESTA: a three-dimensional visualization system for electronic and structural analysis. *Journal of Applied Crystallography*, 41(3), 653-658.  
doi:10.1107/s0021889808012016
- Moore v. Regents of the University of California, 51 Cal.3d 120 , 271 Cal.Rptr. 146; 793 P.2d 479 C.F.R. (1990).
- Morris, M. D., & Mandair, G. S. (2011). Raman assessment of bone quality. *Clinical Orthopaedics and Related Research*, 469(8), 2160-2169. doi:10.1007/s11999-010-1692-y
- Muhamadali, H., Chisanga, M., Subaihi, A., & Goodacre, R. (2015). Combining Raman and FT-IR spectroscopy with quantitative isotopic labeling for differentiation of E. coli cells at community and single cell levels. *Analytical Chemistry*, 87(8), 4578-4586.  
doi:10.1021/acs.analchem.5b00892
- Native American Graves Protection and Repatriation Act of 1990, 25 Cong. Rec. § 3006(b) (1990).
- Nehlich, O., Fuller, B. T., Jay, M., Mora, A., Nicholson, R. A., Smith, C. I., & Richards, M. P. (2011). Application of sulphur isotope ratios to examine weaning patterns and freshwater fish consumption in Roman Oxfordshire, UK. *Geochimica et Cosmochimica Acta*,



75(17), 4963-4977. doi:10.1016/j.gca.2011.06.009

O'Leary, M. H. (1988). Carbon Isotopes in Photosynthesis. *Bioscience*, 38(5), 328-336.

doi:10.2307/1310735

Olsen, K. C., White, C. D., Longstaffe, F. J., von Heyking, K., McGlynn, G., Grupe, G., &

Rühli, F. J. (2014). Intraskkeletal isotopic compositions ( $\delta^{13}\text{C}$ ,  $\delta^{15}\text{N}$ ) of bone collagen:

Nonpathological and pathological variation. *American Journal of Physical Anthropology*,

153(4), 598-604. doi:10.1002/ajpa.22459

Ortiz-Herrero, L., Uribe, B., Armas, L. H., Alonso, M. L., Sarmiento, A., Irurita, J., . . .

Bartolome, L. (2021). Estimation of the post-mortem interval of human skeletal remains

using Raman spectroscopy and chemometrics. *Forensic Science International*, 329,

111087. doi:10.1016/j.forsciint.2021.111087

Parfitt, A. M. (1994). Osteonal and hemi-osteonal remodeling: The spatial and temporal

framework for signal traffic in adult human bone. *Journal of Cellular Biochemistry*,

55(3), 273-286. doi:10.1002/jcb.240550303

Parra, R. C., Anstett, É., Perich, P., & Buikstra, J. E. (2020). Unidentified deceased persons:

Social life, social death and humanitarian action. In R. C. Parra, S. C. Zapico, & D. H.

Ubelaker (Eds.), *Forensic Science and Humanitarian Action: Interacting with the Dead*

*and the Living* (pp. 79-99). Hoboken, NJ: John Wiley & Sons.

Pate, F. D. (1994). Bone chemistry and paleodiet. *Journal of Archaeological Method and*

*Theory*, 1(2), 161-209. doi:10.1007/bf02231415

- Pedregosa, F., Varoquaux, G., Gramfort, A., Michel, V., Thirion, B., Grisel, O., . . . Dubourg, V. (2011). Scikit-learn: Machine learning in Python. *Journal of Machine Learning Research, 12*, 2825-2830.
- Pedrosa, M., Curate, F., Batista de Carvalho, L. A. E., Marques, M. P. M., & Ferreira, M. T. (2020). Beyond metrics and morphology: the potential of FTIR-ATR and chemometrics to estimate age-at-death in human bone. *International Journal of Legal Medicine, 134*(5), 1905-1914. doi:10.1007/s00414-020-02310-3
- Pellegrini, M., & Snoeck, C. (2016). Comparing bioapatite carbonate pre-treatments for isotopic measurements: Part 2 — Impact on carbon and oxygen isotope compositions. *Chemical Geology, 420*, 88-96. doi:10.1016/j.chemgeo.2015.10.038
- Penel, G., Leroy, G., & Bres, E. (1998). New Preparation Method of Bone Samples for Raman Microspectrometry. *Applied Spectroscopy, 52*, 312-313.
- Penel, G., Leroy, G., Rey, C., & Bres, E. (1998). MicroRaman Spectral Study of the PO<sub>4</sub> and CO<sub>3</sub> Vibrational Modes in Synthetic and Biological Apatites. *Calcified Tissue International, 63*(6), 475-481. doi:10.1007/s002239900561
- Perera, S. (2006). 'They Give Evidence': Bodies, Borders and the Disappeared. *Social Identities, 12*(6), 637-656. doi:10.1080/13504630601030859
- Pestle, W. J., Ahmad, F., Vesper, B. J., Cordell, G. A., & Colvard, M. D. (2014). Ancient bone collagen assessment by hand-held vibrational spectroscopy. *Journal of Archaeological Science, 42*, 381-389. doi:10.1016/j.jas.2013.11.014

- Pestle, W. J., Brennan, V., Sierra, R. L., Smith, E. K., Vesper, B. J., Cordell, G. A., & Colvard, M. D. (2015). Hand-held Raman spectroscopy as a pre-screening tool for archaeological bone. *Journal of Archaeological Science*, 58, 113-120. doi:10.1016/j.jas.2015.03.027
- Pestle, W. J., Crowley, B. E., & Weirauch, M. T. (2014). Quantifying inter-laboratory variability in stable isotope analysis of ancient skeletal remains. *PloS One*, 9(7), e102844. doi:10.1371/journal.pone.0102844
- Pucéat, E., Reynard, B., & Lécuyer, C. (2004). Can crystallinity be used to determine the degree of chemical alteration of biogenic apatites? *Chemical Geology*, 205(1-2), 83-97. doi:10.1016/j.chemgeo.2003.12.014
- Pylypa, J. (1998). Power and Bodily Practice: Applying the Work of Foucault to an Anthropology of the Body. *Arizona Anthropologist*, 13, 21-36.
- Rabinow, P., & Rose, N. (2006). Biopower Today. *Biosciences*, 1(2), 195-217.
- Reardon, J., & TallBear, K. (2012). “Your DNA is our history”: genomics, anthropology, and the construction of whiteness as property. *Current Anthropology*, 53(S5), S233-S245.
- Reitsema, L. J. (2013). Beyond diet reconstruction: stable isotope applications to human physiology, health, and nutrition. *American Journal of Human Biology*, 25(4), 445-456. doi:10.1002/ajhb.22398
- Reitsema, L. J., & Kozłowski, T. (2013). Diet and society in Poland before the state: stable isotope evidence from a Wielbark population (2nd c. AD). *Anthropological Review*, 76(1), 1-22. doi:10.2478/anre-2013-0010

- Reynard, L. M., & Tuross, N. (2015). The known, the unknown and the unknowable: weaning times from archaeological bones using nitrogen isotope ratios. *Journal of Archaeological Science*, 53, 618-625. doi:10.1016/j.jas.2014.11.018
- Richards, M. P., Mays, S., & Fuller, B. T. (2002). Stable carbon and nitrogen isotope values of bone and teeth reflect weaning age at the Medieval Wharram Percy site, Yorkshire, UK. *American Journal of Physical Anthropology*, 119(3), 205-210.
- Riding In, J. (1992). Without Ethics and Morality: A Historical Overview of Imperial Archaeology and American Indians. *Arizona State Law Journal*, 24, 11-34.
- Robinson, H. (2017). Dualism. In E. N. Zalta (Ed.), *The Stanford Encyclopedia of Philosophy* (Fall 2017 ed.). <https://plato.stanford.edu/archives/fall2017/entries/dualism/>.
- Robling, A. G., Castillo, A. B., & Turner, C. H. (2006). Biomechanical and molecular regulation of bone remodeling. *Annual Review of Biomedical Engineering*, 8, 455-498. doi:10.1146/annurev.bioeng.8.061505.095721
- Rogers, M. (1976, March 25, 1976). The Double-Edged Helix. *Rolling Stone*, 48-51.
- Sadongei, A., & Cash Cash, P. (2007). Indigenous Value Orientations in the Care of Human Remains. In V. Cassman, N. Odegaard, & J. F. Powell (Eds.), *Human Remains: Guide for Museums and Academic Institutions* (pp. 97-100). New York: AltaMira Press.
- Samuel, A. Z., Mukojima, R., Horii, S., Ando, M., Egashira, S., Nakashima, T., . . . Takeyama, H. (2021). On Selecting a Suitable Spectral Matching Method for Automated Analytical Applications of Raman Spectroscopy. *ACS Omega*, 6(3), 2060-2065.

doi:10.1021/acsomega.0c05041

Sandberg, P. A., Sponheimer, M., Lee-Thorp, J., & Van Gerven, D. (2014). Intra-tooth stable isotope analysis of dentine: A step toward addressing selective mortality in the reconstruction of life history in the archaeological record. *American Journal of Physical Anthropology*, *155*(2), 281-293. doi:10.1002/ajpa.22600

Šavlovskis, J., & Raits, K. (Producer). (2021). Anatomy Standard.

Schlecht, S. H., Pinto, D. C., Agnew, A. M., & Stout, S. D. (2012). Brief communication: The effects of disuse on the mechanical properties of bone: What unloading tells us about the adaptive nature of skeletal tissue. *American Journal of Physical Anthropology*, *149*(4), 599-605. doi:10.1002/ajpa.22150

Schoeller, D. A. (1999). Isotope Fractionation: Why Aren't We What We Eat? *Journal of Archaeological Science*, *26*(6), 667-673. doi:10.1006/jasc.1998.0391

Schoeller, D. A., Minagawa, M., Slater, R., & Kaplan, I. R. (1986). Stable isotopes of carbon, nitrogen and hydrogen in the contemporary north American human food web. *Ecology of Food and Nutrition*, *18*(3), 159-170. doi:10.1080/03670244.1986.9990922

Schoeninger, M. J. (1988). Reconstructing prehistoric human diet. *HOMO - Journal of Comparative Human Biology*, *39*(2), 78-99.

Schulte, F. A., Ruffoni, D., Lambers, F. M., Christen, D., Webster, D. J., Kuhn, G., & Muller, R. (2013). Local mechanical stimuli regulate bone formation and resorption in mice at the tissue level. *PLoS One*, *8*(4), e62172. doi:10.1371/journal.pone.0062172

- Sealy, J., Armstrong, R., & Schrire, C. (1995). Beyond Lifetime Averages: Tracing Life Histories through Isotopic Analysis of Different Calcified Tissues from Archaeological Human Skeletons. *Antiquity*, *69*, 290-300. doi:10.1017/S0003598X00064693
- Sharp, L. A. (2000). The Commodification of the Body and its Parts. *Annual Review Of Anthropology*, *29*(1), 287-328. doi:10.1146/annurev.anthro.29.1.287
- Shea, D. A., & Morris, M. D. (2002). Bone Tissue Fluorescence Reduction for Visible Laser Raman Spectroscopy. *Applied Spectroscopy*, *56*(2), 182-186.  
doi:10.1366/0003702021954647
- Skloot, R. (2010). *The Immortal Life of Henrietta Lacks*. New York: Broadway Books.
- Smith, R., & Rehman, I. (1994). Fourier transform Raman spectroscopic studies of human bone. *Journal of Materials Science: Materials in Medicine*, *5*(9-10), 775-778.  
doi:10.1007/bf00120375
- Snoeck, C., & Pellegrini, M. (2015). Comparing bioapatite carbonate pre-treatments for isotopic measurements: Part 1—Impact on structure and chemical composition. *Chemical Geology*, *417*, 394-403. doi:10.1016/j.chemgeo.2015.10.004
- Somerville, A. D., Fauvelle, M., & Froehle, A. W. (2013). Applying new approaches to modeling diet and status: isotopic evidence for commoner resiliency and elite variability in the Classic Maya lowlands. *Journal of Archaeological Science*, *40*(3), 1539-1553.  
doi:10.1016/j.jas.2012.10.029
- Sponheimer, M., Ryder, C. M., Fewlass, H., Smith, E. K., Pestle, W. J., & Talamo, S. (2019).

- Saving Old Bones: a non-destructive method for bone collagen prescreening. *Science Reports*, 9(1), 13928. doi:10.1038/s41598-019-50443-2
- Squires, K., Booth, T., & Roberts, C. A. (2019). The Ethics of Sampling Human Skeletal Remains for Destructive Analyses. In K. Squires, D. Errickson, & N. Márquez-Grant (Eds.), *Ethical Approaches to Human Remains* (pp. 265-297). Cham: Springer.
- Stathopoulou, E. T., Psycharis, V., Chryssikos, G. D., Gionis, V., & Theodorou, G. (2008). Bone diagenesis: New data from infrared spectroscopy and X-ray diffraction. *Palaeogeography, Palaeoclimatology, Palaeoecology*, 266(3-4), 168-174. doi:10.1016/j.palaeo.2008.03.022
- Still, C. J., Berry, J. A., Collatz, G. J., & DeFries, R. S. (2003). Global distribution of C<sub>3</sub> and C<sub>4</sub> vegetation: Carbon cycle implications. *Global Biogeochemical Cycles*, 17(1), 6-1-6-14. doi:10.1029/2001gb001807
- Sudarsanan, K., & Young, R. A. (1969). Significant precision in crystal structural details. Holly Springs hydroxyapatite. *Acta Crystallographica Section B Structural Crystallography and Crystal Chemistry*, 25(8), 1534-1543. doi:10.1107/s0567740869004298
- Sugiyama, T., Meakin, L. B., Browne, W. J., Galea, G. L., Price, J. S., & Lanyon, L. E. (2012). Bones' adaptive response to mechanical loading is essentially linear between the low strains associated with disuse and the high strains associated with the lamellar/woven bone transition. *Journal of Bone and Mineral Research*, 27(8), 1784-1793. doi:10.1002/jbmr.1599

Sugiyama, T., Price, J. S., & Lanyon, L. E. (2010). Functional adaptation to mechanical loading in both cortical and cancellous bone is controlled locally and is confined to the loaded bones. *Bone*, *46*(2), 314-321. doi:10.1016/j.bone.2009.08.054

Tapp, H. S., & Kemsley, E. K. (2009). Notes on the practical utility of OPLS. *Trends in Analytical Chemistry*, *28*(11), 1322-1327. doi:10.1016/j.trac.2009.08.006

Tauber, A. I. (1999). Is Biology a Political Science? *Bioscience*, *49*(6), 479-486. doi:10.2307/1313555

Tomczak, M., & Tomczak, E. (2014). The need to report effect size estimates revisited. An overview of some recommended measures of effect size. *Trends in Sport Sciences*, *1*(21), 19-25.

Toyne, J. M., White, C. D., Verano, J. W., Uceda Castillo, S., Millaire, J. F., & Longstaffe, F. J. (2014). Residential histories of elites and sacrificial victims at Huacas de Moche, Peru, as reconstructed from oxygen isotopes. *Journal of Archaeological Science*, *42*, 15-28. doi:10.1016/j.jas.2013.10.036

Trent, C., Zejdlik, K., Nyaradi, Z., Gonciar, A., Berger, J., Tykot, R., & Bethard, J. (2020). *Dietary Reconstruction of the Székely Community of Papdomb*. Paper presented at the European Association of Archaeologists Annual Meeting, Virtual.

Trueman, C. N., Privat, K., & Field, J. (2008). Why do crystallinity values fail to predict the extent of diagenetic alteration of bone mineral? *Palaeogeography, Palaeoclimatology, Palaeoecology*, *266*(3-4), 160-167. doi:10.1016/j.palaeo.2008.03.038



- Truog, R. D., Kesselheim, A. S., & Joffe, S. (2012). Paying patients for their tissue: The legacy of Henrietta Lacks. *Science*, 337(6090), 37-38. doi:10.1126/science.1216888
- Tsosie, R. (2007). Cultural Challenges to Biotechnology: Native American Genetic Resources and the Concept of Cultural Harm. *Journal of Law, Medicine and Ethics*, 35(3), 396-411. doi:10.1111/j.1748-720X.2007.00163.x
- Turner, C. H. (1999). Toward a Mathematical Description of Bone Biology: The Principle of Cellular Accommodation. *Calcified Tissue International*, 65(6), 466-471. doi:10.1007/s002239900734
- Turner, T. R. (2005). Introduction: Ethical Concerns in Biological Anthropology. In T. R. Turner (Ed.), *Biological Anthropology and Ethics: From Repatriation to Genetic Identity* (pp. 1-13). Albany: State University of New York Press.
- Turner, T. R. (2012). Ethical Issues in Human Population Biology. *Current Anthropology*, 53, S222-S223.
- Turner, T. R., Wagner, J. K., & Cabana, G. S. (2018). Ethics in Biological Anthropology. *American Journal of Physical Anthropology*, 165, 939-951.
- Tykot, R. H. (2010). Isotope Analyses and the Histories of Maize. In J. Staller, R. Tykot, & B. Benz (Eds.), *Histories of Maize in Mesoamerica: Multidisciplinary Approaches* (pp. 131-142). New York: Left Coast Press, Inc.
- van der Merwe, N. J. (1982). Carbon Isotopes, Photosynthesis, and Archaeology: Different pathways of photosynthesis cause characteristic changes in carbon isotope ratios that

- make possible the study of prehistoric human diets. *American Scientist*, 70(6), 596-606.
- van Oers, R. F. M., Ruimerman, R., Tanck, E., Hilbers, P. A. J., & Huiskes, R. (2008). A unified theory for osteonal and hemi-osteonal remodeling. *Bone*, 42(2), 250-259.  
doi:10.1016/j.bone.2007.10.009
- van Oers, R. F. M., Ruimerman, R., van Rietbergen, B., Hilbers, P. A. J., & Huiskes, R. (2008). Relating osteon diameter to strain. *Bone*, 43(3), 476-482. doi:10.1016/j.bone.2008.05.015
- Verdery, K. (1999). *The Political Lives of Dead Bodies: Reburial and Postsocialist Change*. New York: Columbia University Press.
- Vinh, N. X., Epps, J., & Bailey, J. (2010). Information Theoretic Measures for Clusterings Comparison: Variants, Properties, Normalization and Correction for Chance" (PDF), T, 11 (oct): 2837–54. *The Journal of Machine Learning Research*, 11, 2837-2854.
- Vitkin, V., Polishchuk, A., Chubchenko, I., Popov, E., Grigorenko, K., Kharitonov, A., . . . Mateos, X. (2020). Raman Laser Spectrometer: Application to  $^{12}\text{C}/^{13}\text{C}$  Isotope Identification in  $\text{CH}_4$  and  $\text{CO}_2$  Greenhouse Gases. *Applied Sciences*, 10(21).  
doi:10.3390/app10217473
- Vogel, J. C., & Van Der Merwe, N. J. (1977). Isotopic Evidence for Early Maize Cultivation in New York State. *American Antiquity*, 42(2), 238-242. doi:10.2307/278984
- Walker, P. L. (2008). Bioarchaeological Ethics: A Historical Perspective on the Value of Human Remains. In M. A. Katzenberg & S. R. Saunders (Eds.), *Biological Anthropology of the Human Skeleton* (Second ed., pp. 3-40). Hoboken: John Wiley & Sons Ltd.

- Walsh, J. S. (2018). Normal bone physiology, remodelling and its hormonal regulation. *Surgery (Oxford)*, 36(1), 1-6. doi:10.1016/j.mpsur.2017.10.006
- Warinner, C., & Tuross, N. (2010). Brief communication: tissue isotopic enrichment associated with growth depression in a pig: implications for archaeology and ecology. *American Journal of Physical Anthropology*, 141(3), 486-493. doi:10.1002/ajpa.21222
- Waters-Rist, A. L., & Katzenberg, M. A. (2010). The effect of growth on stable nitrogen isotope ratios in subadult bone collagen. *International Journal of Osteoarchaeology*, 20(2), 172-191. doi:10.1002/oa.1017
- Webb, E. C., White, C. D., & Longstaffe, F. J. (2014). Investigating inherent differences in isotopic composition between human bone and enamel bioapatite: implications for reconstructing residential histories. *Journal of Archaeological Science*, 50, 97-107. doi:10.1016/j.jas.2014.07.001
- Weiner, S. (2010a). Biological Materials: Bone and Teeth. In *Microarchaeology: Beyond the Visible Archaeological Record* (pp. 99-134). New York: Cambridge University Press.
- Weiner, S. (2010b). Reading the Microscopic Record On-Site. In *Microarchaeology: Beyond the Visible Archaeological Record* (pp. 261-274). New York: Cambridge University Press.
- Wiesheu, A. C., Brejcha, R., Mueller, C. W., Kögel-Knabner, I., Elsner, M., Niessner, R., & Ivleva, N. P. (2018). Stable-isotope Raman microspectroscopy for the analysis of soil organic matter. *Analytical and Bioanalytical Chemistry*, 410(3), 923-931. doi:10.1007/s00216-017-0543-z

- Woess, C., Unterberger, S. H., Roider, C., Ritsch-Marte, M., Pemberger, N., Cemper-Kiesslich, J., . . . Pallua, J. D. (2017). Assessing various Infrared (IR) microscopic imaging techniques for post-mortem interval evaluation of human skeletal remains. *PloS One*, *12*(3), e0174552. doi:10.1371/journal.pone.0174552
- Wolff, J. (1986 [1892]). *Law of Bone Remodelling* (P. Maquet & R. Furlong, Trans.). Berlin: Springer-Verlag.
- Wright, L. E., & Schwarcz, H. P. (1996). Infrared and Isotopic Evidence for Diagenesis of Bone Apatite at Dos Pilas, Guatemala: Palaeodietary Implications. *Journal of Archaeological Science*, *23*(6), 933-944. doi:10.1006/jasc.1996.0087
- Wright, L. E., & Schwarcz, H. P. (1998). Stable carbon and oxygen isotopes in human tooth enamel: Identifying breastfeeding and weaning in prehistory. *American Journal of Physical Anthropology*, *106*(1), 1-18. doi:10.1002/(sici)1096-8644(199805)106:1<1::aid-ajpa1>3.0.co;2-w
- Yang, H., Xu, X., Bullock, W., & Main, R. P. (2019). Adaptive changes in micromechanical environments of cancellous and cortical bone in response to in vivo loading and disuse. *Journal of Biomechanics*, *89*, 85-94. doi:10.1016/j.jbiomech.2019.04.021
- Young, H. (2011). The Right to Posthumous Bodily Integrity and Implications of Whether it is a Right of the Dead or of the Living. *SSRN Electronic Journal*. doi:10.2139/ssrn.2637315
- Zejdlik, K., Gonciar, A., Bethard, J., & Nyárádi, Z. (2020). Investigating a Medieval Church and Cemetery (Văleni-Papdomb, Harghita County). *Acta Musei Napocensis*, *57*(II), 143-173.

Zuckerman, M. K., Kamnikar, K. R., & Mathena, S. A. (2014). Recovering the 'Body Politic': a Relational Ethics of Meaning for Bioarchaeology. *Cambridge Archaeological Journal*, 24(3), 513-522. doi:10.1017/s0959774314000766

## APPENDIX

APPENDIX I

INVENTORY OF SKELETAL ELEMENTS AND INDICES OF DIAGENESIS FROM  
RAMAN SPECTRA FOR INDIVIDUALS FROM PATAKFALVA-PAPDOMB AND  
DUPLICATED ANALYSES IN THIS STUDY

Table I.1. Inventory of samples representing individuals from Patakfalva-Papdomb and diagenetic indices calculated from original scans.

| ID   | Element   | Portion           | Age Category | Same as | QC    | CI <sub>raman</sub> | Fluor. Ratio | Amide(I) PO <sub>4</sub> | CO <sub>3</sub> PO <sub>4</sub> |
|------|-----------|-------------------|--------------|---------|-------|---------------------|--------------|--------------------------|---------------------------------|
| S001 | mandible  | gonial portion    | Adult        |         | fair  | 0.301               | 0.876        | 9.899                    | 0.502                           |
| S002 | mandible  | notch             | Adult        |         | great | 0.310               | 0.835        | 12.324                   | 0.317                           |
| S003 | mandible  | ascending ramus   | Adult        |         | good  | 0.301               | 0.901        | 8.570                    | 0.339                           |
| S004 | mandible  | condyle           | Adult        |         | good  | 0.299               | 0.892        | 6.734                    | 0.323                           |
| S005 | ilium     | crest             | Adult        |         | good  | 0.298               | 0.871        | 11.619                   | 0.329                           |
| S006 | ilium     | crest             | Adult        | S005    | great | 0.308               | 0.862        | 10.740                   | 0.278                           |
| S007 | zygomatic | complete          | Adult        |         | fair  | 0.318               | 0.905        | 7.441                    | 0.472                           |
| S008 | temporal  | petrous           | Adult        |         | fair  | 0.280               | 0.933        | 7.953                    | 0.652                           |
| S009 | rib       | midshaft          | Adult        |         | great | 0.287               | 0.832        | 15.322                   | 0.261                           |
| S010 | rib       | distal 1st        | Adult        |         | great | 0.291               | 0.741        | 12.594                   | 0.259                           |
| S011 | rib       | proximal 1st      | Adult        | S010    | great | 0.295               | 0.804        | 12.892                   | 0.295                           |
| S012 | ilium     | crest             | Subadult     |         | good  | 0.367               | 0.921        | 5.361                    | 0.553                           |
| S013 | ulna      | proximal shaft    | Subadult     |         | good  | 0.308               | 0.877        | 9.155                    | 0.365                           |
| S014 | tibia     | proximal shaft    | Subadult     |         | fair  | 0.298               | 0.903        | 8.855                    | 0.412                           |
| S015 | scapula   | blade and glenoid | Subadult     |         | good  | 0.316               | 0.902        | 7.315                    | 0.448                           |
| S016 | ulna      | proximal shaft    | Subadult     |         | good  | 0.287               | 0.890        | 8.842                    | 0.384                           |
| S017 | humerus   | midshaft          | Subadult     |         | fair  | 0.331               | 0.926        | 7.062                    | 0.499                           |
| S018 | femur     | distal shaft      | Subadult     |         | fair  | 0.299               | 0.919        | 7.376                    | 0.501                           |
| S019 | femur     | distal shaft      | Subadult     |         | fair  | 0.279               | 0.917        | 7.659                    | 0.444                           |
| S020 | tibia     | proximal shaft    | Subadult     |         | fair  | 0.266               | 0.944        | 6.566                    | 0.548                           |
| S021 | femur     | midshaft          | Subadult     |         | bad   | 0.301               | 0.947        | 4.859                    | 0.551                           |
| S022 | femur     | midshaft          | Subadult     | S021    | good  | 0.307               | 0.894        | 7.224                    | 0.334                           |
| S023 | femur     | midshaft          | Subadult     |         | good  | 0.295               | 0.922        | 7.742                    | 0.501                           |
| S024 | femur     | distal shaft      | Subadult     | S023    | good  | 0.292               | 0.934        | 5.988                    | 0.472                           |
| S025 | femur     | midshaft          | Subadult     |         | good  | 0.288               | 0.878        | 8.262                    | 0.404                           |
| S026 | femur     | midshaft          | Subadult     | S025    | good  | 0.307               | 0.869        | 14.185                   | 0.376                           |
| S027 | tibia     | midshaft          | Subadult     |         | good  | 0.311               | 0.877        | 10.530                   | 0.366                           |
| S028 | tibia     | proximal shaft    | Subadult     | S027    | fair  | 0.286               | 0.912        | 5.260                    | 0.455                           |
| S029 | long bone | midshaft          | Subadult     |         | good  | 0.317               | 0.915        | 9.966                    | 0.489                           |
| S030 | long bone | midshaft          | Subadult     |         | great | 0.299               | 0.875        | 9.865                    | 0.322                           |
| S031 | cranial   | vault             | Adult        |         | fair  | 0.298               | 0.922        | 6.828                    | 0.497                           |

Table I.1. Continued.

| ID   | Element   | Portion        | Age Category | Same as | QC    | CI <sub>raman</sub> | Fluor. Ratio | <u>Amide(I)</u><br>PO <sub>4</sub> | <u>CO<sub>3</sub></u><br>PO <sub>4</sub> |
|------|-----------|----------------|--------------|---------|-------|---------------------|--------------|------------------------------------|--|
| S032 | cranial   | vault          | Adult        |         | good  | 0.313               | 0.878        | 12.938                             | 0.326                                    |
| S033 | cranial   | vault          | Adult        |         | fair  | 0.294               | 0.884        | 12.286                             | 0.341                                    |
| S034 | cranial   | vault          | Adult        |         | good  | 0.349               | 0.894        | 9.986                              | 0.338                                    |
| S035 | cranial   | vault          | Adult        |         | great | 0.308               | 0.836        | 19.215                             | 0.271                                    |
| S036 | cranial   | vault          | Adult        |         | fair  | 0.297               | 0.904        | 6.050                              | 0.449                                    |
| S037 | cranial   | vault          | Adult        |         | bad   | 0.303               | 0.946        | 3.735                              | 0.732                                    |
| S038 | cranial   | vault          | Adult        |         | good  | 0.317               | 0.897        | 7.890                              | 0.328                                    |
| S039 | cranial   | vault          | Adult        |         | fair  | 0.286               | 0.916        | 13.025                             | 0.431                                    |
| S040 | cranial   | vault          | Adult        |         | fair  | 0.277               | 0.925        | 8.633                              | 0.481                                    |
| S041 | cranial   | vault          | Adult        |         | great | 0.292               | 0.871        | 13.614                             | 0.421                                    |
| S042 | cranial   | vault          | Adult        |         | bad   | 0.403               | 0.965        | 2.988                              | 0.813                                    |
| S043 | cranial   | vault          | Adult        |         | good  | 0.290               | 0.903        | 9.372                              | 0.459                                    |
| S044 | cranial   | vault          | Adult        |         | good  | 0.359               | 0.915        | 6.484                              | 0.387                                    |
| S045 | radius    | distal         | Adult        |         | good  | 0.277               | 0.882        | 7.535                              | 0.331                                    |
| S046 | radius    | proximal       | Adult        |         | fair  | 0.297               | 0.920        | 8.442                              | 0.471                                    |
| S047 | scapula   | coracoid       | Adult        |         | fair  | 0.307               | 0.919        | 7.020                              | 0.542                                    |
| S048 | scapula   | acromion       | Adult        |         | fair  | 0.299               | 0.912        | 7.828                              | 0.406                                    |
| S049 | scapula   | medial border  | Adult        |         | fair  | 0.303               | 0.920        | 8.595                              | 0.411                                    |
| S050 | long bone | shaft          | Adult        |         | good  | 0.333               | 0.924        | 5.163                              | 0.440                                    |
| S051 | femur     | distal shaft   | Adult        |         | good  | 0.313               | 0.910        | 4.703                              | 0.463                                    |
| S052 | long bone | midshaft       | Adult        |         | fair  | 0.312               | 0.922        | 6.451                              | 0.456                                    |
| S053 | ilium     | crest          | Adult        |         | great | 0.295               | 0.850        | 10.031                             | 0.332                                    |
| S054 | femur     | proximal shaft | Adult        |         | good  | 0.307               | 0.925        | 5.376                              | 0.607                                    |
| S055 | fibula    | distal         | Adult        |         | good  | 0.296               | 0.875        | 14.780                             | 0.370                                    |
| S056 | femur     | midshaft       | Adult        |         | good  | 0.283               | 0.910        | 6.343                              | 0.528                                    |
| S057 | tibia     | proximal shaft | Adult        |         | good  | 0.302               | 0.891        | 10.209                             | 0.372                                    |
| S058 | tibia     | proximal shaft | Adult        | S057    | fair  | 0.283               | 0.907        | 9.239                              | 0.508                                    |
| S059 | tibia     | proximal shaft | Adult        | S057    | fair  | 0.255               | 0.925        | 6.904                              | 0.536                                    |
| S060 | humerus   | proximal shaft | Adult        |         | fair  | 0.303               | 0.885        | 9.443                              | 0.384                                    |
| S061 | humerus   | proximal shaft | Adult        | S060    | fair  | 0.342               | 0.898        | 8.708                              | 0.412                                    |
| S062 | ulna      | midshaft       | Adult        |         | good  | 0.298               | 0.887        | 12.147                             | 0.468                                    |
| S063 | ulna      | midshaft       | Adult        | S062    | fair  | 0.295               | 0.915        | 7.774                              | 0.507                                    |
| S064 | ulna      | proximal shaft | Adult        | S062    | fair  | 0.316               | 0.906        | 7.917                              | 0.481                                    |
| S065 | ulna      | proximal shaft | Adult        | S062    | fair  | 0.293               | 0.901        | 8.691                              | 0.449                                    |
| S066 | fibula    | distal shaft   | Adult        |         | good  | 0.282               | 0.890        | 6.888                              | 0.390                                    |
| S067 | fibula    | distal shaft   | Adult        | S066    | fair  | 0.293               | 0.895        | 11.436                             | 0.441                                    |
| S068 | fibula    | distal shaft   | Adult        | S066    | good  | 0.304               | 0.903        | 9.394                              | 0.453                                    |
| S069 | fibula    | midshaft       | Adult        |         | fair  | 0.309               | 0.878        | 11.447                             | 0.373                                    |
| S070 | fibula    | midshaft       | Adult        | S069    | good  | 0.312               | 0.882        | 7.491                              | 0.375                                    |



Table I.1. Continued.

| ID   | Element | Portion        | Age Category | Same as | QC   | CI <sub>raman</sub> | Fluor. Ratio | <u>Amide(I)</u> PO <sub>4</sub> | <u>CO<sub>3</sub></u> PO <sub>4</sub> |
|------|---------|----------------|--------------|---------|------|---------------------|--------------|---------------------------------|---------------------------------------|
| S071 | fibula  | midshaft       | Adult        | S069    | good | 0.316               | 0.837        | 10.637                          | 0.276                                 |
| S072 | humerus | proximal shaft | Adult        |         | fair | 0.315               | 0.921        | 8.080                           | 0.483                                 |
| S073 | humerus | proximal shaft | Adult        | S072    | fair | 0.292               | 0.923        | 5.730                           | 0.590                                 |
| S074 | femur   | midshaft       | Adult        |         | fair | 0.271               | 0.928        | 7.798                           | 0.530                                 |
| S075 | femur   | midshaft       | Adult        | S074    | fair | 0.280               | 0.911        | 5.875                           | 0.378                                 |
| S076 | tibia   | midshaft       | Adult        |         | good | 0.292               | 0.876        | 11.617                          | 0.423                                 |
| S077 | tibia   | midshaft       | Adult        | S076    | fair | 0.308               | 0.918        | 9.920                           | 0.423                                 |
| S078 | tibia   | midshaft       | Adult        |         | fair | 0.352               | 0.911        | 8.689                           | 0.384                                 |
| S079 | tibia   | midshaft       | Adult        | S078    | good | 0.295               | 0.861        | 12.609                          | 0.307                                 |
| S080 | tibia   | midshaft       | Adult        | S078    | fair | 0.318               | 0.902        | 9.607                           | 0.424                                 |
| S081 | tibia   | midshaft       | Adult        | S078    | good | 0.307               | 0.895        | 10.390                          | 0.371                                 |
| S082 | tibia   | midshaft       | Adult        | S078    | fair | 0.326               | 0.945        | 5.001                           | 0.599                                 |
| S083 | femur   | midshaft       | Adult        |         | fair | 0.288               | 0.936        | 5.933                           | 0.417                                 |
| S084 | femur   | midshaft       | Adult        | S083    | bad  | 0.298               | 0.943        | 6.028                           | 0.526                                 |
| S085 | femur   | midshaft       | Adult        | S083    | fair | 0.291               | 0.932        | 5.365                           | 0.536                                 |
| S086 | femur   | midshaft       | Adult        | S083    | bad  | 0.349               | 0.947        | 5.906                           | 0.480                                 |
| S087 | femur   | midshaft       | Adult        |         | fair | 0.305               | 0.931        | 5.653                           | 0.549                                 |
| S088 | femur   | midshaft       | Adult        | S087    | fair | 0.301               | 0.917        | 9.710                           | 0.468                                 |
| S089 | femur   | midshaft       | Adult        |         | fair | 0.324               | 0.911        | 7.798                           | 0.440                                 |
| S090 | femur   | midshaft       | Adult        | S089    | fair | 0.299               | 0.935        | 9.011                           | 0.557                                 |
| S091 | femur   | midshaft       | Adult        |         | good | 0.330               | 0.901        | 9.757                           | 0.332                                 |
| S092 | femur   | proximal shaft | Adult        | S091    | good | 0.287               | 0.872        | 9.930                           | 0.313                                 |
| S093 | femur   | proximal shaft | Adult        | S091    | good | 0.297               | 0.842        | 10.043                          | 0.276                                 |
| S094 | femur   | midshaft       | Adult        |         | good | 0.310               | 0.904        | 7.602                           | 0.353                                 |
| S095 | femur   | proximal shaft | Adult        | S094    | bad  | 0.275               | 0.936        | 5.712                           | 0.536                                 |
| S096 | femur   | proximal shaft | Adult        | S094    | fair | 0.318               | 0.913        | 9.071                           | 0.450                                 |
| S097 | femur   | midshaft       | Adult        |         | fair | 0.293               | 0.932        | 8.362                           | 0.461                                 |
| S098 | femur   | midshaft       | Adult        | S097    | bad  | 0.313               | 0.945        | 6.316                           | 0.575                                 |
| S099 | femur   | midshaft       | Adult        |         | fair | 0.343               | 0.906        | 9.587                           | 0.284                                 |
| S100 | femur   | midshaft       | Adult        |         | good | 0.353               | 0.878        | 9.260                           | 0.220                                 |

Table I.2. Inventory of select duplicated Raman spectra of samples representing individuals from Patakfalva-Papdomb and diagenetic indices calculated from duplicate scans.

| ID     | Element  | Portion         | Age Category | Same as | QC   | CI <sub>raman</sub> | Fluor. Ratio | <u>Amide(I)</u> PO <sub>4</sub> | <u>CO<sub>3</sub></u> PO <sub>4</sub> |
|--------|----------|-----------------|--------------|---------|------|---------------------|--------------|---------------------------------|---------------------------------------|
| S002.2 | mandible | notch           | Adult        |         | good | 0.291               | 0.826        | 14.208                          | 0.299                                 |
| S003.2 | mandible | ascending ramus | Adult        |         | good | 0.291               | 0.911        | 8.332                           | 0.432                                 |
| S004.2 | mandible | condyle         | Adult        |         | good | 0.312               | 0.888        | 7.844                           | 0.331                                 |
| S005.2 | ilium    | crest           | Adult        |         | good | 0.300               | 0.869        | 11.774                          | 0.352                                 |

Table I.2. Continued.

| ID     | Element   | Portion           | Age Category | Same as | QC    | CI <sub>raman</sub> | Fluor. Ratio | <u>Amide(I)</u><br>PO <sub>4</sub> | <u>CO<sub>3</sub></u><br>PO <sub>4</sub> |
|--------|-----------|-------------------|--------------|---------|-------|---------------------|--------------|------------------------------------|--|
| S006.2 | ilium     | crest             | Adult        | S005    | great | 0.300               | 0.864        | 11.048                             | 0.345                                    |
| S009.2 | rib       | midshaft          | Adult        |         | good  | 0.289               | 0.835        | 16.753                             | 0.261                                    |
| S010.2 | rib       | distal 1st        | Adult        |         | great | 0.277               | 0.749        | 13.004                             | 0.221                                    |
| S011.2 | rib       | proximal 1st      | Adult        | S010    | good  | 0.271               | 0.808        | 16.200                             | 0.304                                    |
| S013.2 | ulna      | proximal shaft    | Subadult     |         | good  | 0.293               | 0.877        | 11.639                             | 0.370                                    |
| S015.2 | scapula   | blade and glenoid | Subadult     |         | good  | 0.304               | 0.907        | 8.321                              | 0.414                                    |
| S016.2 | ulna      | proximal shaft    | Subadult     |         | good  | 0.291               | 0.883        | 8.102                              | 0.395                                    |
| S022.2 | femur     | midshaft          | Subadult     | S021    | good  | 0.323               | 0.895        | 6.847                              | 0.334                                    |
| S026.2 | femur     | midshaft          | Subadult     | S025    | good  | 0.307               | 0.871        | 9.556                              | 0.368                                    |
| S029.2 | long bone | midshaft          | Subadult     |         | good  | 0.313               | 0.909        | 7.905                              | 0.431                                    |
| S030.2 | long bone | midshaft          | Subadult     |         | good  | 0.305               | 0.875        | 10.740                             | 0.342                                    |
| S035.2 | cranial   | vault             | Adult        |         | great | 0.284               | 0.853        | 12.515                             | 0.293                                    |
| S038.2 | cranial   | vault             | Adult        |         | good  | 0.322               | 0.897        | 9.775                              | 0.371                                    |
| S041.2 | cranial   | vault             | Adult        |         | good  | 0.305               | 0.873        | 9.912                              | 0.349                                    |
| S043.2 | cranial   | vault             | Adult        |         | good  | 0.291               | 0.913        | 8.497                              | 0.466                                    |
| S053.2 | ilium     | crest             | Adult        |         | great | 0.284               | 0.835        | 11.518                             | 0.317                                    |
| S055.2 | fibula    | distal            | Adult        |         | good  | 0.317               | 0.867        | 10.997                             | 0.325                                    |
| S057.2 | tibia     | proximal shaft    | Adult        |         | good  | 0.293               | 0.894        | 10.373                             | 0.448                                    |
| S066.2 | fibula    | distal shaft      | Adult        |         | good  | 0.275               | 0.898        | 9.728                              | 0.449                                    |
| S068.2 | fibula    | distal shaft      | Adult        | S066    | good  | 0.293               | 0.903        | 8.323                              | 0.464                                    |
| S070.2 | fibula    | midshaft          | Adult        | S069    | good  | 0.317               | 0.882        | 10.097                             | 0.377                                    |
| S071.2 | fibula    | midshaft          | Adult        | S069    | good  | 0.307               | 0.844        | 12.596                             | 0.306                                    |
| S076.2 | tibia     | midshaft          | Adult        |         | good  | 0.292               | 0.882        | 13.672                             | 0.368                                    |
| S079.2 | tibia     | midshaft          | Adult        | S078    | good  | 0.290               | 0.859        | 12.445                             | 0.299                                    |
| S081.2 | tibia     | midshaft          | Adult        | S078    | good  | 0.298               | 0.897        | 8.090                              | 0.366                                    |
| S092.2 | femur     | proximal shaft    | Adult        | S091    | good  | 0.304               | 0.874        | 9.782                              | 0.311                                    |
| S093.2 | femur     | proximal shaft    | Adult        | S091    | good  | 0.303               | 0.850        | 13.084                             | 0.274                                    |
| S100.2 | femur     | midshaft          | Adult        |         | good  | 0.354               | 0.877        | 9.730                              | 0.232                                    |

APPENDIX II

INVENTORY OF DONORS, REPORTED RESIDENCE, AND REPORTED  
 DEMOGRAPHICS FOR INDIVIDUALS FROM THE UNIVERSITY OF TENNESSEE  
 SKELETAL COLLECTION IN THIS STUDY

| Project ID | City         | State | Years of Residence | $\delta^{18}\text{O}_{\text{tap water}}$ | $\delta^{18}\text{O}_{\text{ap-vsmow}}$ | Sex    | Age | Reported Ancestry |
|------------|--------------|-------|--------------------|--|---|--------|-----|-------------------|
| 1099       | Durham       | NC    | 11                 | -5.03                                    | 27.69                                   | Male   | 59  | Black             |
| 1339       | Boise        | ID    | 8                  | -15.98                                   | 20.43                                   | Female | 70  | White             |
| 1560       | Abilene      | TX    | 7                  | 0.05                                     | 31.05                                   | Male   | 51  | White             |
| 1355       | Ubyly        | MI    | 19                 | -8.83                                    | 25.17                                   | Male   | 59  | White             |
| 1540       | Kent         | WA    | 17                 | -10.63                                   | 23.97                                   | Female | 67  | White             |
| 1229       | Jacksonville | FL    | 27                 | -2.46                                    | 29.39                                   | Male   | 27  | White             |
| 407        | Chicago      | IL    | 93                 | -6.40                                    | 26.78                                   | Female | 94  | White             |
| 1614       | Birmingham   | AL    | 39                 | -4.68                                    | 27.92                                   | Female | 57  | White             |
| 1180       | Montgomery   | AL    | 50                 | -3.97                                    | 28.38                                   | Male   | 51  | White             |
| 1109       | Pulaski      | VA    | 65                 | -7.73                                    | 25.90                                   | Male   | 65  | White             |
| 81         | Newton       | IL    | 22                 | -5.76                                    | 27.20                                   | Female | 55  | White             |
| 1194       | Wilmington   | NC    | 60                 | -3.76                                    | 28.53                                   | Male   | 59  | White             |
| 1318       | Pensacola    | FL    | 20                 | -3.68                                    | 28.57                                   | Female | 66  | White             |
| 1068       | Plant City   | FL    | 25                 | -1.83                                    | 29.80                                   | Male   | 72  | Asian             |
| 1000       | Rifle        | CO    | 14                 | -15.16                                   | 20.97                                   | Male   | 56  | White             |
| 505        | Cleveland    | OH    | 58                 | -7.38                                    | 26.13                                   | Female | 58  | White             |
| 17         | Roseburg     | OR    | 13                 | -10.41                                   | 24.12                                   | Male   | 76  | White             |
| 634        | Rome         | GA    | 30                 | -5.08                                    | 27.65                                   | Male   | 68  | White             |
| 447        | Greenville   | SC    | 7                  | -4.57                                    | 27.99                                   | Female | 65  | White             |
| 187        | Victorville  | CA    | 8                  | -9.83                                    | 24.50                                   | Male   | 62  | White             |
| 107        | Memphis      | TN    | 6                  | -5.32                                    | 27.49                                   | Female | 41  | White             |
| 173        | St. Paul     | MN    | 36                 | -8.26                                    | 25.54                                   | Female | 50  | White             |
| 155        | Pasadena     | TX    | 13                 | -3.54                                    | 28.67                                   | Male   | 54  | White             |
| 1426       | Huntsville   | AL    | 14                 | -5.29                                    | 27.51                                   | Male   | 65  | White             |
| 1253       | Tuscaloosa   | AL    | 25                 | -4.47                                    | 28.06                                   | Male   | 68  | White             |
| 632        | Brunswick    | GA    | 15                 | -2.92                                    | 29.08                                   | Male   | 68  | White             |
| 1058       | Chapel Hill  | NC    | 28                 | -4.99                                    | 27.71                                   | Female | 66  | White             |
| 1573       | Knoxville    | TN    | 10                 | -5.76                                    | 27.20                                   | Male   | 70  | White             |
| 1270       | Mobile       | AL    | 31                 | -3.91                                    | 28.42                                   | Male   | 31  | White             |
| 1261       | Fort Worth   | TX    | 37                 | -1.20                                    | 30.22                                   | Male   | 69  | White             |

## APPENDIX III

### INVENTORY OF ISOTOPIC VALUES AND ASSOCIATED MEASURES FOR INDIVIDUALS FROM PATAKFALVA-PAPDOMB AND DUPLICATED ANALYSES IN THIS STUDY

Table III.1. Inventory of isotopic values for Patakfalva-Papdomb individuals and associated measures of analytical consistency.

| ID   | % Yield | $\delta^{13}\text{C}_{\text{apatite}}$ | $\delta^{18}\text{O}_{\text{vpdb}}$ | $\delta^{18}\text{O}_{\text{vsmow}}$ | %CaCO <sub>3</sub> |
|------|---------|--|-------------------------------------|--------------------------------------|--------------------|
| S001 | 68%     | -12.971                                | -7.960                              | 22.711                               | 8.631              |
| S002 | 60%     | -13.879                                | -7.890                              | 22.783                               | 6.166              |
| S003 | 68%     | -13.519                                | -8.199                              | 22.465                               | 7.299              |
| S004 | 71%     | -14.531                                | -7.935                              | 22.737                               | 5.865              |
| S005 | 47%     | -14.154                                | -8.149                              | 22.516                               | 6.471              |
| S006 | 89%     | -14.544                                | -8.562                              | 22.090                               | 6.103              |
| S007 | 70%     | -12.737                                | -7.982                              | 22.688                               | 6.610              |
| S008 | 71%     | -13.409                                | -7.728                              | 22.950                               | 8.012              |
| S009 | 50%     | -14.700                                | -7.819                              | 22.856                               | 6.708              |
| S010 | 44%     | -14.134                                | -7.533                              | 23.151                               | 6.599              |
| S011 | 59%     | -13.934                                | -7.146                              | 23.550                               | 6.310              |
| S012 | 64%     | -12.987                                | -8.035                              | 22.634                               | 7.287              |
| S013 | 70%     | -13.475                                | -7.892                              | 22.781                               | 8.110              |
| S014 | 67%     | -12.845                                | -8.872                              | 21.771                               | 7.239              |
| S015 | 50%     | -15.152                                | -6.577                              | 24.137                               | 5.382              |
| S016 | 37%     | -13.798                                | -7.857                              | 22.817                               | 6.971              |
| S017 | 70%     | -13.096                                | -8.636                              | 22.014                               | 6.436              |
| S018 | 64%     | -13.172                                | -7.074                              | 23.624                               | 6.804              |
| S019 | 60%     | -12.495                                | -9.122                              | 21.513                               | 8.178              |
| S020 | 55%     | -13.278                                | -8.536                              | 22.117                               | 7.291              |
| S021 | 71%     | -13.100                                | -8.227                              | 22.436                               | 7.345              |
| S022 | 77%     | -12.485                                | -7.696                              | 22.983                               | 8.809              |
| S023 | 64%     | -12.937                                | -8.086                              | 22.581                               | 7.154              |
| S024 | 68%     | -13.233                                | -7.750                              | 22.928                               | 6.835              |
| S025 | 77%     | -13.429                                | -7.674                              | 23.006                               | 8.689              |
| S026 | 71%     | -13.455                                | -7.411                              | 23.277                               | 7.410              |
| S027 | 72%     | -12.589                                | -8.610                              | 22.041                               | 9.513              |
| S028 | 55%     | -13.552                                | -6.786                              | 23.921                               | 6.313              |
| S029 | 66%     | -12.824                                | -8.365                              | 22.294                               | 7.617              |
| S030 | 62%     | -13.346                                | -7.624                              | 23.057                               | 8.645              |
| S031 | 62%     | -14.570                                | -7.147                              | 23.549                               | 6.022              |
| S032 | 77%     | -12.897                                | -8.201                              | 22.463                               | 5.603              |

Table III.1. Continued.

| ID   | % Yield | $\delta^{13}\text{C}_{\text{apatite}}$ | $\delta^{18}\text{O}_{\text{vpdb}}$ | $\delta^{18}\text{O}_{\text{vsmow}}$ | %CaCO <sub>3</sub> |
|------|---------|--|-------------------------------------|--------------------------------------|--------------------|
| S033 | 73%     | -13.156                                | -9.256                              | 21.375                               | 7.291              |
| S034 | 64%     | -13.426                                | -8.575                              | 22.077                               | 6.029              |
| S035 | 76%     | -13.841                                | -8.456                              | 22.200                               | 5.631              |
| S036 | 55%     | -14.251                                | -8.006                              | 22.664                               | 6.564              |
| S037 | 73%     | -13.439                                | -8.473                              | 22.182                               | 7.813              |
| S038 | 53%     | -14.327                                | -8.281                              | 22.380                               | 5.700              |
| S039 | 75%     | -12.387                                | -8.978                              | 21.662                               | 6.787              |
| S040 | 72%     | -12.977                                | -8.103                              | 22.564                               | 7.326              |
| S041 | 65%     | -13.871                                | -9.093                              | 21.543                               | 6.707              |
| S042 | 56%     | -14.259                                | -7.685                              | 22.995                               | 5.510              |
| S043 | 78%     | -12.648                                | -8.870                              | 21.773                               | 7.061              |
| S044 | 78%     | -12.822                                | -7.704                              | 22.975                               | 6.269              |
| S045 | 67%     | -13.741                                | -7.769                              | 22.908                               | 7.291              |
| S046 | 69%     | -12.324                                | -7.265                              | 23.428                               | 7.351              |
| S047 | 64%     | -13.102                                | -7.025                              | 23.675                               | 8.401              |
| S048 | 68%     | -13.250                                | -8.756                              | 21.890                               | 7.562              |
| S049 | 64%     | -12.945                                | -7.481                              | 23.205                               | 8.083              |
| S050 | 61%     | -12.596                                | -8.227                              | 22.436                               | 7.804              |
| S051 | 65%     | -12.799                                | -8.910                              | 21.732                               | 7.629              |
| S052 | 72%     | -12.674                                | -7.692                              | 22.987                               | 7.620              |
| S053 | 54%     | -14.290                                | -7.354                              | 23.336                               | 7.742              |
| S054 | 73%     | -12.393                                | -8.244                              | 22.418                               | 7.604              |
| S055 | 63%     | -12.363                                | -9.130                              | 21.505                               | 7.738              |
| S056 | 72%     | -13.756                                | -9.115                              | 21.520                               | 7.122              |
| S057 | 64%     | -12.089                                | -8.124                              | 22.542                               | 8.518              |
| S058 | 52%     | -11.845                                | -9.055                              | 21.582                               | 9.450              |
| S059 | 56%     | -12.093                                | -8.330                              | 22.330                               | 8.491              |
| S060 | 70%     | -12.883                                | -8.926                              | 21.715                               | 6.903              |
| S061 | 75%     | -13.050                                | -9.083                              | 21.553                               | 7.379              |
| S062 | 70%     | -13.181                                | -7.654                              | 23.027                               | 10.070             |
| S063 | 61%     | -13.182                                | -7.556                              | 23.128                               | 9.136              |
| S064 | 56%     | -13.228                                | -7.463                              | 23.223                               | 9.399              |
| S065 | 66%     | -13.033                                | -7.604                              | 23.078                               | 9.420              |
| S066 | 66%     | -12.749                                | -7.812                              | 22.864                               | 9.422              |
| S067 | 66%     | -13.081                                | -8.070                              | 22.598                               | 8.823              |
| S068 | 69%     | -12.490                                | -7.777                              | 22.900                               | 9.505              |
| S069 | 61%     | -13.683                                | -7.663                              | 23.017                               | 9.046              |
| S070 | 65%     | -13.667                                | -7.305                              | 23.386                               | 8.660              |
| S071 | 72%     | -13.903                                | -7.335                              | 23.355                               | 8.593              |
| S072 | 69%     | -13.014                                | -7.663                              | 23.017                               | 8.278              |

Table III.1. Continued.

| ID   | % Yield | $\delta^{13}\text{C}_{\text{apatite}}$ | $\delta^{18}\text{O}_{\text{vpdb}}$ | $\delta^{18}\text{O}_{\text{vsmow}}$ | %CaCO <sub>3</sub> |
|------|---------|--|-------------------------------------|--------------------------------------|--------------------|
| S073 | 62%     | -12.827                                | -7.836                              | 22.839                               | 5.826              |
| S074 | 41%     | -13.094                                | -8.679                              | 21.970                               | 7.137              |
| S075 | 70%     | -13.067                                | -8.191                              | 22.473                               | 7.312              |
| S076 | 62%     | -12.676                                | -7.400                              | 23.288                               | 8.049              |
| S077 | 68%     | -12.575                                | -7.362                              | 23.328                               | 7.949              |
| S078 | 75%     | -12.971                                | -8.543                              | 22.110                               | 7.820              |
| S079 | 50%     | -13.098                                | -8.149                              | 22.516                               | 7.855              |
| S080 | 47%     | -13.259                                | -8.575                              | 22.077                               | 7.513              |
| S081 | 67%     | -13.035                                | -8.184                              | 22.480                               | 7.704              |
| S082 | 71%     | -13.095                                | -8.147                              | 22.518                               | 7.401              |
| S083 | 69%     | -13.145                                | -8.167                              | 22.498                               | 6.872              |
| S084 | 65%     | -13.003                                | -7.996                              | 22.674                               | 7.047              |
| S085 | 64%     | -12.898                                | -8.645                              | 22.005                               | 6.891              |
| S086 | 55%     | -12.926                                | -8.524                              | 22.130                               | 6.152              |
| S087 | 73%     | -13.035                                | -8.176                              | 22.488                               | 6.261              |
| S088 | 58%     | -12.927                                | -8.331                              | 22.329                               | 7.718              |
| S089 | 69%     | -12.267                                | -8.503                              | 22.151                               | 8.197              |
| S090 | 72%     | -11.640                                | -8.384                              | 22.274                               | 9.184              |
| S091 | 71%     | -12.653                                | -8.022                              | 22.647                               | 7.189              |
| S092 | 68%     | -12.383                                | -7.555                              | 23.129                               | 8.259              |
| S093 | 64%     | -12.141                                | -7.979                              | 22.692                               | 7.837              |
| S094 | 69%     | -12.766                                | -7.844                              | 22.831                               | 8.509              |
| S095 | 64%     | -12.542                                | -7.915                              | 22.757                               | 8.176              |
| S096 | 70%     | -12.778                                | -7.825                              | 22.850                               | 7.605              |
| S097 | 74%     | -12.779                                | -8.001                              | 22.669                               | 7.306              |
| S098 | 77%     | -12.872                                | -8.069                              | 22.599                               | 6.744              |
| S099 | 72%     | -13.224                                | -8.829                              | 21.815                               | 5.926              |
| S100 | 70%     | -13.385                                | -8.728                              | 21.919                               | 5.554              |

Table III.2. Inventory of isotopic values for duplicated analyses of Patakfalva-Papdomb individuals and associated measures of analytical consistency.

| ID   | % Yield | $\delta^{13}\text{C}_{\text{apatite}}$ | $\delta_{18}\text{O}_{\text{vpdb}}$ | $\delta^{18}\text{O}_{\text{vsmow}}$ | %CaCO <sub>3</sub> |
|------|---------|--|-------------------------------------|--------------------------------------|--------------------|
| S006 | 63%     | -14.390                                | -8.349                              | 22.310                               | 5.945              |
| S015 | 41%     | -15.470                                | -7.167                              | 23.529                               | 5.940              |
| S030 | 66%     | -13.490                                | -7.606                              | 23.076                               | 8.670              |
| S049 | 54%     | -13.290                                | -7.697                              | 22.982                               | 8.213              |
| S056 | 72%     | -13.598                                | -8.321                              | 22.339                               | 8.364              |
| S069 | 67%     | -13.770                                | -7.678                              | 23.002                               | 8.695              |
| S075 | 64%     | -13.071                                | -8.060                              | 22.608                               | 7.040              |
| S081 | 62%     | -13.032                                | -8.246                              | 22.416                               | 7.516              |

APPENDIX IV

FREQUENCY BANDS SELECTED, COEFFICIENTS, AND SIGNIFICANCE IN RAMAN

SPECTRA FOR THE ISOTOPE RATIO INFRARED SPECTROMETRY LINEAR

REGRESSION MODEL IN THIS STUDY

| Peak Position (cm <sup>-1</sup> ) | IRIS Coefficients<br>$\delta^{13}\text{C}_{\text{apatite}}$ |                   | IRIS Coefficients<br>$\delta^{18}\text{O}_{\text{vpdb}}$ |                   | Interpretation      | References  |
|-----------------------------------|---|-------------------|--|-------------------|---------------------|---|
|                                   | Coefficient   | Relative Strength | Coefficient  | Relative Strength |                     |   |
| 800                               | 0.0311  | 0.03              |  |                   |                     |   |
| 802                               | 0.0157  | 0.02              |  |                   |                     |   |
| 864                               | -0.0193   | 0.02              |  |                   | Proline             | Morris and Mandair (2011)   |
| 914                               | 0.0023  | 0.00              |  |                   | Proline             | Morris and Mandair (2011)   |
| 1002                              | 0.0591  | 0.06              |  |                   | Phenylalanine       | Morris and Mandair (2011)   |
| 1070                              | 0.0329  | 0.03              |  |                   | B-type v1 CO3       | Awonusi et al. (2007); Khan et al. (2007); Penel et al. (1998)                                      |
| 1206                              | -0.0266   | 0.03              | 0.0137   | 0.20              |                     |   |
| 1252                              |   |                   | -0.0519  | 0.75              | Amide III           | Khan et al. (2013); G. McLaughlin and Lednev (2011); Morris and Mandair (2011); Penel et al. (1998) |
| 1376                              | -0.0020   | 0.00              |  |                   |                     |   |
| 1378                              | -0.0258   | 0.03              |  |                   |                     |   |
| 1394                              | -0.0122   | 0.01              |  |                   |                     |   |
| 1408                              | 0.1885  | 0.19              |  |                   |                     |   |
| 1410                              | 0.0910  | 0.09              |  |                   | del NH, C-H bending | Khan et al. (2013); G. McLaughlin and Lednev (2011); Morris and Mandair (2011); Penel et al. (1998) |
| 1500                              | 0.0226  | 0.02              |  |                   | del NH, C-H bending | Khan et al. (2013); G. McLaughlin and Lednev (2011); Morris   |



| Peak<br>Position<br>(cm <sup>-1</sup> ) | IRIS Coefficients<br>$\delta^{13}\text{C}_{\text{apatite}}$ |                      | IRIS Coefficients<br>$\delta^{18}\text{O}_{\text{vpdb}}$ |                      | Interpretation | References  |
|---|---|----------------------|--|----------------------|----------------|---|
|   | Coefficient   | Relative<br>Strength | Coefficient  | Relative<br>Strength |                |   |
| 1506                                    | 0.0115  | 0.01                 |  |                      |                | and Mandair<br>(2011); Penel et<br>al. (1998)   |
| 1526                                    | 0.0001  | 0.00                 |  |                      |                |   |
| 1532                                    |   |                      | -0.0036  | 0.05                 |                |   |
| 1594                                    | 0.0072  | 0.01                 |  |                      | Amide I        | Khan et al. (2013);<br>McLaughlin and<br>Lednev (2011);<br>Morris and<br>Mandair (2011);<br>Penel et al. (1998) |
| 1596                                    | 0.0080  | 0.01                 |  |                      | Amide I        | Khan et al. (2013);<br>McLaughlin and<br>Lednev (2011);<br>Morris and<br>Mandair (2011);<br>Penel et al. (1998) |
| 1634                                    | 0.0201  | 0.02                 |  |                      | Amide I        | Khan et al. (2013);<br>McLaughlin and<br>Lednev (2011);<br>Morris and<br>Mandair (2011);<br>Penel et al. (1998) |
| 1684                                    | -0.1430   | 0.14                 |  |                      | Amide I        | Khan et al. (2013);<br>McLaughlin and<br>Lednev (2011);<br>Morris and<br>Mandair (2011);<br>Penel et al. (1998) |
| 1734                                    | 0.0416  | 0.04                 |  |                      | Amide I        | Khan et al. (2013);<br>McLaughlin and<br>Lednev (2011);<br>Morris and<br>Mandair (2011);<br>Penel et al. (1998) |
| 1762                                    | -0.1268   | 0.12                 |  |                      |                |   |
| 1764                                    | -0.0091   | 0.01                 |  |                      |                |   |
| 1814                                    | -0.0667   | 0.07                 |  |                      |                |   |
| 1838                                    | 0.0471  | 0.05                 |  |                      |                |   |
| 1866                                    | -0.0061   | 0.01                 |  |                      |                |   |

## VITA

Armando Anzellini was born in Venezuela and migrated to the U.S. in 2000. His family settled in Florida where he spent his adolescence and attended high school. He attended the University of Central Florida where he received a Bachelor of Arts in Anthropology (2013) with University Honors and Honors in the Major resulting from the completion of an undergraduate thesis titled “Investigating Patterns of Interpersonal Violence Using Frequency Distributions of Cranial Vault Trauma.” Armando remained at the University of Central Florida to pursue a Master of Arts in Anthropology that he received in 2016 with a thesis titled “Developing Methods for the Estimation of Stature and their Use as a Proxy for Health among the Ancient Chachapoya of Peru.” After receiving his Register of Professional Archaeologists certification, Armando joined a Cultural Resource Management firm where he conducted and supervised Phase I, II, and III projects throughout the eastern and midwestern U.S. Armando began his doctoral studies at the University of Tennessee in the Fall of 2018 with foci on bioarchaeology and forensic anthropology, having collaborated extensively with the Forensic Anthropology Center. In the Fall of 2021, Armando received a Diversity Dissertation Fellowship at Middle Tennessee State University, where he taught and completed his dissertation research during the 2021-2022 academic year. He currently resides in Bethlehem, PA and joined Lehigh University as Assistant Professor of Anthropology beginning August 2022.